

A Study on Hyperparameters Configurations for an Efficient Human Activity Recognition System*

Extended Version

Paulo J.S. Ferreira[†]
 João Mendes-Moreira^{*}
 João M.P. Cardoso^{*}
 up201305617@fe.up.pt
 jmoreira@fe.up.pt
 jmpc@fe.up.pt

INESC TEC, Faculty of Engineering, University of Porto
 Porto, Portugal

ABSTRACT

Human Activity Recognition (HAR) has been a popular research field due to the widespread of devices with sensors and computational power (e.g., smartphones and smartwatches). Applications for HAR systems have been extensively researched in recent literature, mainly due to the benefits of improving quality of life in areas like health and fitness monitoring. However, since persons have different motion patterns when performing physical activities, a HAR system must adapt to user characteristics to maintain or improve accuracy. Mobile devices, such as smartphones, used to implement HAR systems, have limited resources (e.g., battery life). They also have difficulty adapting to the device's constraints to work efficiently for long periods. In this work, we present a k NN-based HAR system and an extensive study of the influence of hyperparameters (window size, overlap, distance function, and the value of k) and parameters (sampling frequency) on the system accuracy, energy consumption, and inference time. We also study how hyperparameter configurations affect the model's user and activity performance. Experimental results show that adapting the hyperparameters makes it possible to adjust the system's behavior to the user, the device, and the target service. These results motivate the development of a HAR system capable of automatically adapting the hyperparameters for the user, the device, and the service.

CCS CONCEPTS

• Human-centered computing → Mobile devices.

KEYWORDS

human activity recognition, HAR, k NN, energy consumption, adaptability, smartphones, hyperparameters, PAMAP2, Pareto-Front, sampling frequency

*This paper, followed by Appendix A.2 with a technical report with extensive content and results, is an extended version of the paper: Paulo J.S. Ferreira, João Mendes-Moreira, and João M.P. Cardoso. 2023. A Study on Hyperparameters Configurations for an Efficient Human Activity Recognition System. In 8th International Workshop on Sensor-Based Activity Recognition and Artificial Intelligence (iWOAR 2023), Sept. 21–22, 2023, Lübeck, Germany. ACM, New York, NY, USA. <https://doi.org/10.1145/3615834.3615851>

[†]All authors contributed equally to this research.

1 INTRODUCTION

Recently, Human Activity Recognition (HAR) [11, 15, 16, 19, 24] has been a popular research field due to the wide spread of devices with sensors (e.g., smartphones and smartwatches). HAR aims at recognizing the activities performed by humans at runtime through the analyses of sensing data and other observations acquired by in situ devices [43]. HAR has enabled novel applications in different areas, such as health and fitness monitoring, security, smart cities and entertainment [34, 36, 37].

Figure 1 shows the main stages of the two views of a ML-based HAR system: the offline training view (Preparation Phase), and the online classification view (with the possibility of incremental/online learning) (Use Phase).

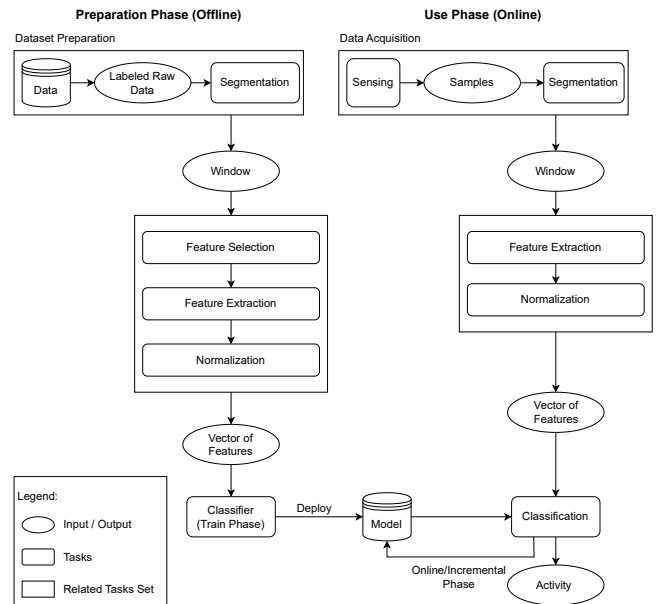


Figure 1: Block diagram of the HAR system considered.

The Preparation Phase is used to train the model to be later used in the classification process. This Phase includes the following steps: data acquisition, pre-processing, and training [34]. At this

Phase, after data acquisition, data is labeled and stored in files to build the dataset used in the system. In the Use Phase, the trained classifiers infer activities. This step can be done online on a mobile device. This Phase includes the following stages: data acquisition, pre-processing, and classification [34]. This Phase can also contain the Incremental Learning step. In this case, data are not stored in files during data acquisition online. Instead, it goes directly to the segmentation. The feature selection is only carried out in the pre-processing step of the Preparation Phase.

Smartphones have been increasingly used to develop HAR systems, due to the capability and diversity of the sensors embedded in these devices [36]. The advantage of smartphones over other wearable devices is associated with (a) their widespread use, (b) their ability to collect and process sensor data [36], (c) the increase in their processing power, (d) the increase in their battery capacity [34], and (e) their use by most people. Although smartphones have seen rapid development in recent years, these devices continue to have limitations concerning battery life and available memory.

In order to be able to recognize different activities accurately, a HAR system uses Machine Learning (ML) algorithms capable of inferring activities from the sensor data. One of the most used ML algorithms in HAR is k -Nearest Neighbours (k NN) [9]. k NN is an instance-based lazy learning algorithm. This fact facilitates the implementation of incremental/online learning HAR systems in mobile devices since k NN does not require a computationally expensive training stage. Besides, k NN has also been proved to obtain very high accuracy in the HAR field (see, e.g., [6, 11, 20, 21, 26, 28, 33, 35, 41]). Using k NN, the implementation of online/incremental learning approaches only needs to add, remove or update the instances in the k NN memory. Updating the k NN is fast and requires low energy because there is no need to retrain the algorithm, which is essential in devices with energy limitations [11].

Typically, an ML algorithm has two types of parameters: model parameters and hyperparameters [23]. Model Parameters are used inside the model and are estimated or learned from the data as a part of the learning process. On the other hand, hyperparameters are external parameters that are not part of the model and thus can not be predicted from the data set but can be configured by subject matter experts or by trial and error until an acceptable accuracy is achieved. Hyperparameters are used to control the learning process and can have wildly varying effects on the resulting model and on its performance [8]. For the same training dataset, with different hyperparameters, an ML algorithm might learn models that have significantly different performances on the testing dataset [39].

This paper studies the influence of hyperparameters on a HAR system's optimal performance, specifically analyzing window size, overlap, k value, distance function, and sampling frequency in a k NN-based approach. Accuracy, response time, and energy consumption are evaluated as performance metrics. While most studies focus on hyperparameters' impact on accuracy, limited research explores their influence on critical measures such as response time and energy consumption. In real-world applications, these factors significantly impact the practicality and usability of HAR systems. Prompt response time is crucial for time-sensitive applications that require real-time activity recognition, while energy consumption is vital for mobile and wearable devices with limited battery life.

Moreover, HAR systems need to be adaptable to changing conditions, such as different users or environments. To achieve adaptability, it is essential to study the hyperparameter's impact on a HAR system's performance under different scenarios. For instance, a HAR system optimized for one user may not perform well for another user due to differences in their physical characteristics or activity patterns. Similarly, a HAR system designed for indoor environments may not perform well in outdoor environments due to changes in lighting, temperature, and other factors.

Therefore, in this study, we address the impact of hyperparameters on the performance of a HAR system in terms of accuracy, response time, and energy consumption. Specifically, we explore the effect of different hyperparameter configurations on the performance of a HAR system using the PAMAP2 [30, 31] dataset. PAMAP2 is one of the most widely used wearable sensor-based datasets in HAR research and also has been widely used to test and implement new approaches for HAR systems [2, 7, 11, 17, 26, 29, 38, 42]. This dataset has data from different sensors, body placements, and users. The results of this study provide valuable insights into the optimal hyperparameter configurations for HAR systems, enabling the design of more efficient, effective, and adaptable systems for real-world applications. We present in [12] an extended version of this study.

Specifically, in this study, we answer the following Research Questions:

- RQ 1 - How do hyperparameter configurations affect the accuracy, response time, and energy consumption of a HAR system globally and across different users and contexts?
- RQ 2 - What are the overall, and specific activities, the impact of window size, overlap, distance function, and k for a k NN-based HAR system regarding its accuracy, response time, and energy consumption?
- RQ 3 - How do the sampling frequencies influence the accuracy of a HAR system for different users and activities?
- RQ 4 - How does reducing the sampling frequency change the trade-off between accuracy and energy consumption for different hyperparameter configurations of a HAR system for a specific user?
- RQ 5 - How does the mismatch between the sampling frequencies of the train and test sets affect the accuracy of a HAR system?

The remainder of this paper is organized as follows. Section 2 describes the related work regarding the study of hyperparameters. Section 3 describes the experimental setup and methodology used to conduct this study. Section 4 presents and discusses the experimental results, including a comparison with the Related Work. Finally, in Section 5, we present the main conclusions for this study and the future work planned.

2 RELATED WORK

HAR is a research field focused on automatically identifying and classifying human activities from sensor data. ML algorithms are commonly used in HAR systems for activity classification. Hyperparameters are essential for building accurate HAR models. They can influence the model's performance significantly, so choosing them carefully is important. Hyperparameters affect the algorithms'

performance in terms of prediction and computation, so many researchers are investigating their impact on HAR systems. The most common hyperparameters in traditional ML algorithms are window size and overlap. These hyperparameters are used to segment the data for both Preparation and User Phases (see Figure 1). Here are some examples of HAR studies that examined some hyperparameters.

Banos et al. [5], uses the REALDISP [4] dataset to evaluate the impact of the window size, using C4.5, k NN, Naïve Bayes, and Nearest Centroid Classifier as inference algorithms. The dataset has data for 33 different activities and was collected at 50 Hz. To measure the performance, the authors use F1-Score. They use windows sizes between 0.25 s and 7 s. Overall, they show that the windows with 2 s achieve the best results. They also concluded that larger window sizes not always translated into better performances for the models.

Garcia et al. study the impact of window size and overlapping. They used the PAMAP2 HAR dataset and built an ensemble classifier with k NN, VFDt, and Naïve Bayes algorithms. The study explored variations in window size (from 100 to 1000 samples with increments of 100) and overlap (from 0.0 to 0.9 with increments of 0.1). Evaluation metrics included accuracy, energy consumption, and execution time. They use the ODROID-XU+E6 board to measure energy consumption. Smaller window sizes showed lower accuracy, while larger sizes improved accuracy. The overlap factor had fluctuations in accuracy, with optimal results between 0.1 and 0.5. Smaller windows consumed less energy and had shorter execution times due to reduced feature calculation effort. Increasing the overlap factor raised energy consumption due to more calculations and classifications. Higher accuracies were associated with increased energy consumption.

Wang et al. [40] conducted a study on the impact of window size in a HAR system. They used a private dataset containing activities such as still, walking, up/down stairs, up/down an elevator, up/down escalator, typing, swinging, phoning, and trouser pocket. The data was collected at a sampling frequency of 50 Hz. The authors varied the window size between 0.5 s and 7 s. They evaluated the performance of different algorithms including SVM, k NN, Decision Tree, Naïve Bayes, and Adaboost, using the F1-Score metric. The results showed that increasing the window size significantly improved the classification performance for all algorithms. However, larger window sizes also resulted in increased recognition latency. Based on their findings, the authors concluded that a window size between 2.5-3.5 s provided the best tradeoff between performance and latency.

Although the window size and overlap are among the most studied hyperparameters, they control data segmentation before being used to train or use the traditional ML algorithms. They are not specific to any ML algorithm. However, traditional ML algorithms have specific hyperparameters (e.g., k NN has the number of k , distance function, and the maximum number of instances). These hyperparameters are defined in the Preparation Phase, more precisely in the training stage of the ML algorithm (see Figure 1). Some authors are also focusing on studying the algorithm's specific hyperparameters.

Mohsen et al. [25] study the impact of the value of k on model accuracy, varying k from 1 to 20 and using the UCI-HAR dataset. The results showed that accuracy improved as k increased, with the best results achieved when k was between 8 and 20. However,

no significant improvement in accuracy was observed for k values greater than 8. Liu et al. [22] also assessed the effect of different values of k on HAR datasets, specifically on HAPT and Smartphone Datasets for Human Activity Recognition in Ambient Assisted Living Data (Smartphone). They examined k values of 3 and 9 in terms of accuracy. The findings demonstrated that increasing the value of k enhanced model accuracy. However, for k values greater than 6, accuracy started to decrease. The optimal value of k for both datasets was determined to be 6, as it yielded the highest accuracy.

Sampling frequency, although not considered a hyperparameter, plays a crucial role in the performance of a Human Activity Recognition (HAR) system. It directly affects inference time, energy consumption, and the performance of machine learning algorithms. Higher sampling frequencies, meaning more samples per second, generally increase energy consumption. Several studies have investigated the impact of sampling frequency on HAR systems.

Santoyo-Ramón et al. [3] study the influence of the sampling frequency in 15 HAR datasets. The datasets have sampling frequencies between 18 Hz and 238 Hz. The metrics used are sensitivity, specificity, and the geometric mean as single descriptors of the global system performance. They use a convolutional neural network (CNN) as an inference algorithm. The results show that the system performance only degrades when the sampling rate of the dataset is between 10 and 15 Hz. The inference improves when the sampling frequency of the dataset is between 20 and 40 Hz.

Niazi et al. [27] conducted a study on the effects of sampling frequency and window duration in a HAR system using a private dataset collected at 100 Hz. Window sizes of 1, 2, 3, 5, and 10s, along with sampling frequencies of 5, 10, 20, 25, 50, and 100 Hz, were considered. Random Forest was used as an inference algorithm. Statistical analysis with weighted least squares and two-way factorial ANOVA was performed to calculate the expected average value (EV) for each combination of window duration and sampling frequency. The optimal combination was found to be 10s/50Hz, especially for young, physically active individuals. Higher sampling rates and window sizes showed higher significance in the EVs, but reducing the sampling rate to 20Hz did not significantly affect accuracy.

Zheng et al. [44] evaluate the impact of the sampling frequency on accuracy and energy consumption with SVM as an inference algorithm. They use a dataset at 1 Hz, 5 Hz, 10 Hz, and 50 Hz sampling frequencies. The data consist of the following activities: Sitting, Standing, Walking, Running, Upstairs, and Downstairs. The results show that the accuracy has only improved slightly with the sampling rate increase from 1 Hz to 50 Hz. In terms of energy consumption, there is an increase with increased sampling frequency, which is more significant when the sampling rate changes from 10 Hz to 50 Hz.

In these studies, the impact of the hyperparameters is more focused on the performance of the resulting model instead of their influence on the computational cost of the system. However, some exceptions exist, like Garcia et al. [13], who, in addition to accuracy, also evaluate the energy consumption for different window sizes and overlap values. Unlike the studies presented in this section, our study considers 5 different hyperparameters of different stages of a HAR system (window size and overlap for data segmentation, sampling frequency for data acquisition, and distance function and the k value for the training of the algorithm) and evaluate their

impact on the performance of the model (accuracy and F1-Score) and the computational cost of the system (inference time and energy consumption).

3 EXPERIMENTAL SETUP AND METHODOLOGY

This section presents the experimental setup and experiments carried out in this study. It includes the dataset and algorithm used in the experiments, the evaluation metrics, the evaluation procedure, the processing of the raw data (feature extraction and normalization), the running platforms and the experiments carried out in our study, and some procedures we used to prepare the data for the experiments.

Dataset: The PAMAP2 [30, 31] HAR dataset contains 1, 926, 896 samples of raw sensor data from 9 different users and 12 different activities. Data were collected from 3 Inertial Measurement Units (IMU) positioned in different body areas (wrist, chest, and ankle), at a sampling frequency of 100 Hz, and a Heart-Rate Monitor at a sampling frequency of 9 Hz. Each IMU has 4 embedded sensors: a 3-axis accelerometer, a 3-axis gyroscope, a 3-axis magnetometer, and a thermometer. The activities are organized as basic activities (walking, running, nordic walking, and cycling); posture activities (lying, sitting, and standing); everyday activities (ascending and descending stairs); household (ironing and vacuum cleaning), and fitness activities (rope jumping). We decided to use only the following sensors: accelerometer, gyroscope, and magnetometer.

Evaluation: To measure the performance of the models obtained using the explored hyperparameters, we use the following ML metrics: accuracy and F1-Score. We also measure the impact of different configurations on the system regarding response time (equals inference time, in our experiments) and energy consumption. Both response times and energy consumption refer to the time and energy needed for each inference. The values for time and energy include the following phases: reading data from the files, feature extraction, and inference. We use the fANOVA (Functional ANOVA (Analysis of Variance))¹ [18] algorithm to assess the importance of the selected hyperparameters. The experiments in this paper follow the leave-one-subject-out (LOSO) approach, where one user is selected for testing the model while the remaining users are used for training. This approach enables us to evaluate the impact of the same set of hyperparameters on different models and highlights the significance of a user-adaptive model.

Feature Extraction: Using fixed-size sliding windows, we extracted 10 features for each 3D sensor: x-axis Mean, y-axis Mean, z-axis Mean, Mean of the sum of the x, y, and z axes, x-axis Standard Deviation, y-axis Standard Deviation, z-axis Standard Deviation, x and y axes Correlation, x, and z axes Correlation, and y and z axes Correlation. The features are extracted from 9 sensors: 3 sensors (accelerometer, gyroscope, and magnetometer) for each body placement (wrist, chest, and ankle). This results in vectors of 90 features that are the input to the ML algorithm. The features are normalized using the Min-Max technique.

Inference ML Algorithm: k -Nearest Neighbour (k NN) [9] is an instance-based classifier based on the majority voting of its k neighbours [37] for classifying an instance. The value of k defines how

many nearest neighbor instances contribute to the classification of each instance. k NN does not use any model to fit and it is only based on memory. k NN is a lazy learning algorithm because it does not have a learning phase; instead, it "memorizes" the training dataset. The more the number of training instances stored in the k NN's memory, the greater the number of distances to be calculated and, consequently, the longer the execution time of the inference phase. Usually, Euclidean distance is used as the distance metric [28]. The selection of k is an important consideration as it affects the classification performance. In this study, the k NN implementation is based on the MOA Java library. The implementation offers three hyperparameters that can be optimized: k value, distance function, and the maximum number of instances that k NN can store.

Running Platforms: We ran the experiments on two platforms: a desktop computer and a board with ARM CPUs. The desktop computer was used to run the exploration experiments. The application was written in Java code and executed with version 1.8 of the Java Runtime Environment (JRE). The experiments related to the HAR system run on an embedded Odroid computing board. They were used to measure energy consumption and response time. It represents a possible mobile/embedded device. We use an ODROID-XU+E6² equipped with an Exynos5 Octa CPU (used in several Samsung smartphones) with four big cores (ARM Cortex-A15 up to 1.6 GHz) and four small cores (ARM Cortex-A7 up to 1.2 GHz). ODROID-XU+E6 has four current/voltage sensors to measure the power consumption of the Big A15 cores, Little A7 cores, GPU and DRAM individually. In our experiments, we only consider the energy consumption for the A15 cores, A7 cores, and DRAM, as we are not using the GPU.

Configurations Search: The goal of the first experiment was to explore the configuration space. We use the multi-objective search in Optuna [1] to select the configurations that optimize two different objectives: maximize the accuracy and minimize response time. We select the hyperparameters window size, overlap, distance function, and the value of k . Table 1 shows the hyperparameters and their search space. To search for the best configurations, we conduct 1000 (out of 5400) trials in Optuna. Each trial represents a different configuration for the hyperparameters. However, due to the characteristics of the sampler used by Optuna (NSGAIISampler) to select the values, it was only possible to obtain 702 different configurations, i.e., 13% of the total number of possible configurations. We split the dataset into training and validation sets to conduct this experiment.

Table 1: Selected Hyperparameters for the 1st exploration.

Hyperparameters	Search Space	# Values
k	[1; 10]	10
distance function	Euclidean, Manhattan, Chebyshev	3
window size	[50; 900] with steps of 50	18
overlap	[0.0; 0.9] with steps of 0.1	10
# Configurations		5400

¹<https://www.automl.org/ixautoml/fanova/>

²<https://www.hardkernel.com/>

Reducing the Number of Training Windows: One important aspect to consider is that the window size and overlap hyperparameters can affect the number of instances obtained from a dataset. To ensure a fair comparison, it matters to establish a consistent number of instances across all possible combinations of window size and overlap. To achieve this, we determine the number of instances based on the pair of window size and overlap that results in the minimum number of instances for the dataset. In our case, we selected a window size of 900 samples with 0% overlap, which yielded a minimum of 1661 instances. Additionally, we ensure that the activity distribution remains consistent with the original dataset. This approach allows for a fair and standardized evaluation of different hyperparameter configurations.

Downsampling the Dataset: Besides the analysed hyperparameter's, we also study the impact of the sampling frequency. For that, we conduct experiments with the following sampling frequencies: 50, 25, 12.5, 5, and 1 Hz. Since the original sampling frequency of the PAMAP2 dataset is 100 Hz, we reduce the sampling frequency of the dataset by downsampling via removing samples until we achieve the intended sampling frequency (e.g., for a frequency of 50 Hz, we remove 1/2 of the samples).

Sampling Frequency: We conduct two experiments to evaluate the effect of the sampling frequency on the accuracy, response time, and energy consumption. In the first experiment, we varied the sampling frequency of the train set and tested it against all considered frequencies. This allowed us to evaluate the effect of sampling frequency on system accuracy. User 9 was excluded from this experiment due to a limited number of samples. For the second experiment, we set the training set frequency at 100 Hz and tested with frequencies of 25 Hz and 1 Hz. We used the 702 configurations obtained from exploration. With this experiment, we intend to study the impact of the sampling frequency in the Pareto-Front and then compare it with the Pareto-Front obtained when the frequency is 100 Hz. When adjusting the sampling frequency of the dataset, we ensure that each sliding window contains the same number of seconds of data regardless of the frequency. This adaptation of the sliding window size is necessary to maintain consistency. However, specific constraints related to window size and overlap arise when dealing with a sampling frequency of 1 Hz. Consequently, only 189 configurations are usable for this particular frequency due to these constraints.

4 RESULTS

This section discusses the results obtained from the experiments and compares the main conclusions with the Related Work.

4.1 Hyperparameters

After analyzing the results of all users, we conclude that the same configurations have different behaviors depending on the User under test, resulting in different Pareto-Fronts for each User. Table 2 summarizes the variation in the accuracy, response time, and energy consumption of the Pareto-Front of each User.

Table 2, shows that the highest accuracy measured in this experiment is 95.35% and for User 7 using the configuration 305 (window size = 900, overlap = 0%, distance = Manhattan, $k=9$). However, this configuration also results in the highest energy consumption

Table 2: Pareto-Front values (PP) for accuracy (Acc), response time (RT), and energy consumption (EC) for all users.

User	Acc (%)	EC (mJ)	RT (ms)	PP
1	[33.05 ; 81.97]	[10.15 ; 121.12]	[5.70 ; 62.92]	57
2	[26.89 ; 95.15]	[9.27 ; 116.58]	[5.11 ; 59.64]	64
3	[20.46 ; 93.95]	[9.16 ; 123.62]	[5.07 ; 61.84]	93
4	[27.85 ; 94.71]	[9.08 ; 99.85]	[4.99 ; 51.40]	77
5	[21.48 ; 91.06]	[9.63 ; 73.22]	[5.29 ; 38.04]	68
6	[27.52 ; 92.80]	[8.92 ; 105.72]	[4.93 ; 53.11]	71
7	[34.26 ; 95.35]	[9.30 ; 130.30]	[5.10 ; 66.97]	51
8	[11.08 ; 86.51]	[8.56 ; 86.55]	[4.64 ; 44.40]	65

(130.30 mJ) and response time (66.97 ms), considering all the Pareto-Front of all users under analysis. On the other hand, for User 1 and configuration 52 (window size = 850, overlap = 0%, distance = Manhattan, $k=10$), the accuracy does not exceed 82%. This User is the one that obtained the lowest maximum accuracy value of all the users studied. Despite User 1 having registered the lowest maximum accuracy, it is the third with the highest energy consumption (121.12 mJ) and the second with the highest response time (62.92 ms). There are Users with higher accuracies than User 1 and lower energy consumption and response times. For example, User 5, with configuration 909 (window size = 900, overlap = 50%, distance = Manhattan, $k=10$), achieved 91.06% accuracy (more 9.09% than User 1) with the lowest energy consumption (73.22 mJ, less 47.90 mJ than User 1) and response time (38.04 ms, less 24.88 ms than User 1). Except for Users 1 and 8, the remaining users achieve a maximum accuracy above 90%. Table 2, shows that each User has different variations in accuracy, response time, energy consumption, and the configurations that belong to the Pareto-Front (answer to RQ 1).

The hyperparameters significantly impact the system's performance. However, there is a significant variation in the values for the hyperparameters. This makes it difficult to conclude which hyperparameters impact the most. To calculate the importance of each of the hyperparameters in the system, we use the fANOVA algorithm [18]. In this experience, we study the hyperparameters' impact on one of the 9 Users. We apply the fANOVA algorithm to the configurations of User 5. Figure 2 shows the importance of the hyperparameters when considering the Pareto-Front configurations.

Figure 2, shows that window size and overlap have the most impact on the system, with the distance function being the hyperparameter with the most negligible impact. The most important factor for accuracy is the overlap. The value of k and window size also has some importance. The importance of the distance function for accuracy is much lower. The window size and overlap are the most important energy consumption and response time hyperparameters. The results show that the window size, overlap, distance function, and k have different levels of impact on the different performance metrics of the model and this should be considered when optimizing the model for a specific task. Depending on the desired performance metric, the relative importance of these hyperparameters may vary. For example, if energy consumption is the most important metric, then optimizing the window size and overlap may

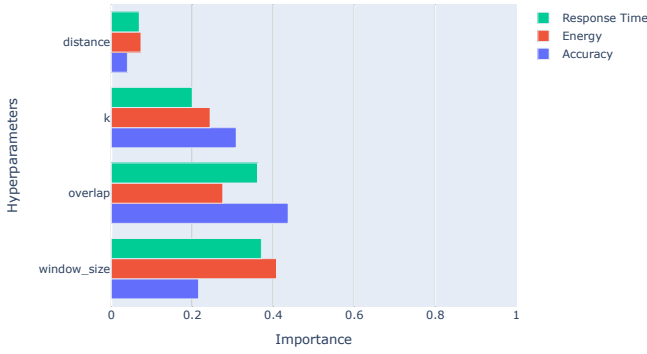


Figure 2: Hyperparameters Importance for the Pareto-front configurations.

lead to the most considerable improvement in energy consumption. In conclusion, the window size and overlap are consistently important for all three performance metrics.

Until now, we were only focusing on the global performance of the model with different configurations, but it is also important to understand the influence of the configurations at an activity level. For that, we calculate the F1-Score of the 12 activities for User 5. To better analyze the impact at an activity level, we consider the scenario where the system’s accuracy must be higher than 75%. Table 3 shows the F1-Score of each activity for each chosen configuration.

As we can see from Table 3, there is a variation in the F1-Score of each activity for different configurations. There are activities where this variation is more significant. The activities running (A8), lying (A5), and cycling (A2) are the ones where the variations are smaller, 3%, 4%, and 6%, respectively. The classification capability of the model for these activities is not significantly affected by the hyperparameters. These activities also have higher values for F1-Score, indicating that the model performs better in recognizing these activities. On the other hand, the activities of sitting (A9), descending stairs (A3), standing (A10), and Nordic walking (A6) are the activities where there is a significant variation in the F1-Score, with variations of 59%, 34%, 21%, and 17%, respectively. The results show that these activities strongly depend on the hyperparameter’s values and the model has a lower performance in recognizing these activities.

For the activity with higher variation in the values of F1-Score, sitting (A9), the minimum F1-Score is 0.3 (configuration 818), and the maximum is 0.89 (configuration 909). Based on the results, the value of the hyperparameters strongly influences the model’s performance for this activity. Analysing Table 3, we can see that the only difference in configurations 537 and 893 is the overlap, with 90% and 70%, respectively. This difference in the overlap allows an improvement of 0.48 in the F1-Score of the algorithm for the activity sitting (A9). These results show that small changes in the hyperparameters can significantly impact at an activity level.

We already concluded that the hyperparameters could impact the model’s overall performance and computational cost of the HAR system. However, these results also show that the hyperparameters can significantly impact the model’s performance at an

activity level. For example, configuration 818 allows a global F1-Score of 0.80, but at an activity level, the performance of the model for activities sitting (A9), standing (A10), and descending stairs (A3) is significantly worse than the remaining activities. On the other hand, some activities are not affected by the variations of the hyperparameter’s values, in the case of activities like running (A8), lying (A5), and cycling (A2). These results also provided important information regarding energy consumption. In a scenario where the user of the system is performing a specific activity for an extended time (for example, A8 - running), the system can change to a configuration (for example, from 909 to 537) that maintains the recognition performance of the model for the activity (F1-Score of 0.96) but requires less energy (73.22 mJ to 22.77 mJ), even though the global performance of the system decreases (0.91 to 0.81). These results reinforced the importance of adaptability in HAR systems because although configuration provides a global high performance for the system, some activities may be negatively affected by the configuration (answer to RQ 2).

4.2 Sampling Frequency

Table 4 summarizes the combinations of the sampling frequency for the train and test sets that allow us to obtain the maximum and minimum accuracy.

The results show that changing the sampling frequencies of the training set and of the test set significantly impacted the model’s accuracy. Overall, all users show a decreased accuracy when the sampling frequency is reduced. However, the decrease in the sampling frequency impacted all users differently. There are users for whom this impact is more significant than others. The biggest drop in the accuracy is shown for User 8, with a decrease in accuracy of about 17%. In this case, the sampling frequency of the training set used to train the model is 1 Hz, and the sampling frequency of the test set is also 1 Hz. There are also other significant drops in the accuracy for Users 3 and 4, where we obtained a decrease of 12.40% and 12.43%, respectively. On the other hand, User 7 reports a slight reduction in accuracy, dropping 4.27%, and User 5 shows a decrease of 5.63% (answer to RQ 3).

The combination of the sampling frequency for the train and test sets that resulted in the lowest accuracy obtained is when both sets have a sampling frequency of 1 Hz (see Table 4). This combination obtains lower accuracy for 50% of the users (Users 1, 3, 4, and 8). Although we report a decrease in the accuracy for all users when changing the sampling frequency, except for Users 1 and 8, all the remaining users obtain minimum accuracy greater than 80%. Regarding Users 1 and 8, the minimum accuracy obtained is 71.48% and 63.38%, respectively. Considering the scenario where the acceptable accuracy for a HAR system is greater than 75%, the sampling frequency of 1 Hz for the train and test sets for Users 1 and 8 are not sufficient to be used in the system.

Although for Users 1 and 7 the highest accuracy achieved is with the model trained and tested with a sampling frequency of 5 Hz, on average, the highest accuracy values are obtained for sampling frequencies greater or equal to 12.5 Hz for the train and test sets. These results are observed for all users. Overall, the accuracy benefits from sampling frequencies greater or equal to 12.5 Hz,

Table 3: F1-Score of each activity for each configuration. (A1 - ascending stairs; A2 - cycling; A3 - descending stairs; A4 - ironing; A5 - lying; A6 - nordic walking; A7 - rope jumping; A8 - running; A9 - sitting; A10 - standing; A11 - vacuum cleaning; A12 - walking; WS - Window Size; Ov - Overlap; EC - Energy Consumption; RT - Response Time)

Config	A1	A2	A3	A4	A5	A6	A7	A8	A9	A10	A11	A12	AVG	WS	Ov	k	EC	RT
818	0.87	0.92	0.69	0.88	0.95	0.86	0.91	0.95	0.30	0.56	0.85	0.89	0.80	500	90	9	22.89	12.99
909	0.90	0.91	0.88	0.89	0.98	0.95	0.97	0.96	0.89	0.76	0.88	0.96	0.91	900	50	10	73.22	38.04
537	0.86	0.92	0.70	0.88	0.95	0.87	0.92	0.96	0.32	0.56	0.84	0.89	0.81	500	90	10	22.77	13.07
893	0.89	0.94	0.81	0.84	0.96	0.96	0.96	0.97	0.80	0.67	0.84	0.93	0.88	500	70	10	33.53	18.02

Table 4: Combinations of sampling frequency for the training and test sets that obtained the maximum and minimum accuracy for each User and respective accuracy (Acc) values.

User	Max (Hz)			Min (Hz)		
	Train	Test	Acc (%)	Train	Test	Acc (%)
1	5	5	80.50	1	1	71.48
2	50	5	93.86	1	5	85.62
	-	-	-	1	25	-
3	100	12.5	-	1	1	80.83
	25	12.5	93.23	-	-	-
	5	12.5	-	-	-	-
4	25	12.5	94.14	1	1	81.71
5	100	50	86.09	5	1	80.46
	25	50	-	-	-	-
6	100	12.5	92.39	25	1	82.67
	50	12.5	-	5	1	-
7	5	5	95.74	12.5	1	91.47
8	25	100	85.22	1	1	68.38

while sampling frequencies equal to or below 5 Hz show significant decreases in accuracy (answer to RQ 5).

Understanding how the sampling frequency affects the algorithm's performance at the activity level is also important. Different sampling frequencies may have other effects depending on the activity. For that, we show the F1-Score for each activity for different sampling frequencies for User 8, because it is the User with whom the sampling frequency has more impact, where there is a variation of 17% between the highest and lower accuracy. Figure 3 shows the effect of the sampling frequency on the activities of PAMAP2 when using the same sampling frequency of the train set (100 Hz) and vary the sampling frequency of the test set for 100 Hz, 12.5 Hz, and 1 Hz.

Figure 3 shows that the sampling frequency of the test set has different effects on the activities of the PAMAP2 dataset. Varying the sampling frequency of the test set does not significantly affect the model's performance for cycling, lying, and vacuum cleaning activities. There is a decreased performance for most activities when the sampling frequency is reduced. This decrease is more significant for Nordic walking, walking, standing, sitting, and ascending stairs. For these activities, the F1-Score decreased with the sampling frequency reduction. The lowest values of the F1-Score are obtained for a sampling frequency of 1 Hz. "Sitting" and "Nordic walking" activities show a more significant decrease in performance when

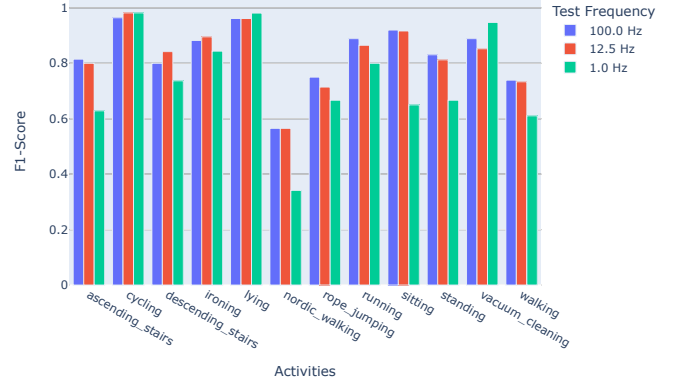


Figure 3: F1-Score per activity for different values of the sampling frequency of the test set, maintaining the sampling frequency of the trained model as 100 Hz (User 8).

the sampling frequency changes from 100 Hz to 1 Hz. However, there is an increase in F1-Score for "vacuum cleaning" when lower sampling frequencies are used for the test set.

Although these results suggest that higher sampling frequencies are generally better for improving the performance of kNN in recognizing different activities, the optimal sampling frequency may depend on the recognized activity. For example, *Nordic walking* is better recognized at 100 Hz than at 1 Hz. The results show that the choice of sampling frequency can significantly impact the performance of the kNN model, as demonstrated by the varying performance across different activities (answer to RQ 3).

We also evaluate the effect of the sampling frequency on the Pareto-Front of User 5. We use a sampling frequency of 100 Hz for the train set and then test them using sampling frequencies of 100 Hz, 25 Hz, and 1 Hz. It is important to note that the window sizes of the configurations are adjusted to the sampling frequency to maintain the same number of seconds. The results of this experiment are presented in Figure 4. We show the Pareto-Front of the original sampling frequency (red line), of the 25 Hz frequency (blue line), and of the 1 Hz frequency (black line). Table 5 presents the lower and upper extreme points of the Pareto-Front for the sampling frequencies of 100 Hz, 25 Hz, and 1 Hz. We also present the variation in response time, energy consumption, and accuracy.

Figure 4 shows that the Pareto-Fronts are different for each of the frequencies under study. The configurations that constitute the Pareto-Fronts are different for each sampling frequency, and

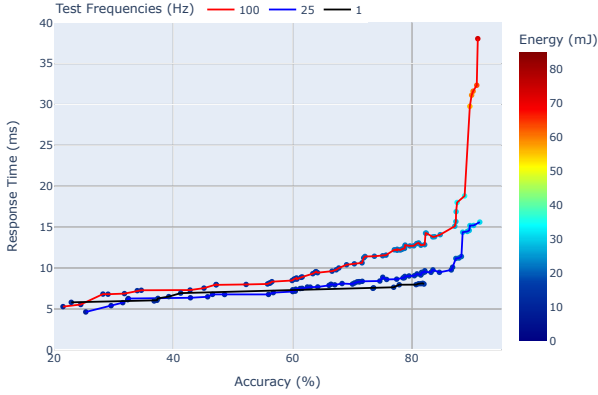


Figure 4: Pareto-frontier of User 5 for different test frequencies (100 Hz, 25 Hz, and 1 Hz).

the number of configurations present in the frontiers is also different. The sampling frequency of 100 Hz has 68 configurations, 25 Hz has 60 configurations, and 1 Hz has only 15 configurations. Focusing only on the sampling frequency of 100 Hz, we observe a significant increase in the energy consumption and response time for accuracies greater or equal to 85%, with a slight increase in the accuracy. However, this behavior is absent for 25 Hz and 1 Hz sampling frequencies. When the sampling frequency is reduced, the energy consumption and response time variation become smaller (see Table 5). The Pareto-Front for the sampling frequency of 1 Hz is where the response time and energy consumption have the lowest variation. For this Pareto-Front, there is a variation of 3.62 mJ in energy consumption and 2.23 ms in response time between the lower and upper extremes of the frontier. At the same time, the accuracy registered an increase of about 59.16%.

Table 5: Variation of the accuracy (Acc), response time (RT), and energy consumption (EC) for the sampling frequencies of 100 Hz, 25 Hz, and 1 Hz. (Freq - Frequency (Hz); LP - Lower Point; UP - Upper Point)

Freq	LP	UP	Acc (%)	EC (mJ)	RT (ms)
100	842	909	[21.48; 91.06]	[9.63; 73.22]	[5.29; 38.40]
25	458	944	[25.30; 91.39]	[8.18; 30.63]	[4.63; 15.62]
1	226	682	[22.87; 82.03]	[11.19; 14.81]	[5.81; 8.04]

Comparing the Pareto-Front for the sampling frequencies of 100 Hz and 25 and focusing only on the configuration that allows us to obtain the maximum accuracy (909 for 100 Hz and 944 for 25 Hz, see Table 5), we can observe a significant reduction in energy consumption and response time. We measured a decrease of 58% in energy consumption and 59% in response time. At the same time, the accuracy does not suffer significant alterations. Considering now the Pareto-Front for the sampling frequencies of 100 Hz and 1 Hz and focusing again only on the configuration that allows us to obtain the maximum accuracy (909 for 100 Hz and 682 for 1

Hz, see Table 5), it is possible to observe a higher reduction on the energy consumption and response time. We observe a decrease of 80% in energy consumption and 79% in response time. However, the sampling frequency of 1 Hz also results in a significant reduction in the accuracy of about 11%. Considering the scenario where we assume that an acceptable accuracy is above 75%, both 25 Hz and 1 Hz sampling frequencies have configurations above the threshold, allowing the use of these frequencies in this hypothetical system (answer to RQ 4).

From this experiment, smaller sampling frequencies significantly reduce the system's energy consumption and response time without losing significant accuracy (keeping the same seconds per window). We note that the results of this experiment and its conclusions are for User 5, we cannot generalize these results to the other Users since each User data has its behavior and characteristics that can have different effects when the sampling frequency is tested.

4.3 Analysis with Respect to Related Work

During this work, we conducted several experiments to evaluate the impact of some parameters (window size, overlap, the value of k , distance function, and sampling frequency) on the performance of a HAR system (accuracy, F1-Score, energy consumption, and response time). As our experimental results and conclusions address the PAMAP2 dataset and the k NN algorithm, we compare them to the findings of the works identified in Section 2. Table 8 resumes the Related Work, to be compared with our study. We analyze each hyperparameter individually to evaluate the impact on the system. To do this, we fixed the values of the remaining hyperparameter and select the configurations where only the hyperparameter under study changes. Table 6 shows the values for the fixed hyperparameters and those used for the hyperparameter under study.

Table 6: Hyperparameter values used to evaluate their individual influence on the HAR system.

	Window Size (WS)	Overlap (%)	$k(k$ NN)
WS	100, 150, 250, 300, 350, 500, 550, 600, 650, 750, 800, 850, 900	250	250
Overlap	50	0, 10, 30, 40, 60, 70, 80, 90	80
k	10	9	1, 2, 3, 5, 6, 9, 10

As we already concluded, each User has its behavior when using the same configurations. To compare our results with the Related Work, we first need to know the influence of each hyperparameter individually for each User. We calculate the Pearson Correlation between the hyperparameters studied and the performance metrics used to evaluate the system. Table 7 shows the values of the correlations between the hyperparameters and performance metrics for each User.

Window size positively correlates with accuracy, energy consumption, and response time. This indicates that these performance

Table 7: Pearson Correlation between each hyperparameter and each performance metric (Acc - Accuracy; EC - Energy Consumption; RT - Response Time).

User	Window Size			Overlap			k (kNN)		
	Acc	EC	RT	ACC	EC	RT	ACC	EC	RT
1	0.5456	0.9994	0.9992	-0.5055	-0.9991	-0.9996	0.9830	0.9407	0.8265
2	0.9454	0.9992	0.9993	-0.9397	-0.9983	-0.9953	0.9238	0.8856	0.9670
3	0.8939	0.9993	0.9987	-0.7819	-0.9997	-0.9998	0.8717	0.8587	0.7764
4	0.9100	0.9993	0.9990	-0.9696	-0.9993	-0.9997	0.9481	0.8184	0.8769
5	0.8618	0.9996	0.9992	-0.7672	-0.9985	-0.9975	0.9777	0.9455	0.9467
6	0.7969	0.9992	0.9992	-0.9457	-0.9993	-0.9987	0.8505	0.8784	0.8743
7	0.3993	0.9992	0.9993	-0.8288	-0.9997	-0.9994	0.6678	0.8965	0.6645
8	0.8437	0.9984	0.9993	-0.2874	-0.9997	-0.9996	0.9932	0.9404	0.8393

metrics increase when the window size also increases. This correlation is stronger for energy consumption and response time. Regarding accuracy, the correlation is stronger for some users. For example, for User 7, the correlation between window size and accuracy is weaker than for the remaining Users. For this specific case, the accuracy increases (from 71% to 89%) until a window size of 500, and after that, it starts decreasing (from 89% to 82%). Overall, larger window sizes, at some extent, lead to higher accuracy.

The overlap increase leads to decreased accuracy, energy consumption, and response time, per inference. However, the increase in the overlap leads to more inferences and globally to an increase in the energy consumption. The negative correlation between overlap and the performance metrics confirms this. Like window size, the correlation is stronger for energy consumption and response time. For all Users, higher overlapping decreases energy consumption and response time. As for accuracy, some users are less affected by the overlap, such as Users 1 and 8. For these Users, the influence of overlap in the accuracy differs significantly from the remaining Users. For example, the highest accuracy is achieved for an overlap of 60%. In contrast, for the remaining users, the maximum accuracy is achieved for an overlap inferior to 50% and superior or equal to 10%. The overlap values between 10% and 50% allow better accuracy. For overlaps higher than 50%, the accuracy starts to decrease significantly.

The value of k is the hyperparameter with a weaker influence on the performance metrics. Changes in the k lead to small accuracy, energy consumption, and response time changes. For most users, these changes are inferior to 5% for accuracy, 2 mJ for energy consumption, and 2 ms for response time. However, overall, higher values of k lead to higher accuracies, energy consumption, and response time.

Mohsen et al. [25] and Liu et al. [22] study the influence of the value of k on a k NN-base HAR system. Mohsen et al. [25] evaluate their studies on the UCI-HAR dataset and conclude that the accuracy increases with the increase of the value of k . The best accuracy is obtained using values of k between 8 and 20. Increasing the value of k above 8 does not yield any significant improvement. On the other hand, Liu et al. [22] evaluate the effect of different values of k , between 3 and 9, on the accuracy using the HAPT [32] and Smartphone [10] dataset. They conclude that increasing the value of k increases the accuracy of the models. However, beyond a k value of 6, the accuracy decreases with the increase of k . Although our results on the effect of the value of k on the HAR system are aligned with the related work, we do not observe significant increases in accuracy. The accuracy increase with the increase of the value of

k , is inferior to 5%. Also, we do not observe a decrease in the accuracy for k values beyond 6, such as Liu et al. [22]. As expected, we also observe an increase in energy consumption and response time when increasing the value of k . However, we cannot compare it with the related work since none of the authors explored the effect of the value of k in these performance metrics.

Another hyperparameter explored in the work presented in the Related Work is overlap. Garcia et al. [13] study the influence of the overlap in accuracy, energy consumption, and execution time for the PAMAP2 dataset. They conclude that the overlap shows more fluctuations in terms of accuracy. The best values are and as in our case, between 10% and 50%. Increasing the overlap factor also increases the energy spent and execution time. Our results are similar to the author's, and larger overlappings lead to higher energy consumption and execution time. However, when considering per inference instead globally, we concluded that higher overlapping leads to decreased energy consumption and response time.

The window size is one of the most studied hyperparameters in HAR research. Banos et al. [5] study the influence of window size, on the REALDISP dataset, between 0.25 s and 7 s. They conclude that windows with a size of 2 seconds achieved the best results and larger window sizes do not always lead to improved performance. Garcia et al. [13] explored window sizes ranging from 100 to 1000 samples on the PAMAP2 dataset, considering accuracy, energy consumption, and execution time. They found that smaller window sizes resulted in lower accuracy, while larger sizes improved accuracy. Additionally, smaller windows consumed less energy and had shorter execution times compared to larger windows. Wang et al. [40] utilized a private dataset and investigated window sizes between 0.5 and 7 seconds. They observed a significant enhancement in classification performance with larger window sizes. However, larger window sizes also introduced increased recognition latency. Niazi et al. [27] evaluated window sizes of 1, 2, 3, 5, and 10 seconds for a private dataset. They found that better results were obtained with larger window sizes. Comparing our findings with these studies, we confirm that larger window sizes generally lead to improved recognition performance, as observed by Garcia et al. [13], Wang et al. [40], and Niazi et al. [27]. Similar to Wang et al. [40] and Garcia et al. [13], we show that larger window sizes result in longer response times and higher energy requirements. However, our results differ from Banos et al. [5], as we found that larger windows can increase the model's accuracy.

Although the sampling frequency is not a hyperparameter, it can significantly influence the system's performance. Niazi et al. [27] use 5, 10, 20, 25, 50, and 100 Hz for sampling frequency. The best results are spread around high sampling rates. Zheng et al. [44] use 1, 5, 10, and 50 Hz sampling frequencies and evaluate their impact on the accuracy and energy consumption. The results show that the accuracy has only improved slightly with the sampling rate increase from 1 to 50 Hz. In terms of energy, there is an increase in energy consumption with increased sampling frequency. Santoyo-Ramón et al. [3] show that the system performance only degrades when the sampling rate is set to 10–15 Hz. The detection ratio improves when the initial rate is reduced to values between 20 and 40 Hz. The conclusions achieved by Santoyo-Ramón et al. [3] is the most similar to ours. Regarding the model's performance, we show no significant difference in sampling frequencies between 12.5 and 100

Hz. However, specifically, for a sampling frequency of 1 Hz, we observe a significant degradation in the model's performance. For the computational cost, smaller sampling frequencies lead to lower energy consumption and response time. Zheng et al. [44] also confirm that higher sampling frequencies translate into higher energy consumption. They also achieve the lowest accuracy for a sampling frequency of 1 Hz. Our conclusions differ from Niazi et al. [27] as they observed better results for higher sampling frequencies (in the case of 50 Hz). However, we verify that for some cases, sampling frequencies of 12.5 Hz achieve better results than the other higher frequencies.

Overall, our result is aligned with most of the work identified in the Related Work, even though different datasets and inference algorithms are being used. Our conclusion is stronger in similarity to the conclusions of Garcia et al. [13] since both use the same dataset and experimental setup. However, there are some exceptions. For example, Niazi et al. [27] show that the best model performance is achieved for a maximum sampling frequency of 50 Hz. Our results show that lower sampling frequencies perform better than bigger ones in some situations. The conclusion for the sampling frequency is more influenced by the datasets used since a large variety of devices were used to collect the data. Most of the studies presented in the Related Work evaluate the influence on the model's performance. Only some exceptions (Garcia et al. [13] and Zheng et al. [44]) have studied the influence on energy consumption and execution time. When targeting the implementation of a HAR system on a device to use in real life, it is essential to consider, in addition to the model's performance, its impact on the device in terms of energy consumption and response time.

5 CONCLUSION

Human activity recognition (HAR) is a research area that has been increasingly addressed due to the widespread of mobile devices such as smartphones. These devices have enough processing power and memory to implement HAR systems. The more sensors embedded in these devices also allow a more accurate HAR system. However, the use of more sensors can increase energy consumption, which decreases the device's battery life.

HAR systems must be able to adapt to the device constraints, the user, and the environment to be more efficient. For example, when the device is running out of battery, the system should be able to adjust its behavior to reduce energy consumption and, in this way, increase the battery life of the device. In addition, people have different walking and motion patterns, and these patterns for the same person may change during a lifetime, caused by aging, diseases, or accidents. Not addressing this problem can result in a loss of accuracy.

One way to change the system's behavior is by changing its hyperparameters. To understand how the hyperparameters can influence the system, in this paper, we studied the impact of a selected set of hyperparameters, namely window size, overlap, the value of k , and distance function, and also sampling frequency, on a k NN-based HAR system in terms of accuracy, response time, and energy consumption, using the PAMAP2 dataset.

Based on the obtained results, we conclude that hyperparameters significantly impact the system's accuracy, response time,

and energy consumption and that the same configurations have different implications for different users. Each user had a different number and configurations belonging to the Pareto-Front, and the range values of the performance metrics were also different. For example, User 1 requires more energy to achieve an accuracy of 82% than most users to achieve an accuracy higher than 90%. In another example, Users 1 and 8 did not achieve an accuracy higher than 82% and 87%, respectively, while all other users achieved an accuracy greater than 90%. These results reinforce the importance of studying the hyperparameters and the necessity of a system adapting to the user.

Overall, window size and overlap were the hyperparameters with a more significant impact on the accuracy, response time, and energy consumption. Windows with more samples require more time and energy to extract the features necessary to train and test the models. Higher overlaps imply more calls to the inference task and globally more energy consumption.

At activity levels, there is a need to consider adaptability. A configuration with high global performance for some activities may not be the most adequate for a specific activity. The results show the importance of considering the activities individually when developing a HAR system instead of considering only the global performance of the model.

The sampling frequency also significantly impacts a HAR system and has different behaviors depending on the User. For example, there are Users much more affected by the reduction of the sampling frequency. Once again, this emphasizes the importance of a self-adaptive system. The sampling frequency also has more impact on some activities. Although lowering the sampling frequency leads to lower energy consumption and response time, it may impact the accuracy of the system.

When implementing a HAR system on a device for use in real-life scenarios, it is important to evaluate both the performance of the model and the impact on the device regarding energy consumption and response time. We conclude that the hyperparameters significantly impact a HAR system and should be studied before implementing the system. These conclusions also motivate continuing this work and the necessity of a self-adaptive HAR system for the user, the device, and the target service.

In future work, we intend to continue studying hyperparameters' impact on a HAR system and consider other ML algorithms and datasets.

REFERENCES

- [1] Takuya Akiba, Shotaro Sano, Toshihiko Yanase, Takeru Ohta, and Masanori Koyama. 2019. Optuna: A Next-Generation Hyperparameter Optimization Framework. In *Proceedings of the 25th ACM SIGKDD International Conference on Knowledge Discovery & Data Mining* (Anchorage, AK, USA) (KDD '19). Association for Computing Machinery, New York, NY, USA, 2623–2631. <https://doi.org/10.1145/3292500.3330701>
- [2] Mohammed A. A. Al-qaness, Abdelghani Dahou, Mohamed Abd Elaziz, and A. M. Helmi. 2023. Multi-ResAtt: Multilevel Residual Network With Attention for Human Activity Recognition Using Wearable Sensors. *IEEE Transactions on Industrial Informatics* 19, 1 (2023), 144–152. <https://doi.org/10.1109/TII.2022.3165875>
- [3] José Antonio Santoyo-Ramón, Eduardo Casilari, and José Manuel Cano-García. 2022. A study of the influence of the sensor sampling frequency on the performance of wearable fall detectors. *Measurement* 193 (2022), 110945. <https://doi.org/10.1016/j.measurement.2022.110945>
- [4] Oresti Baños, Miguel Damas, Héctor Pomares, Ignacio Rojas, Máté Attila Tóth, and Oliver Amft. 2012. A Benchmark Dataset to Evaluate Sensor Displacement in Activity Recognition. In *Proceedings of the 2012 ACM Conference on Ubiquitous Computing* (Pittsburgh, Pennsylvania) (UbiComp '12). Association for Computing Machinery, New York, NY, USA, 1026–1035. <https://doi.org/10.1145/2370216.2370437>
- [5] Oresti Banos, Juan-Manuel Galvez, Miguel Damas, Hector Pomares, and Ignacio Rojas. 2014. Window Size Impact in Human Activity Recognition. *Sensors* 14, 4 (2014), 6474–6499. <https://doi.org/10.3390/s140406474>
- [6] Yunus Celik, Samuel Stuart, Wai Lok Woo, Liam T. Pearson, and Alan Godfrey. 2022. Exploring human activity recognition using feature level fusion of inertial and electromyography data. In *2022 44th Annual International Conference of the IEEE Engineering in Medicine & Biology Society (EMBC)*. IEEE, Glasgow, Scotland, 1766–1769. <https://doi.org/10.1109/EMBC48229.2022.9870909>
- [7] Xin Cheng, Lei Zhang, Yin Tang, Yue Liu, Hao Wu, and Jun He. 2022. Real-Time Human Activity Recognition Using Conditionally Parametrized Convolutions on Mobile and Wearable Devices. *IEEE Sensors Journal* 22, 6 (2022), 5889–5901. <https://doi.org/10.1109/JSEN.2022.3149337>
- [8] Marc Claesen and Bart De Moor. 2015. Hyperparameter Search in Machine Learning. *CoRR* abs/1502.02127 (2015), 5 pages. arXiv:1502.02127 <http://arxiv.org/abs/1502.02127>
- [9] T. Cover and P. Hart. 1967. Nearest neighbor pattern classification. *IEEE Transactions on Information Theory* 13, 1 (1967), 21–27.
- [10] Dheeru Dua and Casey Graff. 2017. UCI Machine Learning Repository. <http://archive.ics.uci.edu/ml>
- [11] Paulo J. S. Ferreira, João M. P. Cardoso, and João Mendes-Moreira. 2020. kNN Prototyping Schemes for Embedded Human Activity Recognition with Online Learning. *Computers* 9, 4 (2020), 20 pages.
- [12] Anonymous for blind review. Jun, 2023. A Study on Hyperparameters Configurations for an efficient Self-Adaptive Human Activity Recognition System. *To be available online*. N/A (Jun, 2023).
- [13] Kemilly D. Garcia, Tiago Carvalho, João Mendes-Moreira, João M. P. Cardoso, and André C. P. L. F. de Carvalho. 2020. A Study on Hyperparameter Configuration for Human Activity Recognition. In *14th International Conference on Soft Computing Models in Industrial and Environmental Applications (SOCO 2019)*, Francisco Martínez Álvarez, Alicia Troncoso Lora, José António Sáez Muñoz, Héctor Quintián, and Emilio Corchado (Eds.). Springer International Publishing, Cham, 47–56.
- [14] Daniel Garcia-Gonzalez, Daniel Rivero, Enrique Fernandez-Blanco, and Miguel R. Luaces. 2020. A Public Domain Dataset for Real-Life Human Activity Recognition Using Smartphone Sensors. *Sensors* 20, 8 (2020), 14 pages. <https://doi.org/10.3390/s20082200>
- [15] Ashish Gupta and Hari Prabhat Gupta. 2021. YogaHelp: Leveraging Motion Sensors for Learning Correct Execution of Yoga With Feedback. *IEEE Transactions on Artificial Intelligence* 2, 4 (2021), 362–371. <https://doi.org/10.1109/tai.2021.3096175>
- [16] Vincent Hernandez, Tomoya Suzuki, and Gentiane Venture. 2020. Convolutional and recurrent neural network for human activity recognition: Application on American sign language. *PLOS ONE* 15 (02 2020), e0228869. <https://doi.org/10.1371/journal.pone.0228869>
- [17] Wenbo Huang, Lei Zhang, Shuoyuan Wang, Hao Wu, and Aiguo Song. 2022. Deep Ensemble Learning for Human Activity Recognition Using Wearable Sensors via Filter Activation. *ACM Trans. Embed. Comput. Syst.* 22, 1, Article 15 (oct 2022), 23 pages. <https://doi.org/10.1145/3551486>
- [18] Frank Hutter, Holger Hoos, and Kevin Leyton-Brown. 2014. An Efficient Approach for Assessing Hyperparameter Importance. In *Proceedings of the 31st International Conference on Machine Learning (Proceedings of Machine Learning Research, Vol. 32)*, Eric P. Xing and Tony Jebara (Eds.). PMLR, Beijing, China, 754–762.
- [19] Ankita Jain and Vivek Kanhangad. 2018. Human Activity Classification in Smartphones Using Accelerometer and Gyroscope Sensors. *IEEE Sensors Journal* 18, 3 (2018), 1169–1177. <https://doi.org/10.1109/JSEN.2017.2782492>
- [20] Sahak Kaghyan and Hakob Sarukhanyan. 2012. Activity recognition using K-nearest neighbor algorithm on smartphone with Tri-axial accelerometer. *International Journal of Informatics Models and Analysis (IJIMA)*, ITHEA International Scientific Society, Bulgaria 1 (2012), 146–156.
- [21] Mustafa Kose, Ozlem Durmaz Incel, and Cem Ersoy. 2012. Online human activity recognition on smart phones. *Workshop on Mobile Sensing: From Smartphones and Wearables to Big Data* 16, 2012 (2012), 11–15.
- [22] Zongying Liu, Shaoxi Li, Jiangling Hao, Jingfeng Hu, and Mingyang Pan. 2021. An Efficient and Fast Model Reduced Kernel KNN for Human Activity Recognition. *Journal of Advanced Transportation* 2021 (06 2021), 1–9. <https://doi.org/10.1155/2021/2026895>
- [23] Gang Luo. 2016. A review of automatic selection methods for machine learning algorithms and hyper-parameter values. *Network Modeling Analysis in Health Informatics and Bioinformatics* 5, 1 (2016), 1–16.
- [24] Saad Mohamad, Moamar Sayed-Mouchaweh, and Abdelhamid Bouchachia. 2020. Online active learning for human activity recognition from sensory data streams. *Neurocomputing* 390 (2020), 341–358. <https://doi.org/10.1016/j.neucom.2019.08.092>
- [25] Saeed Mohsen, Ahmed Elkaseer, and Steffen G. Scholz. 2022. Human Activity Recognition Using K-Nearest Neighbor Machine Learning Algorithm. In *Sustainable Design and Manufacturing*, Steffen G. Scholz, Robert J. Howlett, and Rossi Setchi (Eds.). Springer Singapore, Singapore, 304–313.
- [26] Gael S. Mubiyah and Jalal Almhana. 2022. Improving Human Activity Recognition using ML and Wearable Sensors. In *ICC 2022 - IEEE International Conference on Communications*. IEEE, Seoul, Republic of Korea, 165–170. <https://doi.org/10.1109/ICC45855.2022.9839267>
- [27] Anzah H. Niazi, Delaram Yazdansepar, Jennifer L. Gay, Frederick W. Maier, Lakshminish Ramaswamy, Khaled Rasheed, and Matthew Buman. 2017. Statistical analysis of window sizes and sampling rates in human activity recognition. In *HEALTHINF 2017 - 10th International Conference on Health Informatics, Proceedings; Part of 10th International Joint Conference on Biomedical Engineering Systems and Technologies, BIOSTEC 2017*, Egon L. van den Broek, Ana Fred, Hugo Gamboa, and Mario Vaz (Eds.). SciTePress, Porto, Portugal, 319–325. <https://doi.org/10.5220/0006148503190325>
- [28] P. Paul and T. George. 2015. An effective approach for human activity recognition on smartphone. In *2015 IEEE International Conference on Engineering and Technology (ICETECH)*. IEEE, Coimbatore, India, 1–3.
- [29] Yuxun Qu, Yongqiang Tang, Xuebing Yang, Yanlong Wen, and Wensheng Zhang. 2023. Context-aware mutual learning for semi-supervised human activity recognition using wearable sensors. *Expert Systems with Applications* 219 (2023), 119679. <https://doi.org/10.1016/j.eswa.2023.119679>
- [30] Attila Reiss and Didier Stricker. 2012. Creating and Benchmarking a New Dataset for Physical Activity Monitoring. In *Proceedings of the 5th International Conference on Pervasive Technologies Related to Assistive Environments* (Heraklion, Crete, Greece) (PETRA '12). Association for Computing Machinery, New York, NY, USA, Article 40, 8 pages. <https://doi.org/10.1145/2413097.2413148>
- [31] A. Reiss and D. Stricker. 2012. Introducing a New Benchmarked Dataset for Activity Monitoring. In *2012 16th International Symposium on Wearable Computers*. IEEE, Newcastle, UK, 108–109.
- [32] Jorge-L. Reyes-Ortiz, Luca Oneto, Albert Samà, Xavier Parra, and Davide Anguita. 2016. Transition-Aware Human Activity Recognition Using Smartphones. *Neurocomputing* 171 (2016), 754–767. <https://doi.org/10.1016/j.neucom.2015.07.085>
- [33] Sadiq Sani, Nirmalie Wiratunga, and Stewart Massie. 2017. Learning deep features for kNN-based human activity recognition. In *ICCB, Antonio A. Sanchez-Ruiz and Anders Kofod-Petersen* (Eds.). CEUR Workshop Proceedings, Trondheim, Norway, 95–103.
- [34] Muhammad Shoaib, Stephan Bosch, Ozlem Incel, Hans Scholten, and Paul Havinga. 2015. A Survey of Online Activity Recognition Using Mobile Phones. *Sensors* 15 (01 2015), 2059–2085. <https://doi.org/10.3390/s150102059>
- [35] Pekka Siirtola and Juha Röning. 2012. User-Independent Human Activity Recognition Using a Mobile Phone: Offline Recognition vs. Real-Time on Device Recognition. In *Distributed Computing and Artificial Intelligence*, Sigeru Omatu, Juan F. De Paz Santana, Sara Rodríguez González, Jose M. Molina, Ana M. Bernardos, and Juan M. Corchado Rodríguez (Eds.). Springer Berlin Heidelberg, Berlin, Heidelberg, 617–627.
- [36] Wesllen Sousa Lima, Eduardo Souto, Khalil El-Khatib, Roozbeh Jalali, and João Gama. 2019. Human Activity Recognition Using Inertial Sensors in a Smartphone: An Overview. *Sensors* 19 (07 2019), 3213. <https://doi.org/10.3390/s19143213>
- [37] Xing Su, Hanghang Tong, and Ping Ji. 2014. Activity Recognition with Smartphone Sensors. *Tsinghua Science and Technology* 19 (06 2014), 235–249. <https://doi.org/10.1109/TST.2014.6838194>
- [38] Linh Trinh and Bach Ha. 2022. An Incorporation of Deep Temporal Convolutional Networks with Hidden Markov Models Post-Processing for Sensor-Based Human Activity Recognition. In *Proceedings of the 11th International Symposium on Information and Communication Technology* (Hanoi, Vietnam) (SoICT '22). Association for Computing Machinery, New York, NY, USA, 96–102. <https://doi.org/10.1145/3568562.3568610>

- [39] B. Wang and N. Z. Gong. 2018. Stealing Hyperparameters in Machine Learning. In *2018 IEEE Symposium on Security and Privacy (SP)*. IEEE, San Francisco, CA, USA, 36–52. <https://doi.org/10.1109/SP.2018.00038>
- [40] Gaojing Wang, Qingquan Li, Lei Wang, Wei Wang, Mengqi Wu, and Tao Liu. 2018. Impact of Sliding Window Length in Indoor Human Motion Modes and Pose Pattern Recognition Based on Smartphone Sensors. *Sensors* 18, 6 (2018), 20 pages. <https://doi.org/10.3390/s18061965>
- [41] Yiwei Xia, Jun Ma, ChuYue Yu, XunHuan Ren, Boriskevich Anatoliy Antonovich, and Viktor Yurevich Tsviatkou. 2022. Recognition System Of Human Activities Based On Time-Frequency Features Of Accelerometer Data. In *2022 International Conference on Intelligent Systems and Computer Vision (ISCV)*. IEEE, Fez, Morocco, 1–5. <https://doi.org/10.1109/ISCV54655.2022.9806107>
- [42] Zhe Yang, Mengjie Qu, Yun Pan, and Ruohong Huan. 2022. Comparing Cross-Subject Performance on Human Activities Recognition Using Learning Models. *IEEE Access* 10 (2022), 95179–95196. <https://doi.org/10.1109/ACCESS.2022.3204739>
- [43] Shugang Zhang, Zhiqiang Wei, Jie Nie, Lei Huang, Shuang Wang, and Zhen Li. 2017. A Review on Human Activity Recognition Using Vision-Based Method. *Journal of Healthcare Engineering* 2017 (07 2017), 1–31. <https://doi.org/10.1155/2017/3090343>
- [44] Lingxiang Zheng, Dihong Wu, Xiaoyang Ruan, Shaolin Weng, Ao Peng, Biyu Tang, Hai Lu, Haibin Shi, and Huiru Zheng. 2017. A Novel Energy-Efficient Approach for Human Activity Recognition. *Sensors* 17, 9 (2017), 21 pages. <https://doi.org/10.3390/s17092064>

A APPENDIX

A.1 Comparison with Related Work

Table 8: Detailed information regarding the Related Work.

Study	Hyperparameters	Dataset	Number of Activities	Metrics	Inference Algorithm
Banos et al. [5]	Window Size (s) (0.25 to 7)	REALDISP [4]	33	F1-Score	C4.5, <i>k</i> NN, Naïve Bayes, Nearest Centroid
Garcia et al. [13]	Window Size (samples) (100 to 1000) Overlap (0.0 to 0.9)	PAMAP2 [30, 31]	12	Accuracy, Energy, Execution Time	<i>k</i> NN, VFDT, Naive Bayes, Ensemble
Wang et al. [40]	Window Size (s) (0.5 to 7)	Private	12	F1-Score	SVM, <i>k</i> NN, Decision Tree, Naïve Bayes, Adaboost
Mohsen et al. [25]	<i>k</i> (1 to 20)	UCI-HAR [14]	6	Accuracy	<i>k</i> NN
Liu et al. [22]	<i>k</i> (3 to 9)	HAPT [32] Smartphone [10]	9 6	Accuracy	<i>k</i> NN
Ramón et al. [3]	Sampling Frequency (Hz) (18 to 238)	15 HAR Datasets	6 to 44	Mean geometric of sensitivity and specificity	CNN
Niazi et al. [27]	Sampling Frequency (Hz) (5, 10, 20, 25, 50, 100) Window Size (s) (1, 2, 3, 5, 10)	Private	23	Average expected value	Random Forest
Zheng et al. [44]	Sampling Frequency (Hz) (1, 5, 10, 50)	Private	6	Accuracy Energy	SVM
This Work	Sampling Frequency (Hz) (1, 5, 12.5, 25, 50, 100) Window Size (samples) (50 to 900) Overlap (0 to 0.9) <i>k</i> (1 to 10) Distance (E, M, C)	PAMAP2 [30, 31]	12	Accuracy, F1-Score, Energy, Inference Time	<i>k</i> NN

A.2 Extended Version

An Experimental Study on Hyperparameters Configurations Bearing in Mind Self-Adaptivity Human Activity Recognition Systems

Paulo J.S. Ferreira^[0000-0001-6553-4220], João
Mendes-Moreira^[0000-0002-2471-2833], and João M.P.
Cardoso^[0000-0002-7353-1799]

INESC TEC, Faculty of Engineering, University of Porto, R. Dr. Roberto Frias s/n,
4200-465 Porto, Portugal
{up201305617,jmoreira,jmpc}@fe.up.pt

Abstract. Human Activity Recognition (HAR) has been a popular research field due to the widespread of devices with sensors and computational power (e.g., smartphones and smartwatches). HAR is a task for inferring human physical activities from sensor data. Applications for HAR systems have been extensively researched in recent literature, mainly due to the benefits of improving quality of life in areas like health and fitness monitoring. However, since persons have different motion patterns when performing physical activities, a HAR system needs to be adapted to the characteristics of a person in order to maintain or improve accuracy. Additionally, mobile devices, such as smartphones, are used to implement HAR systems, it is also necessary to manage their limited resources (for example, battery life) and adapt to the device's constraints to work efficiently for long periods. In this work, we present a k NN-based HAR system and an extensive study of the influence of hyperparameters (window size, overlap, distance function, and the value of k) and parameters (sampling frequency) on the system accuracy, energy consumption, and response time. We also investigate how hyperparameter configurations affect the model's performance for the users and the activities. Experimental results show that adjusting the system's behavior to the user, the device, and the target service is possible by adjusting the hyperparameters and parameters. These results motivate the development of a HAR system capable of automatically adapting the hyperparameters for the user, the device, and the service.

Keywords: human activity recognition · HAR · k NN · energy consumption · adaptability · smartphones · hyperparameters · PAMAP2 · Pareto-front · sampling frequency

1 Introduction

Recently, Human Activity Recognition (HAR) [1–5] has been a popular research field due to the wide spread of devices with sensors (e.g., smartphones and

smartwatches). HAR aims at recognizing the activities performed by humans at runtime through the analyses of sensing data and other observations acquired by in situ devices [6]. HAR has enabled novel applications in different areas, such as health and fitness monitoring, security, smart cities and entertainment [7–9].

Figure 1 shows the main stages of the two views of a HAR system: the offline training view (Preparation Phase), and the online classification view (with the possibility of incremental/online learning) (Use Phase).

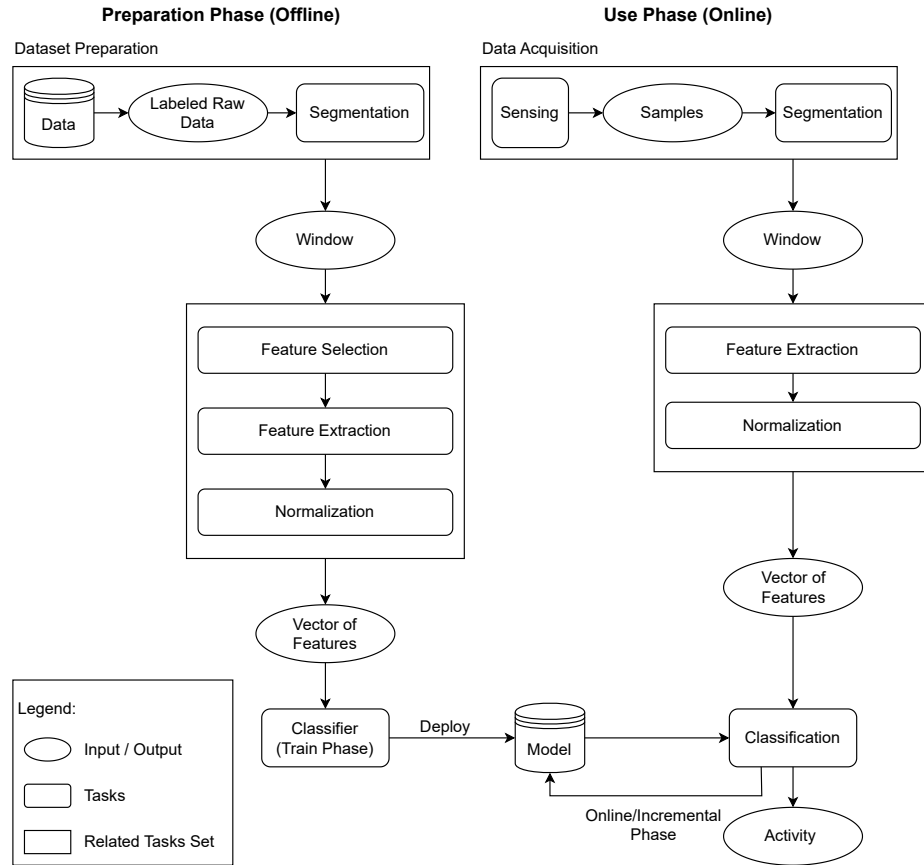


Fig. 1. Block diagram of the HAR system considered.

The Preparation Phase is used to train the model to be later used in the classification process. This Phase includes the following steps: data acquisition, pre-processing, and training [7]. At this Phase, after data acquisition, data is labeled and stored in files to create the dataset used in the system.

In the Use Phase, the trained classifiers infer activities. This step can be done online on a mobile device. This Phase includes the following stages: data acquisition, pre-processing, and classification [7]. This Phase can also contain the Incremental Learning step. In this case, data are not stored in files during data acquisition online. Instead, it goes directly to the segmentation. Furthermore, in this Phase, the pre-processing stage includes feature extraction and normalization. Usually, the feature selection is not carried out at this stage since it has already been carried out in the pre-processing step of the Preparation Phase.

Smartphones have been increasingly used to develop HAR systems, due to the capability and diversity of the sensors embedded in these devices [9]. Most modern smartphones include sensors, such as a microphone, camera, accelerometer, gyroscope, and GPS. The advantage of smartphones over other wearable devices is associated with (a) their widespread use, (b) their ability to collect and process sensor data [9], (c) the increase in their processing power, and (d) the increase in their battery capacity [7], (e) their use by most people. Although smartphones have seen rapid development in recent years, these devices continue to have limitations concerning battery life and available memory.

In order to be able to recognize different activities accurately, a HAR system uses Machine Learning (ML) algorithms capable of inferring activities from the sensor data. One of the most used Machine Learning algorithms in HAR is k -Nearest Neighbours (k NN) [10]. k NN is a simple yet effective Machine Learning algorithm widely applied. k NN is an instance-based algorithm, i.e., instead of performing generalization, it compares instances to be classified with instances seen in training, which have been stored in memory. Because classification is delayed until a new instance is observed, these algorithms are sometimes called "lazy learners". This fact facilitates the implementation of incremental/online learning HAR systems in mobile devices since k NN does not require a computationally expensive task, the training stage. Besides, k NN has also been proved to obtain very high accuracy in the HAR field (see, e.g., [11–18, 1]). The use of k NN facilitates the implementation of online/incremental learning approaches since it is only necessary to add, remove or update the instances in the k NN memory. Updating the k NN is faster and requires less energy because there is no need to retrain the algorithm, which is essential in devices with energy limitations [1].

Typically, an ML algorithm has two types of parameters: model parameters and hyperparameters [19]. Model Parameters consist of configurable variables used inside the model. Their values are estimated or learned from the data as a part of the learning process. Some examples of model parameters are weights in an artificial neural network, support vectors in support vector machines, and coefficients in regression. On the other side, hyperparameters are external parameters that are not part of the model and thus can not be predicted from the data set but can be configured by subject matter experts or by trial and error until an acceptable accuracy is achieved. Hyperparameters are used to control the learning process and can have wildly varying effects on the resulting model and on its performance [20]. For the same training dataset, with different hyperparameters, a Machine Learning algorithm might learn models that have

significantly different performances on the testing dataset [21]. Some examples of hyperparameters are learning rate, optimizer, number of hidden layers and size of each layer for Neural Networks, the value of k for k NN, window size, and overlap.

The optimal performance of a HAR system depends on several hyperparameters. In this paper, we study the impact of a selected set of hyperparameters, namely window size, overlap, the value of k , distance function, and sampling frequency, on a k NN-based HAR system in terms of accuracy, response time, and energy consumption. While most studies focus on the impact of hyperparameters on the accuracy of HAR systems, there is limited research exploring their impact on other critical performance metrics, such as response time and energy consumption. In real-world applications, a HAR system's response time and energy consumption are critical factors that determine its practicality and usability. Response time is crucial, especially for time-sensitive applications where the system must recognize real-time activities. Similarly, energy consumption is essential for mobile and wearable applications, where devices have limited battery life.

Moreover, HAR systems need to be adaptable to changing conditions, such as different users or environments. To achieve adaptability, it is essential to study the hyperparameter's impact on a HAR system's performance under different scenarios. For instance, a HAR system optimized for one user may not perform well for another user due to differences in their physical characteristics or activity patterns. Similarly, a HAR system designed for indoor environments may not perform well in outdoor environments due to changes in lighting, temperature, and other factors.

Therefore, in this study, we aim to investigate the impact of hyperparameters on the performance of a HAR system in terms of accuracy, response time, and energy consumption. Specifically, we explore the effect of different hyperparameter configurations on the performance of a HAR system using the PAMAP2 [22, 23] dataset. PAMAP2 is one of the most widely used wearable sensor-based datasets in HAR research and also has been widely used to test and implement new approaches for HAR systems [1, 24, 17, 25–29]. This dataset has data from different sensors, body placements, and users. Including data from 9 different users allows us to study different users and acquire the importance of a self-adaptive HAR system to the user. Our study aims to address the need to explore the impact of hyperparameters on the adaptability of HAR systems, going beyond the traditional focus on accuracy. The results of this study provide valuable insights into the optimal hyperparameter configurations for HAR systems, enabling the design of more efficient, effective, and adaptable systems for real-world applications.

Specifically, in this study, we answer the following Research Questions:

- RQ 1 - How do hyperparameter configurations affect the accuracy, response time, and energy consumption of a HAR system globally and across different users?

- RQ 2 - What are the overall, and specific activities, the impact of window size, overlap, distance function, and k for a k NN-based HAR system regarding its accuracy, response time, and energy consumption?
- RQ 3 - How do the sampling frequencies influence the accuracy of a HAR system for different users and activities?
- RQ 4 - How does reducing the sampling frequency change the trade-off between accuracy and energy consumption for different hyperparameter configurations of a HAR system for a specific user?
- RQ 5 - How does the mismatch between the sampling frequencies of the train and test sets affect the accuracy of a HAR system?
- RQ 6 - How much energy can be saved by using Pareto-optimal hyperparameter configurations for a HAR system that meets the minimum accuracy required for a specific Quality of Service (QoS) level?

The remainder of this paper is organized as follows. Section 2 describes the related work regarding the study of the selected hyperparameters. Section 3 describes the experimental setup used to conduct this study, including the datasets and algorithms used, the platforms where the experiments were conducted, and the evaluation strategy and metrics. In Section 4, we describe all the experiments conducted. Section 5 presents and discusses the experimental results, including a comparison with the Related Work. Finally, in Section 6, we present the main conclusions for this study and the future work we intend to do.

2 Related Work

Human activity recognition (HAR) is a rapidly evolving field of research that addresses techniques for automatically identifying and classifying human activities based on sensor data. Most HAR systems use Machine Learning algorithms to classify the sensor data. One critical aspect of developing accurate HAR models is selecting the optimal hyperparameters. As hyperparameters can significantly affect the performance of the HAR model, selecting them is essential. In this context, exploring hyperparameters in HAR involves evaluating the impact of various hyperparameter configurations on the performance of the HAR model. This exploration process can involve various techniques, such as grid search [30], random search [31], population-based search [32], and Bayesian optimization [33], to determine the optimal selection of hyperparameters that maximizes the HAR model's performance.

Since hyperparameters can significantly impact the performance of the algorithms in terms of predictive capability and computational cost, many authors are studying their impact on HAR systems. The most explored hyperparameters in traditional ML algorithms are window size and overlap. Window size and overlap are hyperparameters that are used in the segmentation of the data for both Preparation and User Phases (see Figure 1). They can significantly impact the model's performance and the system's computational cost and also they are common to all approaches that use traditional ML algorithms.

The following are examples of HAR studies that explored some hyperparameters.

Banos et al. [34], using the REALDISP [35] dataset, evaluate the impact of the window size for the algorithms C4.5, k NN, Naïve Bayes, and Nearest Centroid Classifier. The dataset has data for 33 different activities and was collected at 50 Hz. To measure the performance of the algorithms with different window sizes, the authors use the F1-Score. They use windows sizes between 0.25 s and 7 s. Overall, they show that the windows with 2 s achieve the best results. They also concluded that larger window sizes not always translated into better performances for the models.

Garcia et al. [36] explore the impact of window size (from 100 to 1000 samples with increments of 100) and the overlapping between windows (from 0.0 to 0.9 with increments of 0.1). The authors used the PAMAP2 [22, 23] HAR dataset to train and test an ensemble classifier composed of three individual classifiers: k NN, VFDT, and Naive Bayes. This dataset has data for 12 different activities and was collected at 100 Hz. They evaluate the impact of the hyperparameters in terms of accuracy, energy consumption, and execution time. They use the ODROID-XU+E6 board to measure energy consumption. They concluded that smaller window sizes present less accuracy, while larger ones provide a more accurate model. The overlap showed more fluctuations in terms of accuracy with the best factors concentrated between 0.1 and 0.5. In terms of energy and execution time, smaller windows consume less energy and take less time than bigger windows because of the increased effort to calculate features for larger window sizes. Also, increasing the overlap factor increases the energy due to the increased number of feature calculations and classifications to be carried out. Relating the energy consumption to accuracy, it is observable that best accuracies are associated with higher energy consumption.

Wang et al. [37] also studied the impact of different window sizes. The authors use a private dataset for the experiments in the paper. The dataset has data for the following activities: still, walking, up/down stairs, up/down an elevator, up/down escalator, typing, swinging, phoning, and trouser pocket. The data were collected at 50 Hz. They varied the window size between 0.5 s and 7 s. To evaluate the performance of the algorithms SVM, k NN, Decision Tree, Naïve Bayes, and Adaboost, they present the F1-Score. The results show that a notable improvement in classification performance using an increased window size occurs across all adopted methods. However, considerable window size leads to significant recognition latency. The authors conclude that a window size between 2.5–3.5 s provides the best tradeoff between performance and latency.

Although the window size and overlap are among the hyperparameters mostly studied, these hyperparameters control data segmentation before being used to train or use the traditional ML algorithms. They are not specific to any ML algorithm. However, even traditional ML algorithms have specific hyperparameters. Decision Trees have the max depth, split criteria, and minimum samples split, among others. k NN has the number of neighbors, distance function, and the maximum number of instances the algorithm can keep. The Support Vector

Machines (SVM) have, for example, the value of C , kernel, degree, and decision function shape. These hyperparameters are defined in the Preparation Phase, more precisely in the training stage of the ML algorithm (see Figure 1). Some authors are also focusing on studying the algorithm’s specific hyperparameters.

Although not in the context of HAR, Hu et al. [38] study the impact of the distance function on the performance of a k NN algorithm. They study the distances: Euclidian, Manhattan, Cosine, and Chi-square. The performance of the distance functions is evaluated on three different types of datasets: numerical, categorical, and mixed (categorical and numerical). They contain 10, 17, and 10 datasets, respectively. Moreover, each dataset type has different numbers of attributes, samples, and classes. In their studies, they conclude that Chi-square distance is the best among the three different types of datasets. On the other hand, the Euclidean distance performs reasonably well over the categorical and numerical datasets but not for the mixed type of datasets.

Mohsen et al. [39] present a k NN-based HAR system using the UCI-HAR dataset [40]. The authors studied the impact of the value of k on the model’s accuracy. They vary the value of k between 1 and 20. The results show that the accuracy increases with the increase of the value of k . The best accuracy is obtained using values of k between 8 and 20. However, for k values greater than 8, there is no significant improvement in the accuracy. In this paper, the authors do not study the impact of the value of k in the inference time. Liu et al. [41] also evaluated the impact of different values of k in the HAR datasets Smartphone-Based Recognition of Human Activities and Postural Transitions Data Set (HAPT) [42], and Smartphone Dataset for Human Activity Recognition in Ambient Assisted Living Data (Smartphone) [43]. They study k values 3 and 9 in terms of accuracy. The results show that increasing the value of k increases the accuracy of the models. However, for k values greater than 6, the accuracy decrease. For both datasets, the best value of k , i.e., the one that allows a higher accuracy, is 6.

Sampling frequency, although not considered a hyperparameter, plays a crucial role in the performance of a Human Activity Recognition (HAR) system. It directly affects inference time, energy consumption, and the performance of machine learning algorithms. Higher sampling frequencies, meaning more samples per second, generally increase energy consumption. Several studies have investigated the impact of sampling frequency on HAR systems.

Santoyo-Ramón et al. [44] study the influence of the sampling frequency in 15 HAR datasets. The datasets have sampling frequencies between 18 Hz and 238 Hz. They use the following metrics: sensitivity, specificity, and geometric mean as single descriptors of the global system performance. They use a convolutional neural network (CNN) as inference algorithm. The results show that the system performance only degrades when the sampling rate of the dataset is between 10 and 15 Hz. The inference improves when the sampling frequency of the dataset is between 20 and 40 Hz.

Niazi et al. [45] study the sampling frequency and window duration. For the study, the authors collected a dataset using 77 volunteers for 23 different ac-

tivities using acceleration data from an activity monitor positioned along the anterior axillary line of the non-dominant hip. The original data were collected at a sampling frequency of 100 Hz. To obtain versions with lower frequencies, the authors downsampled the original data. They use 1s, 2s, 3s, 5s, and 10s for the window size and 5 Hz, 10 Hz, 20 Hz, 25 Hz, 50 Hz, and 100 Hz for sampling frequency. They use Random Forest as the ML algorithm. They use two-way factorial ANOVA with weighted least squares to calculate the expected average value (EV) for every combination of window duration and sampling frequency. The results suggest that 10s/50Hz is the optimal combination of window duration/sampling frequency, especially if the study subjects are young, able-bodied, and physically active. Most highly significant EVs are spread around high sampling rates and window sizes, although there is enough evidence to suggest no significant loss in accuracy if the sampling rate is decreased to 20Hz.

Zheng et al. [46] evaluated the impact of the sampling frequency on accuracy and energy consumption. They use a dataset at 1 HZ, 5Hz, 10 Hz and 50 Hz sampling frequencies. The data consist of the following activities: Sitting, Standing, Walking, Running, Upstairs, and Downstairs. As an inference algorithm, the authors use a version of an SVM. The results show that the accuracy has only improved slightly with the sampling rate increase from 1 Hz to 50 Hz. In terms of energy consumption, there is an increase with increased sampling frequency. It is more significant when the sampling rate changes from 10 Hz to 50 Hz.

3 Experimental Setup

This section presents all the experimental setups used in this study. It includes the dataset and algorithm used in the experiments, the evaluation metrics, the evaluation procedure, the processing of the raw data (feature extraction and normalization), and the running platforms where the experiments were carried out.

3.1 Dataset

The *PAMAP2* [22, 23] HAR dataset contains 1,926,896 samples of raw sensor data from 9 different users and 12 different activities. Data were collected from 3 Inertial Measurement Units (IMU) positioned in different body areas (wrist, chest and ankle), at a sampling frequency of 100 Hz, and a Heart-Rate Monitor at a sampling frequency of 9 Hz. Each IMU has 4 embedded sensors: a 3-axis accelerometer, a 3-axis gyroscope, a 3-axis magnetometer, and a thermometer. The activities are organized as basic activities (walking, running, nordic walking and cycling); posture activities (lying, sitting and standing); everyday activities (ascending and descending stairs); household (ironing and vacuum cleaning) and fitness activities (rope jumping).

Figure 2 shows the distribution of samples per activity. Some activities have fewer samples than others. Activity "Rope Jumping" is the activity with the least number of samples followed by the activities "Running," "Descending Stairs,"

and "Ascending Stairs." The other activities present on the dataset have a similar number of samples.

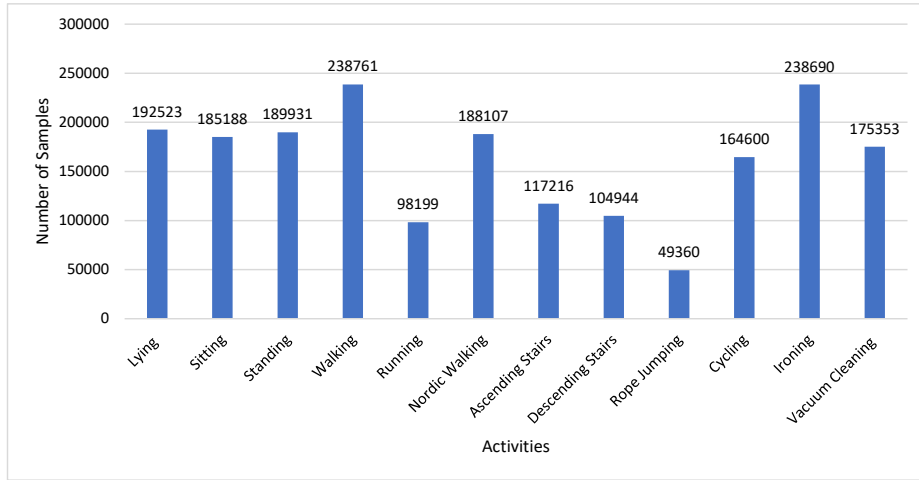


Fig. 2. Distribution of samples per activity in PAMAP2 [22, 23].

After analyzing this dataset, we decided to use only the available motion sensors (accelerometer, gyroscope, and magnetometer), discarding the data from the thermometers. We also did not use the data from the Heart-Rate Monitor because there is a big difference in terms of sampling frequency between the Heart-Rate Monitor and the IMUs. Besides that, the data from the Heart-Rate Monitor were mostly invalid data due to communication problems during data collection.

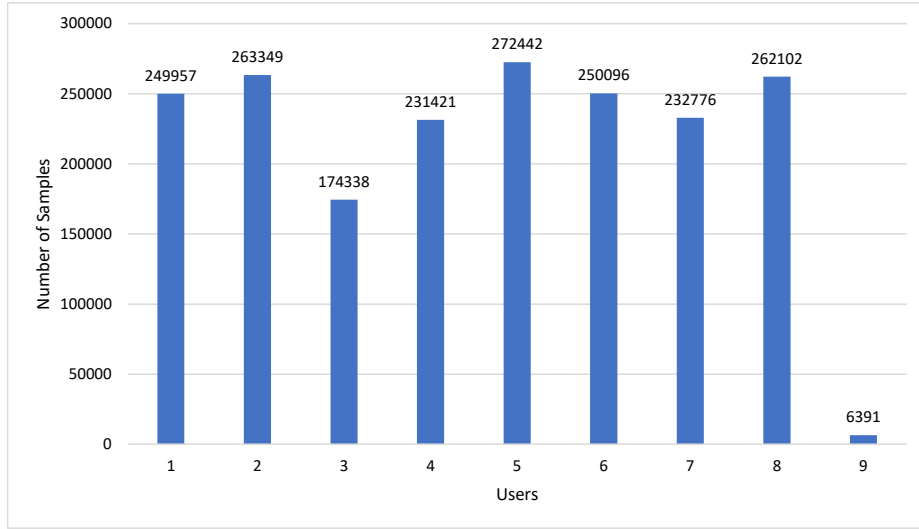


Fig. 3. Distribution of samples per User in PAMAP2 [22, 23].

3.2 Evaluation Metrics

To measure the performance of the models obtained using the explored hyper-parameters, we use the following ML metrics: accuracy, recall, precision, and F1-Score. Table I describes these metrics and shows the respective equations.

Table I. Accuracy, recall, precision and F-measure metrics. TP means true positives, TN true negatives, FP false positives and FN means false negatives.

Metric	Equation	Description
Accuracy	$\frac{TP+TN}{TP+TN+FN+FP}$	Ratio of correct predictions divided by the total predictions.
Precision	$\frac{TP}{TP+FP}$	Ratio of true positives and total positives predicted.
Recall	$\frac{TP}{TP+FN}$	Ratio of true positives to all the positives in ground truth.
F1-Score	$2 \times \frac{Precision \times Recall}{Precision + Recall}$	Harmonic mean of Precision and Recall.

We also measure the impact of different configurations (see Section 4.1) on the system regarding response time (equals inference time, in our experiments) and energy consumption. Both response times and energy consumption refer to the time and energy needed for each inference. The values for time and energy include the following phases: reading data from the files, feature extraction, and inference.

Finally, we use the fANOVA (functional ANOVA) [47] algorithm to assess the importance of the selected hyperparameters. fANOVA¹ is a tool for assessing the importance of an algorithm’s hyperparameters. It takes as input performance data gathered with different hyperparameters. It fits a random forest to capture the relationship between hyperparameters (e.g., window size, overlap, distance function, and value of k) and performance (accuracy, response time, and energy consumption). It then applies functional ANOVA to assess each hyperparameter’s importance to performance.

3.3 Evaluation Procedure

When performing a supervised machine learning experiment, it is necessary to split the data into train and test sets (used for evaluating the performance of the algorithm [48]). Splitting data into training and test sets can be done using various methods, such as hold-out, k -fold cross-validation (k -CV), leave-one-out cross-validation (LOOCV) and leave-one-subject-out (LOSO).

Since the dataset used in this paper has the data split by Users, we used this fact to apply the leave-one-subject-out cross-validation approach to our experiments. With this approach, one user is used to test the resulting model, and the remaining users are used to train the model. Moreover, this approach allows us to study the impact of the same set of hyperparameters for different models and demonstrate the importance of a model capable of adapting to the user.

3.4 Feature Extraction

In this study, features are extracted from fixed-size sliding windows of raw data. We extracted 10 features for each 3D sensor: x-axis Mean, y-axis Mean, z-axis Mean, Mean of the sum of the x, y, and z axes, x-axis Standard Deviation, y-axis Standard Deviation, z-axis Standard Deviation, x and y axes Correlation, x and z axes Correlation, and y and z axes Correlation. The features are extracted from 9 sensors (3 sensors (accelerometer, gyroscope and magnetometer) for each body placement (wrist, chest and ankle)). This results in a total of 90 features. The 90 features result in vectors of 90 features that are the input to the ML algorithm. The features are normalized using the Linear Scaling technique (See Equation 1).

$$x' = (x - x_{min}) / (x_{max} - x_{min}) \quad (1)$$

3.5 Algorithm

k -Nearest Neighbour (k NN) [10] is an instance-based classifier based on the majority voting of its k neighbours [8] for classifying an instance. k NN uses the class information of those instances most similar to the new instance. The value

¹ <https://www.automl.org/ixautoml/fanova/>

of k defines how many nearest neighbor instances contribute to the classification of each instance. Figure 4 exemplifies the classification process for an instance.

k NN does not use any model to fit and it is only based on memory. k NN is a lazy learning algorithm because it does not have a learning phase; instead, it "memorizes" the training dataset. A lazy learner stores the training data, and only when it sees a test instance starts an instance-based approach to classify the test instance based on its nearest stored training instances (i.e., the k nearest neighbors). The more the number of training instances stored in the k NN's memory, the greater the number of distances to be calculated and, consequently, the longer the execution time of the test phase. Usually, Euclidean distance is used as the distance metric [13].

An important factor to take into account when using k NN is the value of k . The best choice of k depends upon the data; generally, larger values of k reduce the effect of noise on the classification but create boundaries between less distinct classes. So, a very large value may include neighbors that are very different from the instance to be classified.

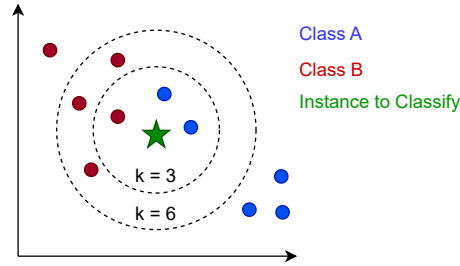


Fig. 4. How the value of k can affect the classification of an instance. In this example, the star represents the instance to classify. With a $k = 3$, 2 instances of class B and 1 of class A are the nearest neighbors. If $k = 3$, the instance is classified as class B. With $k = 6$, the instance is classified as class A.

The k NN version we use is based on the implementation of MOA [49] Java library. This specific implementation has three different hyperparameters that we can optimize: the value of k , the distance function used, and the maximum number of instances that k NN can store.

3.6 Running Platforms

We ran the experiments on two platforms: a desktop computer and a board with ARM CPUs. The desktop computer was used to run the exploration experiments. The application was written in Java code and executed with version 1.8 of the Java Runtime Environment (JRE).

The experiments related to the HAR system run on an embedded Odroid computing board. They were used to measure energy consumption and response time. It represents a possible mobile/embedded device. We use an ODROID-XU+E6² equipped with an Exynos5 Octa CPU (used in several Samsung smartphones) with four big cores (ARM Cortex-A15 up to 1.6 GHz) and four small cores (ARM Cortex-A7 up to 1.2 GHz). ODROID-XU+E6 has four current/voltage sensors to measure the power consumption of the Big A15 cores, Little A7 cores, GPU and DRAM individually. In our experiments, we only consider the energy consumption for the A15 cores, A7 cores, and DRAM, as we are not using the GPU.

4 Experiment Description

This section describes all the experiments carried out in our study and some procedures we used to prepare the data for the experiments.

4.1 Configurations Search

The goal of the first experiment was to explore the configuration space and find the best configurations, i.e., a set of values for the hyperparameters that result in acceptable accuracy and response time. We use multi-objective search in Optuna [50] to select the configurations that optimize two different objectives: accuracy and response time. We intend to maximize the accuracy and minimize the response time.

In this first exploration of hyperparameters, we only focus on a subset of the available hyperparameters. We select the hyperparameters window size, overlap, distance function and the value of k . Table II shows the hyperparameters and their search space.

Table II. Selected Hyperparameters for the 1st exploration.

Hyperparameters	Search Space	# Values
k	[1; 10]	10
distance function	Euclidean, Manhattan and Chebyshev	3
window size	[50; 900] with steps of 50	18
overlap	[0.0; 0.9] with steps of 0.1	10
# Configurations		5400

To search for the best configurations, we conduct 1000 (out of 5400) trials in Optuna. Each trial represents a different configuration for the hyperparameters. However, due to the characteristics of the sampler used by Optuna (NS-GAIIISampler) to select the values, it was only possible to obtain 702 different configurations, i.e., 13% of the total number of possible configurations. We split the dataset into training and validation sets to conduct this experiment.

² <https://www.hardkernel.com/>

4.2 Energy Consumption

In this experience, we ran the obtained configurations on Odroid to measure the response time and energy consumption for each configuration. The energy measured refers to the energy consumption per inference/instance. For these experiments, we use a leave-one-subject-out approach for creating the train and test sets. For example, when the test user is User 1, the users used for training were Users 2, 3, 4, 5, 6, 7, 8, and 9.

4.3 Reducing the Number of Training Windows

Two of the selected hyperparameters can change the number of instances we can obtain from a dataset, namely the window size and the overlap between consecutive windows. Since window size and overlap are two hyperparameters whose values will vary during the tuning phase, we would obtain different numbers of instances with each new configuration. Because of that, it is essential to establish the same number of instances for all the possible combinations between window size and overlap, to allow a fair comparison. We define the number of instances for all configurations based on the pair of window size and overlap that allows us to obtain the minimum number of instances for a dataset. In this case, we used a window size of 900 samples and 0% overlap. With this combination of values, the minimum number of instances was set to 1661. We also guarantee the same activity distribution as the original dataset.

4.4 Downsampling the Dataset

Besides analyzing the hyperparameter’s window size, overlap, distance function, and the value of k , we also intended to study the impact of the sampling frequency. For that, we conducted experiments with different sampling frequencies. We decide to experiment with the following sampling frequencies: 50 Hz, 25 Hz, 12.5 Hz, 5 Hz, and 1 Hz. Since the original sampling frequency of the PAMAP2 dataset is 100 Hz, to reduce the sampling frequency of the dataset by down-sampling via removing samples, for a frequency of 50 Hz, we remove 1/2 of the samples. For a frequency of 25 Hz, we remove 3/4 of the samples. For a frequency of 12.5 Hz, we remove 7/8 of the samples. For a frequency of 5 Hz, we remove 19/20 of the samples. Finally, for a frequency of 1 Hz, we remove 99/100 of the samples.

4.5 Sampling Frequency

We conduct two experiments to evaluate the effect of the sampling frequency on the accuracy, response time, and energy consumption. In the first experiment, we variate the frequency of the train and test set. For that, we change the sampling frequency of the train set for one of the considered frequencies, then tested it against all sampling frequencies. We repeated this experiment until we had experimented with all the considered sampling frequencies for the training

set (see Table III). In this experiment, we intend to evaluate the sampling frequency’s impact on the system’s accuracy. We tested on all Users except User 9. We decide to exclude User 9 from this experiment since this User has a small number of samples (see Figure 3), and those samples refer to just one activity. It would not be possible to conduct the same experiments on this User.

Table III. Variation of the sampling frequency for the train and test sets.

Train Set Frequency (Hz)	Test Set Frequency (Hz)
100	100, 50, 25, 12.5, 5, 1
50	100, 50, 25, 12.5, 5, 1
25	100, 50, 25, 12.5, 5, 1
12.5	100, 50, 25, 12.5, 5, 1
5	100, 50, 25, 12.5, 5, 1
1	100, 50, 25, 12.5, 5, 1

For the second experiment, we set the sampling frequency of the training set as 100 Hz (the dataset’s original frequency) and the test set’s frequency as 25 Hz and 1 Hz. Then we used the 702 configurations obtained from Optuna and tested first for 25 Hz and then for 1 Hz. With this experiment, we intend to study the impact of the sampling frequency in the Pareto-front and then compare it with the Pareto-front obtained when the test set’s frequency is 100 Hz. In this experiment, we intend to evaluate the sampling frequency’s impact on the system’s accuracy, response time, and energy consumption. For this experiment, we tested on User 5 (simulating the user of the system). We run this experiment on the Odroid board to measure energy consumption.

When we change the sampling frequency of the dataset, we also have to consider the number of samples per sliding window because the number of seconds of data per window will be different depending on the frequency. Based on that, we adapt the sliding window size to the sampling frequency to guarantee that each window has the same number of sec, regardless of sampling frequency. For example, if we consider a window size of 900 samples for a frequency of 100 Hz, each window has 9 sec of data. To keep the 9 sec of data, the window size has to be 425 for a frequency of 50 Hz, 225 for 25 Hz, 113 for 12.5 Hz, 45 for 5 Hz, and 9 for 1 Hz.

However, some constraints must be considered when considering the sampling frequency of 1 Hz. Not all 702 configurations can be used when the sampling frequency is 1 Hz. For example, for a window size of 2 samples (200 samples if 100 Hz), the only overlap possible is 50%. Table IV shows the possible values for the overlap for window sizes considering a sampling frequency of 1 Hz. Another limitation is that a window’s size below 50 samples for 100 Hz cannot be used when the frequency is 1 Hz because we cannot have 0.5 sec of data in a window. Because of these limitations, the number of usable configurations for a sampling frequency of 1 Hz is 189. Since we cannot create windows with 0.5 sec of data, the window sizes of 150, 250, 350, 450, 550, 650, 750, and 850 were rounded for

the next possible window size, i.e., 200, 300, 400, 500, 600, 700, 800, and 900, respectively.

Table IV. Possible values of overlap for the window sizes considering a sampling frequency of 1 Hz.

Window Size (samples)	Possible Overlaps (%)
1	[0]
2	[0, 50]
3	[0, 20, 60]
4	[0, 20, 50, 70]
5	[0, 20, 40, 60, 80]
6	[0, 10, 30, 50, 60, 70]
7	[0, 10, 20, 40, 50, 60, 70, 80]
8	[0, 10, 20, 30, 50, 60, 70, 80]
9	[0, 10, 20, 30, 40, 50, 60, 70, 80]

5 Results

This section discusses the results obtained from the experiments and compares the main conclusions with the Related Work.

5.1 Hyperparameters

We conduct a study on all 9 users of the PAMAP2 dataset to evaluate the influence of different configurations of hyperparameters on the system for each user. Figure 5 shows an example of the results obtained. Figure 5 shows the accuracy, response time, and energy consumption of the 702 configurations and the Pareto-Front for User 1. The charts for the remaining users can be found in Appendix A.1.

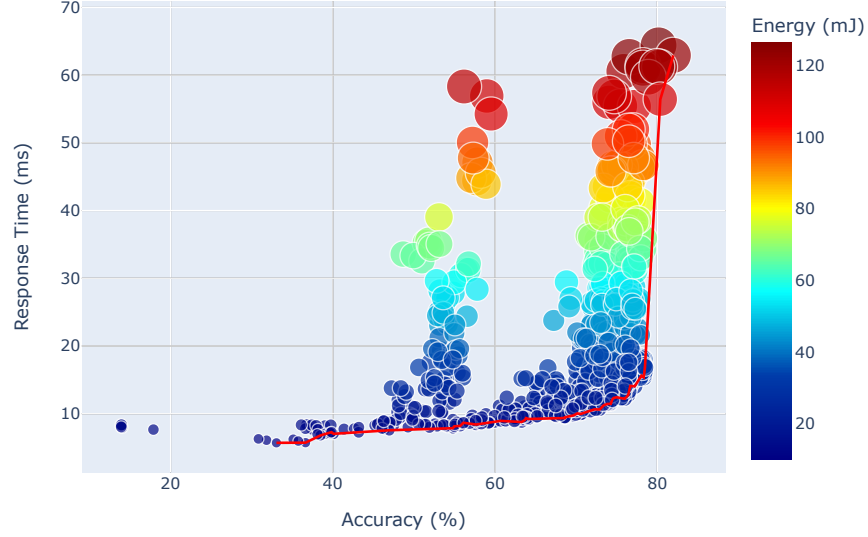


Fig. 5. Energy Consumption, Response Time, and Accuracy of the configurations for User 1.

Table V summarizes the variation in the accuracy, response time, and energy consumption for all Users of the PAMAP2 dataset. The Table shows the variation when considering all the 702 configurations and considering only the Pareto-Front configurations.

Table V. Variation for accuracy, response time and energy consumption for all users (PFP - Pareto-Front Points).

User	# PFP	Accuracy (%)		Response Time (ms)		Energy Consumption (mJ)	
		All Points	PFP	All Points	PFP	All Points	PFP
1	57	[14; 82]	[33; 82]	[6; 64]	[6; 63]	[10; 126]	[10; 121]
2	64	[15; 95]	[27; 95]	[5; 63]	[5; 60]	[9; 123]	[9; 117]
3	93	[15; 94]	[20; 94]	[5; 68]	[5; 61]	[9; 137]	[9; 123]
4	77	[18; 94]	[27; 94]	[5; 67]	[5; 51]	[9; 129]	[9; 99]
5	68	[17; 91]	[21; 91]	[5; 64]	[5; 38]	[9; 126]	[9; 73]
6	71	[12; 93]	[27; 93]	[5; 64]	[5; 53]	[8; 125]	[8; 105]
7	51	[16; 95]	[34; 95]	[5; 67]	[5; 67]	[9; 130]	[9; 130]
8	65	[9; 86]	[11; 86]	[4; 66]	[4; 44]	[8; 130]	[8; 86]
9	21	[0; 100]	[0; 100]	[8; 218]	[8; 25]	[16; 579]	[16; 59]

After analyzing the results of all users, we conclude that the same configurations have different behaviors depending on the User under test, resulting in different Pareto-Fronts for each User. The number of Pareto-Front points for each User is also different. For example, User 3 has more configurations in the Pareto-Front. Table V, shows that the highest accuracy measured in this experiment was 95.35% and was registered for User 7 using the configuration 305 (window size = 900, overlap = 0%, distance = Manhattan, $k = 9$). However, this configuration also resulted in the highest energy consumption (130.30 mJ) and response time (66.97 ms), considering all the Pareto-Front of all users under analysis. On the other hand, for User 1 and configuration 52 (window size = 850, overlap = 0%, distance = Manhattan, $k = 10$), the accuracy does not exceed 82%. This User is the one that obtained the lowest maximum accuracy value of all the users studied. Despite User 1 registering the lowest maximum accuracy, it is the third with the highest energy consumption (121.12 mJ) and the second with the highest response time (62.92 ms). There are Users with higher accuracies than User 1 and lower energy consumption and response times. For example, User 5, with configuration 909 (window size = 900, overlap = 50%, distance = Manhattan, $k = 10$), achieved 91.06% accuracy (more 9.09% than User 1) with the lowest energy consumption (73.22 mJ, less 47.90 mJ than User 1) and response time (38.04 ms, less 24.88 ms than User 1). Except for Users 1 and 8, the remaining users achieve a maximum accuracy above 90%.

User 9 differs from the other 8 analyzed Users because it only has samples for one activity (in this case, Rope Jumping). Besides, User 9 also has considerably fewer samples when compared with the other 8 Users. Because User 9 has fewer samples for specific configurations, the number of instances obtained is less than 10. As shown in Table V, there are considerably high energy consumption and response time values. These higher values occur for configurations where the number of instances is less than 20. This behavior occurs because of the Java JIT compiler. The first instance takes significant time to be processed and classified. This happens because the JIT compiler has to load all the classes and methods. All the necessary classes were already loaded for the following instances, and less time is needed to classify the instances. The higher values for response time and energy consumption only appear in User 9 because since we calculate the average energy consumption and response time, the high value registered for the first instance is diluted in the other instances. Since User 9 has only samples for one activity and has fewer samples, we cannot analyze them as for the other Users.

We focus our study on the Pareto-Fronts of each User. As a possible acceptable scenario, we define an accuracy greater than 75%. Considering the scenario, we focus only on the Pareto-Front configurations that meet the scenario requirements. Figure 6 shows an example of the Pareto-Front with configurations with an accuracy greater than 75%. The charts for the remaining Users are available in Appendix A.2. In each Figure, we highlight some configurations.

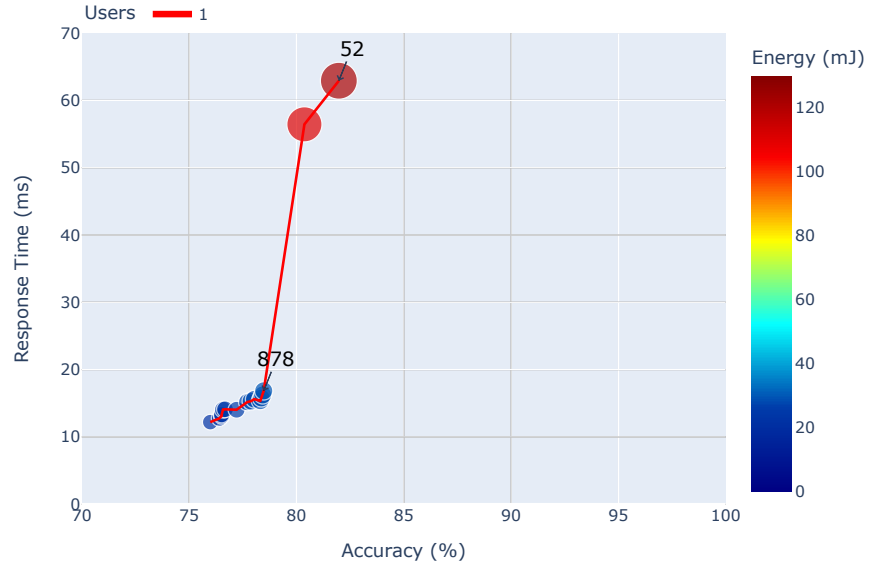


Fig. 6. Pareto-Front for User 1 with configurations with an accuracy greater than 75%. Some configurations highlighted (configuration ID is shown).

Table VI summarizes all the highlight configurations for each user, the energy consumption, response time, and accuracy associated with the configuration, and the values of the hyperparameters. We exclude User 9 from this comparison due to its limited data, consisting of only one activity and a minimal number of samples. Including User 9 would result in an unfair and skewed comparison.

Table VI. Specific configurations of the Pareto-Front for each User (Acc - Accuracy; RT - Response Time; EC - Energy Consumption; WS - Window Size; Ov - Overlap).

User	Conf ID	Acc (%)	RT (ms)	EC (mJ)	WS	Ov (%)	Distance	k
1	52	81.97	62.92	121.12	850	0	Manhattan	10
	878	78.47	16.84	29.62	850	90	Manhattan	6
2	881	95.15	59.64	116.58	850	0	Manhattan	4
	333	89.66	19.91	37.19	400	50	Manhattan	5
3	795	93.95	61.85	123.62	900	10	Manhattan	9
	778	87.02	17.23	30.99	850	90	Manhattan	9
4	524	94.71	51.39	99.85	850	20	Manhattan	9
	250	87.2	19.33	36.83	250	20	Manhattan	6
5	909	91.06	38.04	73.22	900	50	Manhattan	10
	919	88.45	18.82	34.5	700	80	Manhattan	10
6	281	92.8	53.11	105.72	900	20	Manhattan	10
	973	89.51	25.08	47.75	800	70	Manhattan	8
7	305	95.35	66.97	130.3	900	0	Manhattan	9
	150	89.4	15.07	27.04	750	90	Euclidean	10
8	356	81.51	41.94	80.4	550	0	Manhattan	10
	402	78.45	16.12	28.74	750	90	Manhattan	10

Analyzing the highlighted configurations presented in Table VI, we can observe that it is possible to significantly reduce energy consumption and response time without compromising the system's accuracy for all users. Let's consider User 1 as an example. By transitioning from configuration 52 to 878, we can decrease energy consumption from 121.12 mJ to 29.62 mJ (a 75% reduction) and reduce response time from 62.92 ms to 16.84 ms (a 73% reduction), while only experiencing a 3.5% decrease in accuracy. This behavior is observed when switching configurations for all users.

During our study, we observe that some configurations appear multiple times in the Pareto-Front of the Users. To better perceive the most common configurations among the users, we show the number of times each configuration appear in the Pareto-Front. Figure 7 shows the configurations that appear in more than 5 Users and the normalized values of accuracy, response time and energy consumption.

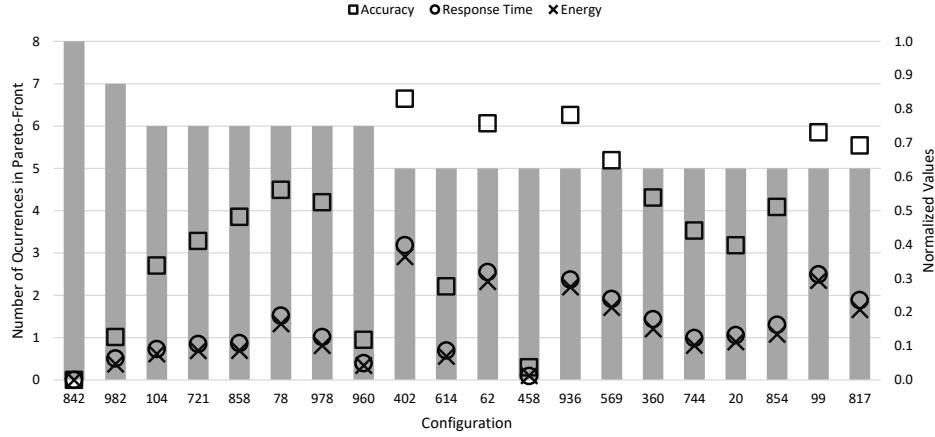


Fig. 7. Most frequent configurations on Pareto fronts and the values for accuracy, response time and energy consumption normalized.

The most frequent configurations in the Pareto-Front of the Users under study are 842 and 982. Configuration 842 appears in 8 Users as the lower extreme of the Pareto-Front, except User 9. Configuration 982 appears in 7 of the 8 Pareto-Front of the Users. Configuration 842 has a variation in the accuracy from 11.08% (User 8) to 34.26% (User 7), on the energy consumption from 8.56 mJ (User 8) to 10.15 mJ (User 1), and in the response time from 4.64 ms (User 8) to 5.70 ms (User 1). As for configuration 982, the accuracy varies between 22.41% (User 8) and 41.65% (User 7), the energy consumption between 10.98 mJ (User 2) and 12.32 mJ (User 1), and the response time from 6.43 ms (User 2) to 7.27 ms (User 1). Although configurations 842 and 982 are the most frequent in the Pareto-Front, the maximum accuracy obtained with these configurations is 41.65% (this value was obtained with configuration 982 for User 7). We note that an accuracy of 41.65% is not suitable for most HAR systems.

Additionally, HAR systems often play a crucial role in safety-critical applications, such as fall detection for older individuals. In such cases, even a slight decrease in accuracy can result in false negatives or positives, leading to potentially serious consequences. Moreover, even in non-critical services like fitness tracking, an accuracy rate of 41.65% would be inadequate. While the implications of low accuracy may not be as dire as in safety-critical scenarios, fitness tracking systems are still expected to deliver a certain level of performance to be beneficial. A low accuracy level would result in imprecise tracking of users' activities and exercises, adversely affecting their ability to monitor progress and tailor their fitness routines accordingly. Hence, an accuracy of 41.65% is deemed unacceptable for a HAR system. We define a minimum accuracy threshold of 75% to establish an acceptable benchmark. This level of accuracy is generally sufficient for most practical applications, as it enables the system to identify and classify

a majority of the intended activities correctly. However, it is important to note that the required accuracy level may vary depending on the specific application and the potential consequences of misclassification. We present the frequency of configurations appearing on the Pareto Front with an accuracy exceeding 75%. Figure 8 illustrates the configurations shared among more than three users. It is important to mention that the Pareto Front of User 9 configurations are not included in this analysis.

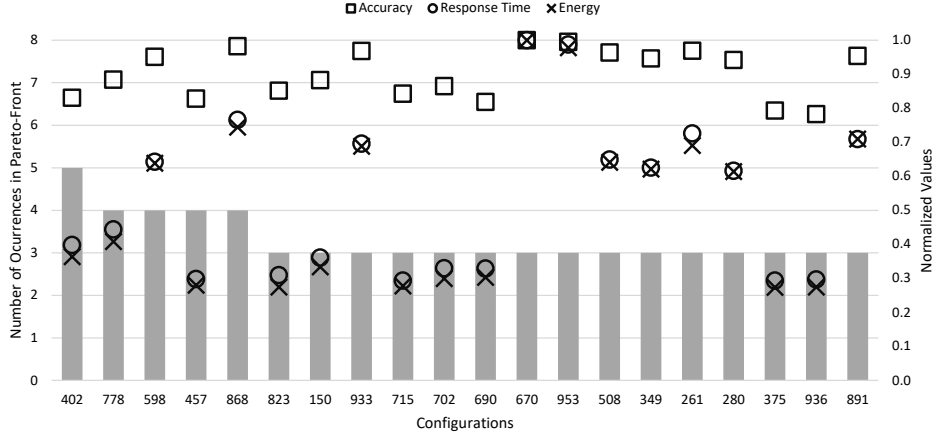


Fig. 8. Most frequent configurations on Pareto fronts with accuracy greater than 75% and the values for accuracy, response time and energy consumption normalized.

Figure 8 shows that the most common configuration in the Pareto-Front of the Users and with an accuracy superior to 75% is configuration 402 (window size = 750; overlap = 90%; distance = Manhattan; $k = 10$). This configuration belongs to the Pareto-Front of Users 1, 2, 4, 5, and 8. This configuration has a variation in accuracy from 75.94% (User 4) to 87.39% (User 5), in energy consumption from 27.27 mJ (User 2) to 28.74 mJ (User 8), and in response time from 15.43 ms (User 2) to 16.12 ms (User 8). Configurations 778, 598, 457, and 868 also have a strong presence in the Pareto-Front, appearing in 4 users. As already mentioned, these configurations allow an accuracy superior to 75%. Although a higher accuracy was achieved with these configurations, they require also an increase in energy consumption and response time.

All 702 configurations remain consistent across all users; however, we observe distinct outcomes for different configurations. The reason for this discrepancy lies in the unique characteristics of each user's data. The leave-one-out approach employed here mimics real-life scenarios where a HAR system is trained using data from N users and subsequently deployed for use by a new user. Despite having identical configurations, the model's performance varies because each

user's data is collected under distinct conditions. These conditions encompass sensor placement, noise, activity types, and intensity levels.

Additionally, user data distribution is not uniform, as some users possess more or less data than others. Moreover, variations exist in the quality of data collected by individual users. These inherent variations significantly impact the model's performance, resulting in different user outcomes regarding accuracy, energy consumption, and response time.

These results show the necessity of a self-adaptive HAR system. The need for a self-adaptive HAR system for a user is justified by the unique characteristics and varying conditions associated with individual users. Different users exhibit different data patterns due to sensor placement, noise levels, activity types, intensity levels, data distribution, and data quality. A self-adaptive HAR system can effectively address these variations and tailor its performance to meet the specific needs and conditions of each user. By continuously monitoring and analyzing the user's data, a self-adaptive system can dynamically adjust its hyperparameters, algorithms, and models to optimize accuracy, energy consumption, and response time for that particular user. The self-adaptive nature of the HAR system allows it to learn and adapt to the user's unique characteristics over time. This ensures the system remains effective and accurate even as the user's activities and data patterns evolve. By providing personalized and optimized performance, a self-adaptive HAR system enhances the user experience, enables better monitoring, and facilitates the customization of fitness routines. In summary, the need for a self-adaptive HAR system arises from inherent user data and conditions variations. Such a system can adapt its algorithms, hyperparameters, and models to accommodate each user's unique characteristics, ultimately improving accuracy and overall performance for personalized activity recognition.

Hyperparameter Importance The hyperparameters significantly impact the system performance regarding accuracy, response time, and energy consumption. However, there is a significant variation in the combinations of values for the selected hyperparameters. This makes it difficult to conclude which hyperparameters impacted the most.

To calculate the importance of each of the hyperparameters in the system, we used the fANOVA algorithm [47]. fANOVA stands for "Functional ANOVA," a statistical technique used to analyze the relationship between a response variable and multiple predictor variables. A generalization of ANOVA (Analysis of Variance) allows for modeling non-linear and interaction effects between the predictor variables. fANOVA can be used to identify which predictor variables have the most significant impact on the response variable and to estimate the magnitude of these effects.

It takes as input performance data gathered with different configurations. It fits a random forest to capture the relationship between hyperparameters (in our case, window size, overlap, distance function, and value of k) and performance (in our case, accuracy, response time, and energy consumption). Then apply

functional ANOVA (Analysis of Variance) to assess each hyperparameter’s importance.

In this experience, we study the hyperparameters’ impact on one of the 9 Users. We decide to apply the fANOVA algorithm to the results of the configurations for User 5. We use the fANOVA algorithm in two scenarios. In the first scenario, we apply the fANOVA algorithm to all the 702 configurations, and in the second one, we use it only for the Pareto-Front configurations. Figures 9 and 10 show the importance of the hyperparameters when considering all configurations and the Pareto-front configurations, respectively.

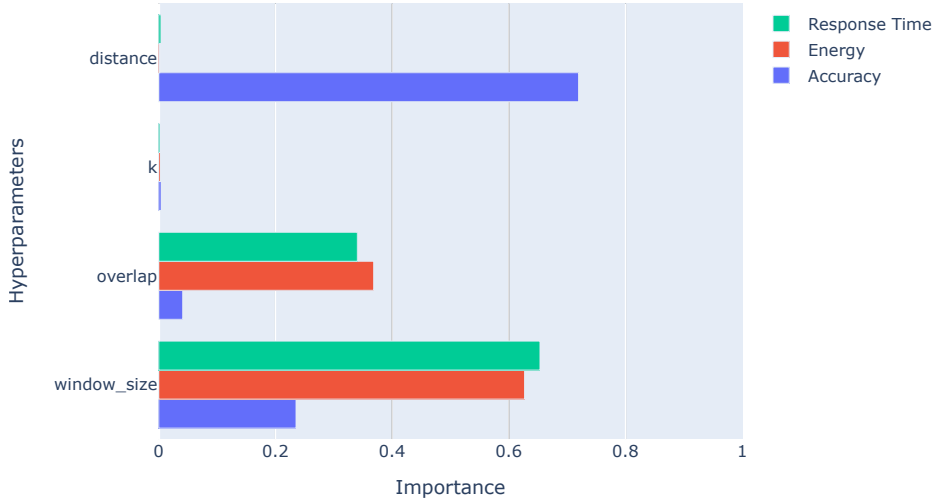


Fig. 9. Hyperparameters Importance for all configurations.

Figure 9 shows that overall the hyperparameter with the most significant impact on the system is the window size. On the other hand, the value of k does not significantly impact the system performance. The most important factor for accuracy is the distance function. This suggests that the choice of distance function has a significant impact on the accuracy of the system. The window size is the most important factor in energy consumption and response time. This suggests that the window size significantly impacts the system’s energy consumption and response time. We can also note that overlap had a similar effect on the response time and energy consumption as windows size.

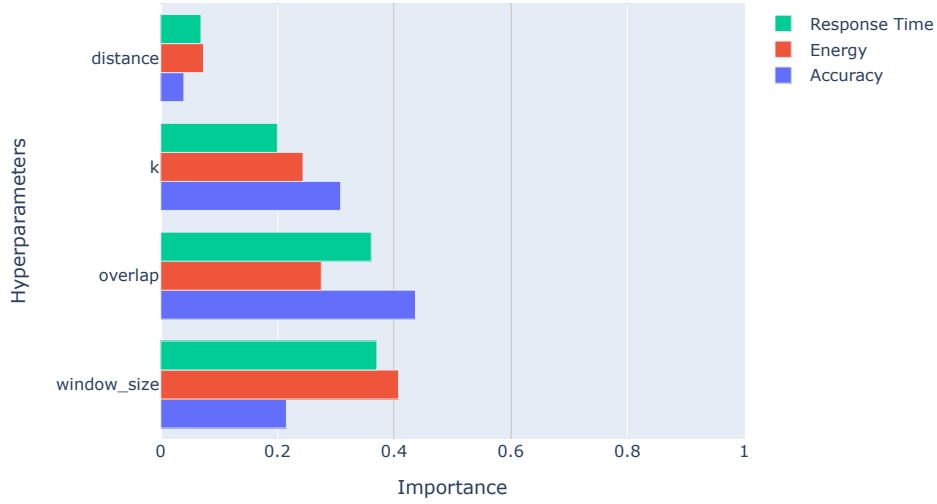


Fig. 10. Hyperparameters Importance for the Pareto-front configurations.

In the case of the Pareto-front configurations, Figure 10, shows that window size and overlap have the most impact on the system, with the distance function being the hyperparameter with the most negligible impact. The most important factor for accuracy is the overlap. The value of k and window size also has some importance. The importance of the distance function for accuracy is much lower. The window size and overlap are the most important energy consumption and response time hyperparameters.

Comparing the results for all configurations and Pareto-Front configurations, we can see that the importance of the different hyperparameters varies depending on the model's specific configuration. However, in both cases, the window size is the most important factor in determining energy consumption and execution time. Considering all configurations, the distance function is the most important factor in determining accuracy. In contrast, in the case of Pareto-front configurations, overlap is the most important factor in determining accuracy. Unlike the result obtained for all configurations, the value of k has much more influence on the system when considering only the Pareto-front configurations.

In conclusion, our study provides insights with respect to the impact of hyperparameters on the performance of a HAR system using the PAMAP2 dataset. The results show that the window size, overlap, distance function, and k have different levels of impact on the different performance metrics of the model and this should be considered when optimizing the model for a specific task. Depending on the desired performance metric, the relative importance of these hyperparameters may vary. For example, if energy consumption is the most important metric, then optimizing the window size and overlap may lead to the most con-

siderable improvement in energy consumption. In conclusion, the window size and overlap are consistently important for all three performance metrics.

The window size and overlap play an essential role in the system performance, as they determine the amount of data used to train the model. The window size determines the number of samples used to represent the data, while the overlap determines the amount of overlap between consecutive windows. Larger window size and higher overlap can lead to more detailed representations of the data showing better accuracy but requires more computation and memory, which translates into higher energy consumption and response time. Therefore, it is essential to carefully evaluate the trade-offs between the different performance metrics when selecting the optimal values for the hyperparameters.

The results suggest that a balance of all four hyperparameters is crucial for achieving good performance in accuracy, energy consumption, and execution time. These findings can be helpful in the design and optimization of real-time systems that operate under resource constraints. It can also be used to research new methods and algorithms that can automatically select the optimal hyperparameter values based on the specific requirements and limitations of the application. This would simplify choosing the optimal hyperparameter values and make it easier to apply these methods to other datasets and users.

Activity Level Until now, we were only focusing on the global performance of the model with different configurations, but it is also important to understand the influence of the configurations at an activity level. For that, we calculate the F1-Score of the 12 activities for User 5. To better analyze the impact at an activity level, we consider the scenario where the system’s accuracy must be higher than 75%. Table VII shows the F1-Score of each activity for each chosen configuration.

Table VII. F1-Score of each activity for each configuration. (A1 - ascending stairs; A2 - cycling; A3 - descending stairs; A4 - ironing; A5 - lying; A6 - nordic walking; A7 - rope jumping; A8 - running; A9 - sitting; A10 - standing; A11 - vacuum cleaning; A12 - walking)

Config ID	A1	A2	A3	A4	A5	A6	A7	A8	A9	A10	A11	A12	AVG
2	0.83	0.92	0.64	0.88	0.95	0.79	0.94	0.97	0.70	0.62	0.82	0.92	0.83
229	0.88	0.93	0.75	0.89	0.96	0.87	0.95	0.97	0.77	0.70	0.88	0.91	0.87
375	0.81	0.90	0.58	0.85	0.96	0.82	0.93	0.97	0.67	0.59	0.82	0.88	0.82
402	0.84	0.93	0.71	0.89	0.96	0.86	0.95	0.97	0.79	0.71	0.90	0.93	0.87
416	0.90	0.94	0.82	0.90	0.97	0.93	0.95	0.96	0.84	0.76	0.92	0.89	0.90
433	0.89	0.94	0.74	0.89	0.94	0.87	0.93	0.94	0.36	0.58	0.86	0.91	0.82
537	0.86	0.92	0.70	0.88	0.95	0.87	0.92	0.96	0.32	0.56	0.84	0.89	0.81
670	0.89	0.93	0.81	0.92	0.98	0.94	0.98	0.96	0.84	0.75	0.88	0.93	0.90
690	0.84	0.93	0.65	0.87	0.94	0.80	0.94	0.97	0.71	0.63	0.82	0.92	0.84
702	0.86	0.94	0.66	0.88	0.95	0.83	0.95	0.97	0.72	0.63	0.84	0.93	0.85
778	0.82	0.95	0.71	0.89	0.95	0.84	0.96	0.97	0.80	0.71	0.90	0.93	0.87
818	0.87	0.92	0.69	0.88	0.95	0.86	0.91	0.95	0.30	0.56	0.85	0.89	0.80
893	0.89	0.94	0.81	0.84	0.96	0.96	0.96	0.97	0.80	0.67	0.84	0.93	0.88
909	0.90	0.91	0.88	0.89	0.98	0.95	0.97	0.96	0.89	0.76	0.88	0.96	0.91
919	0.89	0.95	0.81	0.85	0.96	0.95	0.95	0.97	0.82	0.71	0.89	0.92	0.89
936	0.82	0.90	0.61	0.85	0.96	0.82	0.94	0.97	0.68	0.60	0.82	0.88	0.82
944	0.87	0.94	0.84	0.90	0.98	0.94	0.97	0.97	0.89	0.77	0.90	0.92	0.91
953	0.90	0.94	0.77	0.91	0.98	0.93	0.98	0.96	0.86	0.76	0.87	0.90	0.90
962	0.80	0.89	0.54	0.83	0.96	0.79	0.92	0.97	0.66	0.59	0.82	0.87	0.80
986	0.89	0.93	0.75	0.88	0.94	0.86	0.92	0.95	0.36	0.58	0.86	0.89	0.82

The configurations presented in Table VII have accuracies between 80.33% and 91.06%. These configurations have the same distance function, the Manhattan Distance. Table VIII shows the values of the hyperparameters for the selected configurations. There is a 10.73% difference between the minimum and maximum accuracy. As we can see from Table VII, there is a variation in the F1-Score of each activity for different configurations. There are activities where this variation is more significant. The activities running (A8), lying (A5), and cycling (A2) are the ones where the variations are smaller, 3%, 4%, and 6%, respectively. The classification capability of the model for these activities is not significantly affected by the window size, overlap, or the value of k. These activities also have higher values for F1-Score, indicating that the model, regardless of the configurations, performs better in recognizing these activities. On the other side, the activities of sitting (A9), descending stairs (A3), standing (A10), and nordic walking (A6) are the activities where there is a significant variation in the F1-Score, with variations of 59%, 34%, 21%, and 17%, respectively. The results show that these activities strongly depend on the hyperparameter's values. The activities of sitting (A9), standing (A10), and descending stairs (A3) are the ones with the lowest values of F1-Score. This indicates that the model has a lower performance in recognizing these activities when compared with the remaining ones.

Table VIII. Hyperparameters values for the selected configurations.

Config ID	Accuracy (%)	Window Size	Overlap (%)	Distance	k	EC (mJ)	RT (ms)
2	83.51	400	80	Manhattan	6	24.69	13.81
229	87.20	700	90	Manhattan	10	26.81	15.11
375	81.52	250	70	Manhattan	9	22.91	12.79
402	87.39	750	90	Manhattan	10	27.98	15.68
416	89.73	650	50	Manhattan	10	55.92	29.77
433	82.41	600	90	Manhattan	9	24.59	14.27
537	81.14	500	90	Manhattan	10	22.77	13.07
670	90.27	850	60	Manhattan	10	60.17	31.62
690	83.83	400	80	Manhattan	7	24.84	13.83
702	84.76	400	80	Manhattan	9	24.71	14.08
778	87.42	850	90	Manhattan	9	30.36	16.89
818	80.81	500	90	Manhattan	9	22.89	12.99
893	87.59	500	70	Manhattan	10	33.53	18.02
909	91.06	900	50	Manhattan	10	73.22	38.04
919	88.85	700	80	Manhattan	10	34.50	18.82
936	82.15	250	70	Manhattan	10	23.00	12.86
944	90.89	900	60	Manhattan	10	62.39	32.35
953	90.02	850	60	Manhattan	7	59.05	31.14
962	80.33	250	70	Manhattan	7	22.94	12.72
986	82.30	600	90	Manhattan	8	24.59	14.27

For the activity with higher variation in the values of F1-Score, sitting (A9), the minimum F1-Score is 0.3 (for configuration 818), and the maximum is 0.89 (for configuration 909 and 944). Based on the results, the value of the hyperparameters strongly influences the model's performance for this activity. Analysing Table VIII, we can see that the only difference in configurations 537 and 893 is the overlap, with 90% and 70%, respectively. This slight difference in the overlap (20%) allows an improvement of 0.48 in the F1-Score of the algorithm for the activity sitting (A9). Another example is configurations 537 and 229, where the F1-Score for the activity sitting (A9) is 0.32 and 0.77. The only difference in configurations 537 and 229 (see Table VIII) is the window size, 500 and 700, respectively. An increase in the window size by 200 samples increases the F1-Score of the model for the activity sitting by 0.45. These results show that small changes in the hyperparameters of the configurations can significantly impact an activity level.

We already concluded that the hyperparameters could impact the model's overall performance and computational cost of the HAR system. However, these results also show that the hyperparameters can significantly impact the model's performance at an activity level. For example, configuration 818 allows a global accuracy of 80.81% for the model, but at an activity level, the performance of the model for activities sitting (A9), standing (A10), and descending stairs (A3) is significantly worse than the remaining activities. On the other hand, some activities are not affected by the variations of the hyperparameter's values, in the case of activities like running (A8), lying (A5), and cycling (A2). These results

also provided important information regarding energy consumption. For example, we can see in Table VII that activity A1 (ascending stairs) has the same high recognition performance for configurations 416 and 909. However, configuration 909 requires much more energy than configuration 416. In a scenario where the user of the system is performing a specific activity for an extended time (for example, A8 - running), the system can change to a configuration (for example, from 944 to 402) that maintains the recognition performance of the model for the activity (F1-Score of 0.97) but requires less energy (62.39 mJ to 22.91 mJ), even though the global accuracy of the system decreases (90.89% to 81.51%). These results reinforced the importance of adaptability in HAR systems because although configuration provides a global high performance for the system (accuracy superior to 80%), some activities may be negatively affected by the configuration.

5.2 Sampling Frequency

For the first experiment involving the sampling frequency, we aim to assess the impact of varying the train frequency and test data on the system's accuracy. We chose one of the 702 configurations obtained from the previous exploration to study the sampling frequency. We select the configuration with the highest accuracy, which is configuration 305. Using this configuration, we achieve an accuracy of 95.35% for User 7. Next, we modify the sampling frequency of the train and test sets of each user. It is worth mentioning that to maintain the same number of seconds per window, we need to adjust the window size of the configuration due to the change in sampling frequency. However, the remaining values of the configuration's hyperparameters remain unchanged. Figure 11 shows the results when changing the sampling frequency of the train and test sets for User 1. The charts for the remaining users can be found in Appendix B.

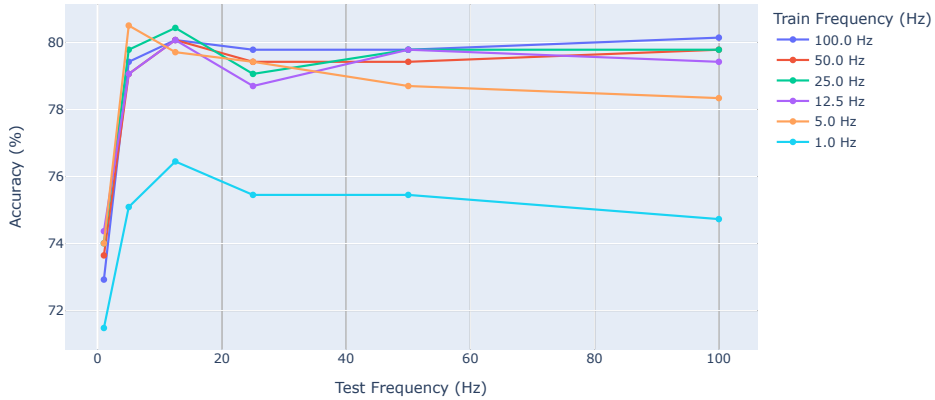


Fig. 11. Variation of the sampling frequency of the train and test sets for User 1, from 1 Hz to 100 Hz.

Table IX summarizes the combinations of the sampling frequency for the train and test sets that allow us to obtain the maximum and minimum accuracies for each user.

Table IX. Combinations of sampling frequency for the training and test sets that obtained the maximum and minimum accuracy for each User and respective accuracy values.

User	Max			Min		
	Train (Hz)	Test (Hz)	Acc (%)	Train (Hz)	Test (Hz)	Acc (%)
1	5	5	80.50	1	1	71.48
2	50	5	93.86	1	5	85.62
	-	-	-	1	25	-
3	100	12.5	-	1	1	80.83
	25	12.5	93.23	-	-	-
	5	12.5	-	-	-	-
4	25	12.5	94.14	1	1	81.71
5	100	50	86.09	5	1	80.46
	25	50	-	-	-	-
6	100	12.5	92.39	25	1	82.67
	50	12.5	-	5	1	-
7	5	5	95.74	12.5	1	91.47
8	25	100	85.22	1	1	68.38

The results indicate that modifying the sampling frequencies of the training set used to train the k NN and the test set significantly impacts the system's accuracy. In general, all users experience a decrease in accuracy when we lower the sampling frequency. However, the extent of this decrease varies among users, with some users being more affected than others. We observe the most substantial drop in accuracy for User 8, with a reduction of approximately 17%. In this case, the training and test sets have a sampling frequency of 1 Hz. Users 3 and 4 also exhibit notable accuracy decreases, with 12.40% and 12.43%, respectively. On the other hand, User 7 demonstrates a slight decrease in accuracy, with a drop of 4.27%. User 5 experiences a decrease of 5.63% in accuracy.

Combining a sampling frequency of 1 Hz for both the train and test sets resulted in the lowest accuracy, as shown in Table IX. This combination yields lower accuracy for 50% of the users (Users 1, 3, 4, and 8). Although there is a decrease in accuracy for all users when the sampling frequency is changed, except for Users 1 and 8, all other users still achieve minimum accuracies above 80%. Users 1 and 8, however, obtain minimum accuracies of 71.48% and 63.38%, respectively. Considering the previous scenario where an acceptable accuracy for a HAR system is greater than 75%, it is clear that the sampling frequency of 1 Hz for the train and test sets is insufficient for Users 1 and 8 to be used in the system.

Most Users obtain maximum accuracy when the sampling frequency is greater or equal to 12.5 Hz. However, for Users 1 and 7, the highest accuracy achieved is with the model trained and tested with a sampling frequency of 5 Hz. Overall, for the PAMAP2 dataset and using a leave-one-user-out approach with a k NN as the activity inference algorithm, the accuracy benefits from sampling frequencies greater or equal to 12.5 Hz, while sampling frequencies equal to or below 5 Hz show significant decreases in the accuracy.

Activity Level Understanding how the sampling frequency impacts the algorithm’s performance at the activity level is also crucial. Different sampling frequencies can have varying effects depending on the activity being performed. To explore this, we present the F1-Score for each activity at different sampling frequencies for User 5. Additionally, we include User 8 in our analysis because this user experiences the most significant impact from changes in sampling frequency, with a variation of 17% between the highest and lowest accuracies obtained.

We present two charts to evaluate the effect of sampling frequency on PAMAP2 activities. In the first chart (Figure 12 and 13), we keep the training set’s sampling frequency constant at 100 Hz and vary the sampling frequency of the test set to 100 Hz, 12.5 Hz, and 1 Hz. The second chart (Figure 16 and 13) displays the F1-Score values for each activity when the algorithm is trained and tested using sampling frequencies of 100 Hz and 1 Hz, representing the highest and lowest tested sampling frequencies, respectively.

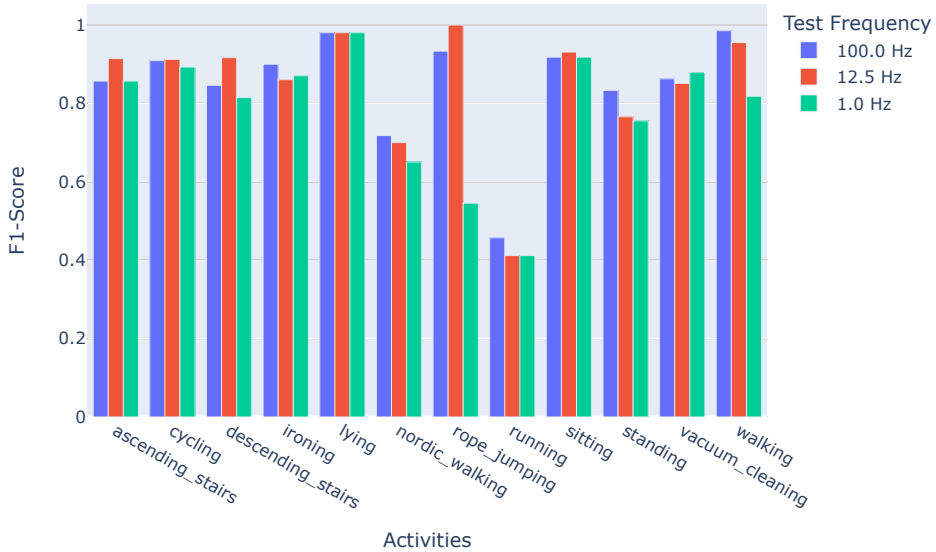


Fig. 12. F1-Score per activity for different values of the sampling frequency of the test set, maintaining the sampling frequency of the trained model as 100 Hz (User 5).

Figure 12 illustrates that, in the case of User 5, most activities within the PAMAP2 dataset are not significantly impacted by variations in the test set’s sampling frequency. However, certain activities are negatively affected when the sampling frequency is reduced. Specifically, the activity ”rope jumping” substantially decreases its F1-Score when the test set frequency is decreased from 100 Hz to 1 Hz. On the other hand, activities like ”running,” ”walking,” and ”standing” experience less significant reductions in their F1-Scores with the decrease in sampling frequency.

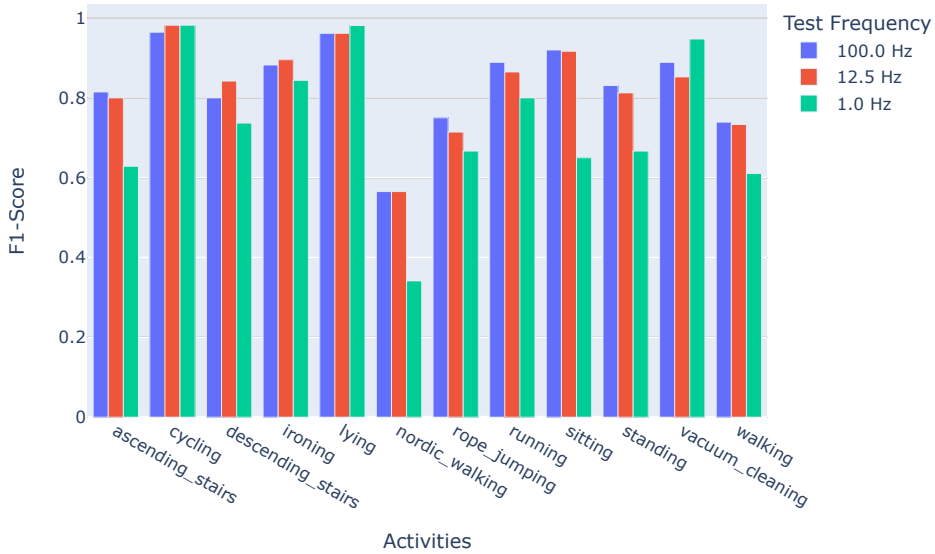


Fig. 13. F1-Score per activity for different values of the sampling frequency of the test set, maintaining the sampling frequency of the trained model as 100 Hz (User 8).

Regarding User 8, Figure 13 demonstrates that the sampling frequency of the test set has distinct effects on the activities within the PAMAP2 dataset. When the sampling frequency of the test set is varied, the algorithm’s performance remains relatively unaffected for activities such as ”cycling,” ”lying,” and ”vacuum cleaning.” However, most activities experience a decline in performance as the sampling frequency is reduced. This decline is particularly notable for ”nordic walking,” ”walking,” ”standing,” ”sitting,” and ”ascending stairs.” For these activities, the F1-Score decreases with the reduction in sampling frequency, with the lowest values observed at a sampling frequency of 1 Hz. Notably, the activities ”sitting” and ”nordic walking” exhibit a more pronounced decrease in performance when the sampling frequency changes from 100 Hz to 1 Hz. On the other hand, the F1-Score for ”vacuum cleaning” shows an increase when lower sampling frequencies are utilized for the test set.

Figures 14 and 15 show the differences in the signal of the ankle accelerometer for the sampling frequencies of 100 Hz, 12.5 Hz, and 1 Hz for the activities of "nordic walking" and "lying", respectively. For each sampling frequency, we show in the charts 1 minute of raw data for the x, y, and z axis.

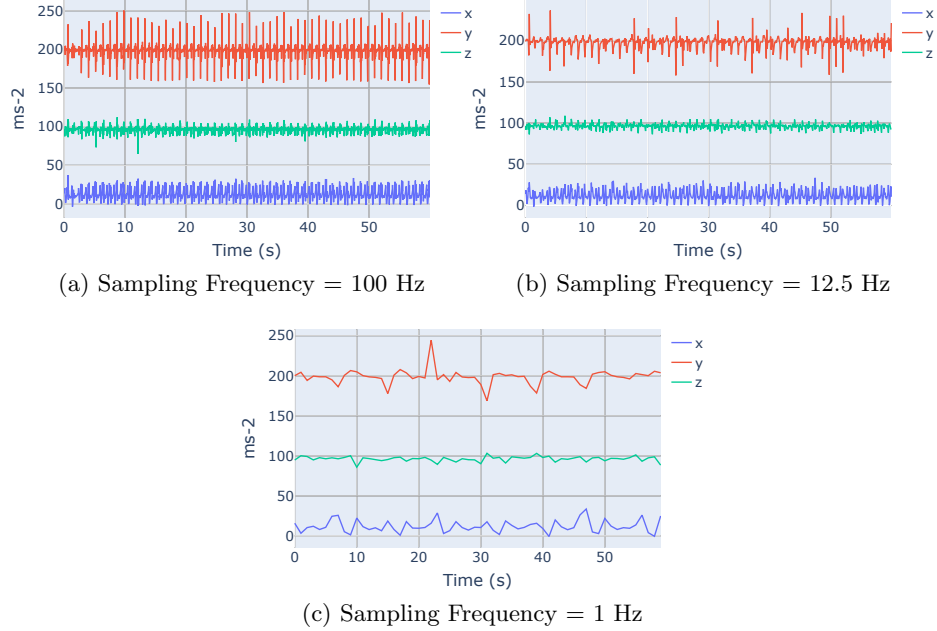


Fig. 14. Behavior of the signal of the accelerometer for activity nordic walking (User 8).

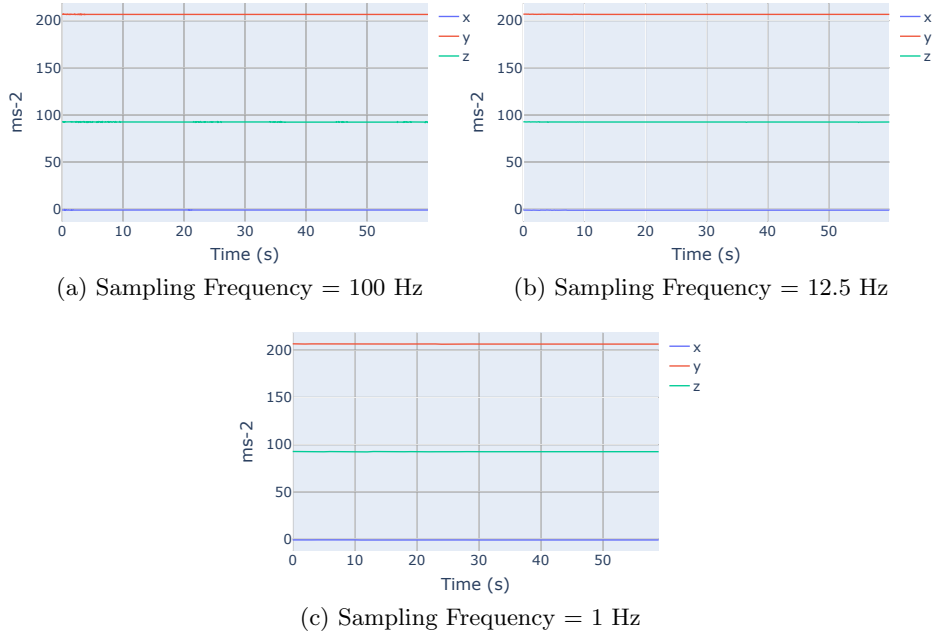


Fig. 15. Behavior of the signal of the accelerometer for activity lying (User 8).

When comparing the signal of "nordic walking" in Figure 14 (an activity whose recognition performance decreases with the reduction of the sampling frequency) and the signal of "lying" in Figure 15 (an activity unaffected by the sampling frequency), a noticeable degradation of the accelerometer signal becomes apparent as the sampling frequency is reduced. Conversely, for the "lying" activity, we observe that the signal remains unaffected by the decrease in sampling frequencies. The signal of the "nordic walking" activity experiences a loss of information, which explains the negative impact on the recognition performance due to the sampling frequency reduction. However, it is worth noting that despite the evident loss of information in the accelerometer signal, our approach involves extracting features from the signal rather than utilizing raw accelerometer data. Other sensors placed on different parts of the user's body also capture supplementary aspects of the motion pattern. These factors contribute to the justification as to why the performance of the k NN algorithm for the "nordic walking" activity does not degrade significantly further. The features extracted from the signal can still capture crucial aspects, and the additional sensors help provide complementary information, thereby mitigating the overall degradation in performance.

Focusing on the model trained and tested with the highest considered sampling frequency (100 Hz) and the lowest considered sampling frequency (1 Hz), we observe significant changes in the F1-Scores for User 5 (refer to Figure 16).

Out of the 12 activities, 10 exhibit a decrease in their F1-Scores when the sampling frequency is reduced to 1 Hz, compared to the original 100 Hz sampling frequency. Activities such as "ascending stairs," "rope jumping," and "walking" are particularly affected by the reduction in sampling frequency, experiencing notable decreases in their F1-Scores. However, there is an increase in the F1-Score for the "running" activity.

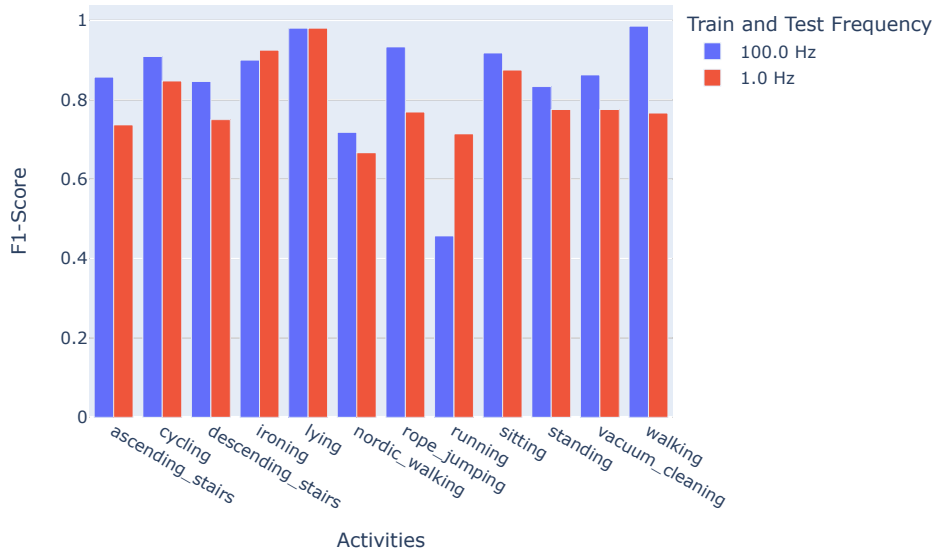


Fig. 16. F1-Score per activity for a model trained and tested with a sampling frequency of 100 Hz and 1 Hz (User 5).

Regarding User 8 (refer to Figure 17), we note that 11 out of the 12 activities exhibit a decrease in the F1-Score when the sampling frequency is reduced to 1 Hz, as compared to the original 100 Hz sampling frequency. In contrast, there is a reduction in the algorithm's performance for these 11 activities. Not all experience a significant decrease in the F1-Score. Activities such as "descending stairs," "vacuum cleaning," and "cycling" demonstrate only minor reductions in their F1-Scores. However, we observe a substantial decrease in the F1-Score for the "nordic walking" and "rope jumping" activities.

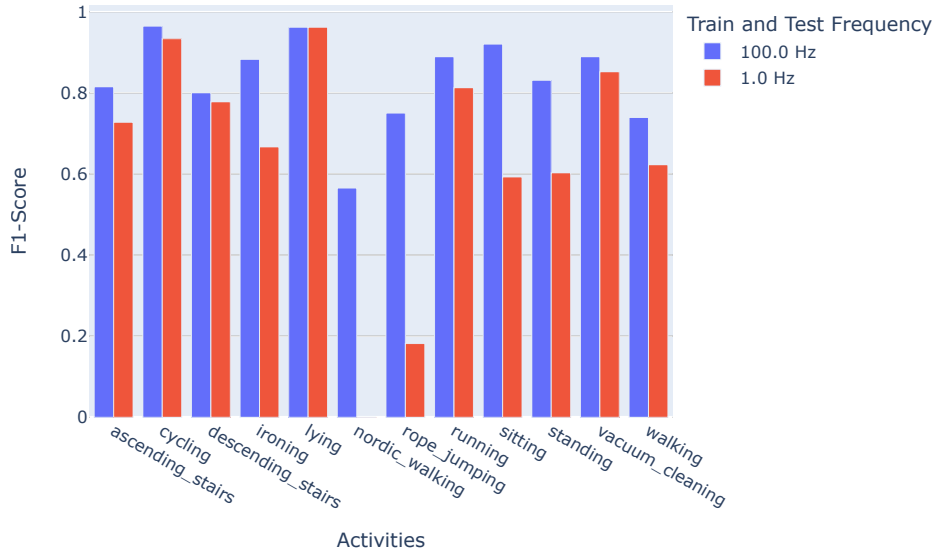


Fig. 17. F1-Score per activity for a model trained and tested with a sampling frequency of 100 Hz and 1 Hz (User 8).

Although these results suggest that higher sampling frequencies generally lead to improved performance of k NN in recognizing different activities, the optimal sampling frequency may vary depending on the specific activity. The findings highlight the significant impact of the choice of sampling frequency on the performance of the k NN, as evidenced by the varying performance across different activities. For example, User 8 achieved an F1-Score value of 0 for “nordic walking” at a sampling frequency of 1 Hz. This may be attributed to the fact that the movements involved in “nordic walking” are relatively subtle and require higher sampling frequencies to capture them accurately.

Pareto-Front and Frequency With this experiment, we evaluate the effect of sampling frequency on the Pareto-Front for User 5. We specifically chose this user based on previous experiments [1], where we aimed to emulate the system user. In this experiment, we trained the algorithm using a sampling frequency of 100 Hz and subsequently tested them using sampling frequencies of 100 Hz, 25 Hz, and 1 Hz. For the 1 Hz sampling frequency, certain constraints regarding overlap and window size reduced usable configurations from 702 to 189 (refer to Section 4.5). It is worth noting that the window sizes of the configurations were adjusted according to the sampling frequency to maintain a consistent number of seconds. The results of this experiment are presented in Figure 18, illustrating the Pareto-Front for the original sampling frequency, the 25 Hz frequency, and the 1 Hz frequency.

Additionally, Table X provides the lower and upper extreme points of the Pareto-Front for the tested sampling frequencies. We also include information on the variations in response time, energy consumption, and accuracy. Furthermore, Table XI provides detailed configurations that make up the lower and upper extremes of the Pareto-Front.

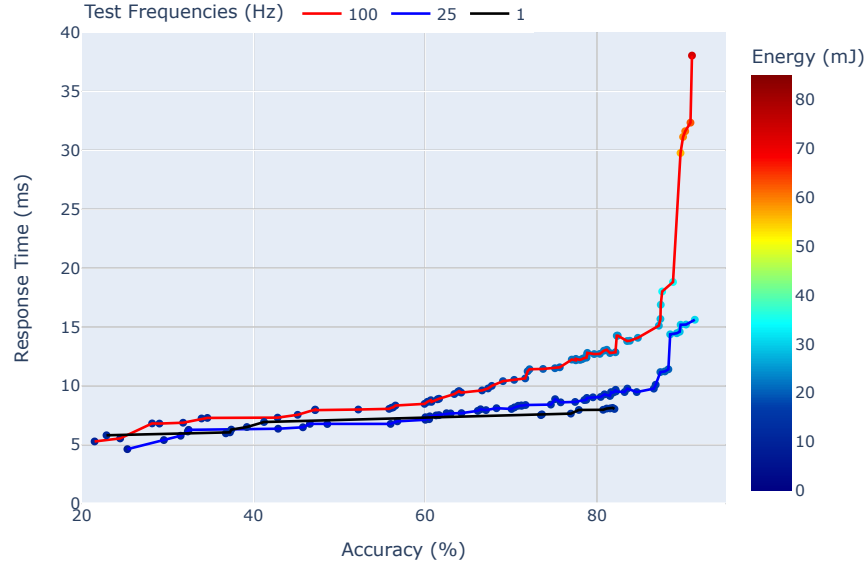


Fig. 18. Pareto-frontier of User 5 for different test frequencies (100 Hz, 25 Hz, and 1 Hz).

Figure 18 illustrates the distinct Pareto-Fronts for each sampling frequency examined. The configurations comprising the Pareto fronts differ for each sampling frequency, and the number of configurations in these fronts also varies. Specifically, the 100 Hz sampling frequency has 68 configurations, 25 Hz has 60 configurations, and 1 Hz has only 15 configurations. Directing our attention to the 100 Hz sampling frequency, we observe a significant increase in energy consumption and response time for accuracies equal to or greater than 85%, accompanied by a slight increase in accuracy. However, this behavior is not observed for the 25 Hz and 1 Hz sampling frequencies. As the sampling frequency decreases, the energy consumption and response time variations become smaller (refer to Table X). The Pareto-Front for the 1 Hz sampling frequency exhibits the slightest variation in response time and energy consumption. The

energy consumption varies by 3.62 mJ, and the response time varies by 2.23 ms between the lower and upper extremes of the frontier. Simultaneously, the accuracy demonstrates an increase of approximately 59.16%.

Table X. Variation of the accuracy, response time and energy consumption for the sampling frequencies of 100 Hz, 25 Hz and 1 Hz. (Freq - Frequency (Hz); LP - Lower Point; UP - Upper Point; ACC - Accuracy (%); EC - Energy Consumption (mJ); RT - Response Time (ms))

Freq	LP	UP	ACC	EC	RT	#Points
100	842	909	[21.48 ; 91.06]	[9.63 ; 73.22]	[5.29 ; 38.4]	68
25	458	944	[25.30 ; 91.39]	[8.18 ; 30.63]	[4.63 ; 15.62]	60
1	226	682	[22.87 ; 82.03]	[11.19 ; 14.81]	[5.81 ; 8.04]	15

Comparing the Pareto-Fronts for the sampling frequencies of 100 Hz and 25 Hz and focusing solely on the configurations that yield the maximum accuracy (909 for 100 Hz and 944 for 25 Hz, refer to Table X), we observe a significant reduction in energy consumption and response time. Specifically, we measured a decrease of 58% in energy consumption and 59% in response time. Meanwhile, the accuracy does not undergo significant alterations. Shifting our attention to the Pareto-Front for the sampling frequencies of 100 Hz and 1 Hz, and once again focusing on the configurations that result in the maximum accuracy (909 for 100 Hz and 682 for 1 Hz, see Table X), we observe a more significant reduction in energy consumption and response time. In this case, we observe a decrease of 80% in energy consumption and 79% in response time. However, the 1 Hz sampling frequency also significantly reduces accuracy, approximately 11%. Considering a scenario where an acceptable accuracy threshold is set above 75%, both the 25 Hz and 1 Hz sampling frequencies have configurations that meet this threshold, thus allowing the use of these frequencies in this hypothetical system.

Table XI. Detailed configurations. (WS - Window Size)

ID	WS	Overlap	Distance	k (<i>k</i> NN)
842	50	80%	Chebyshev	1
909	900	50%	Manhattan	10
458	13	70%	Chebyshev	1
944	225	60%	Manhattan	10
226	2	50%	Chebyshev	5
682	9	80%	Manhattan	7

The observed reduction in response time and energy consumption when using the sampling frequencies of 25 Hz and 1 Hz occurs because of smaller window sizes, meaning fewer samples per window. To illustrate, consider the upper extreme configuration (944) of the Pareto-Front for a frequency of 25 Hz. It has

a window size of 225 and 9 seconds of data, corresponding to a window size of 900 when the sampling frequency is 100 Hz. We reduce the window size to maintain the exact duration of data per window when the original sampling frequency is used (100 Hz). In this manner, for a frequency of 25 Hz, the window size varies between 13 and 225 samples, while for a frequency of 1 Hz, it varies between 1 and 9 samples. By adjusting the window sizes, we ensure that the number of seconds of data per window remains consistent across different sampling frequencies. If the window sizes were always the same for all frequencies, the data per window would be significantly higher when using lower frequencies. However, with smaller window sizes, each window contains fewer samples. Consequently, the time and energy required to extract features and classify instances are reduced.

This experiment shows that lower sampling frequencies can significantly decrease the system’s energy consumption and response time without incurring significant accuracy loss. However, it is crucial to adjust the window size according to the sampling frequency to maintain a consistent duration of data per window. It is important to note that these results and conclusions are specific to User 5. As observed in previous experiments, these findings cannot be generalized to other users since each user’s data exhibit unique behaviors and characteristics, which can result in different effects when varying the sampling frequency.

5.3 Answering Research Questions

We identify 6 Research Questions that we address in this study.

RQ 1 The RQ1 aims to investigate how hyperparameter configurations affect the accuracy, response time, and energy consumption of a Human Activity Recognition (HAR) system. Hyperparameters play a crucial role in the behavior and performance of ML algorithms. RQ 1 specifically emphasizes considering the global impact of hyperparameter configurations across diverse users. This is important because users may have different activity patterns, body movements, or preferences that can influence the effectiveness of specific hyperparameter settings. Understanding the effect of hyperparameters in different user groups and contexts enables personalized and adaptive system design.

During the experimentation and analysis of various hyperparameter configurations, we observed that specific configurations required more energy and time per inference in a HAR system. These configurations typically involved computationally intensive operations. As a result, the increased computational workload led to higher energy consumption and longer response times.

Furthermore, different hyperparameter configurations exhibited varying levels of accuracy. Some configurations achieved higher accuracies compared to others. The differences in accuracy can be attributed to the impact of hyperparameters on the learning process and the algorithm’s overall performance. Moreover, the same hyperparameter configurations produced different outcomes

for accuracy, energy consumption, and response time across users. Users with distinct activity patterns, body movements, or device placements experienced varying performance results even when using the same hyperparameter settings.

In summary, the findings of RQ 1 confirm that hyperparameter configurations significantly impact the performance of a HAR system. Some configurations require more energy and time, while others achieve higher accuracies. Additionally, the effect of hyperparameters can differ among users with diverse characteristics. These insights are valuable for optimizing hyperparameter configurations, ensuring efficient energy usage, and improving the accuracy and responsiveness of HAR systems for different users.

RQ 2 RQ2 aims to investigate the impact of window size, overlap, distance function, and the value of k on the accuracy, response time, and energy consumption of a k NN-based HAR system. We intend to understand how these factors influence the performance of the HAR system. By examining the overall and specific activities, the study seeks to determine the relationship between the chosen factors and the system’s accuracy in recognizing different activities. This involves analyzing how changing the window size, overlap, distance function, and value of k affects the system’s ability to classify activities correctly. In addition to accuracy, we also investigate the impact of these factors on the response time and energy consumption of the HAR system.

The results show that the window size and overlap are the hyperparameters that significantly influence the accuracy, response time, and energy consumption of the k NN-based HAR system. Changes in these parameters can substantially impact the system’s performance. While specific configurations of window size, overlap, distance function, and k may exhibit good overall performance, we observe that some activities may experience poor results with these configurations. This suggests that different activities within the HAR system can be more sensitive to changes in the hyperparameters. This implies that the optimal configuration for achieving high accuracy, minimal response time, and low energy consumption can vary depending on the specific recognized activity.

Even minor adjustments in the hyperparameters, especially window size, and overlap, can have a substantial impact on both the overall system performance and the performance at the activity level. This highlights the importance of carefully selecting and fine-tuning these hyperparameters to achieve optimal results.

In summary, the study reveals that window size and overlap significantly influence the accuracy, response time, and energy consumption of the k NN-based HAR system. It emphasizes the need to consider the specific activities being recognized and the sensitivity of those activities to hyperparameter changes. Additionally, it highlights the potential impact of small adjustments in the hyperparameters on the overall system performance.

RQ 3 The goal of RQ 3 is to investigate the influence of sampling frequencies on the accuracy of a HAR system, considering different users and activities. We intend to understand how varying sampling frequencies impact the performance

of the HAR system in accurately recognizing human activities. The study seeks to examine how different sampling frequencies affect the accuracy of the HAR system for different users. Individuals may exhibit variations in their movement patterns and activity styles, which can influence the effectiveness of the recognition system at different sampling frequencies. Furthermore, we also consider the impact of sampling frequencies on activity recognition accuracy for different activities. Different activities may have distinct characteristics and movement patterns, and the effectiveness of the HAR system in accurately identifying these activities can be influenced by the sampling frequency used.

Overall, reducing the sampling frequency of the HAR system leads to a reduction in its accuracy. Lower sampling frequencies result in less data being collected and analyzed, leading to decreased accuracy in activity recognition. We observe that some users are more affected by the reduction in sampling frequency compared to others. This suggests that individual differences in movement patterns, activity styles, or other factors can influence how much the accuracy of the HAR system is compromised when the sampling frequency is decreased.

We also verify that certain activities are more affected by the reduction of the sampling frequency than others. Different activities may have distinct movement characteristics, duration, or intensity levels, affecting the system's ability to recognize them accurately when the sampling frequency is lower. Even at an activity level, we note that some users have a smaller impact on activity recognition when the sampling frequency is reduced. This implies that specific individuals may possess movement patterns or styles that are more discernible or distinct, allowing the system to identify their activities even with lower sampling frequencies accurately.

In summary, the study indicates that reducing the sampling frequency of a HAR system generally leads to a decrease in performance. However, the impact of this reduction can vary depending on the user and the specific activity being recognized. Some users and activities may be more sensitive to changes in sampling frequency, while others may exhibit more robust recognition even with lower sampling rates. These findings highlight the need to consider individual differences and activity characteristics when determining the optimal sampling frequency for accurate activity recognition in HAR systems.

RQ 4 The goal of the RQ 4 is to investigate the trade-off between accuracy and energy consumption when reducing the sampling frequency for different hyperparameter configurations of a HAR system, specifically for a specific user (User 5). We aim to understand how decreasing the sampling frequency affects the balance between the accuracy and the energy consumption of the HAR system. The study evaluates this trade-off for different hyperparameter configurations of the HAR system. By explicitly considering a specific user, we aim to investigate how reducing the sampling frequency impacts the accuracy and energy consumption of the HAR system for that particular individual. User-specific characteristics, such as movement patterns, activity styles, or physiological factors, can influence the system's performance at different sampling frequencies.

The objective is to identify the optimal trade-off point between accuracy and energy consumption for different hyperparameter configurations under reduced sampling frequencies. This information can be used to determine the most efficient and effective configuration settings for the HAR system, tailored to the specific user while minimizing energy consumption without sacrificing accuracy.

The study examines three sampling frequencies: 100 Hz, 25 Hz, and 1 Hz. We use these frequencies to investigate the trade-off between accuracy and energy consumption for different hyperparameter configurations of the HAR system. Each sampling frequency studied resulted in a distinct Pareto-Front, representing the trade-off between accuracy and energy consumption. The number of points in the Pareto-Front also varied for different frequencies, indicating different possible configurations with varying levels of accuracy and energy consumption. We observe that reducing the sampling frequency significantly reduced the energy consumption of the HAR system across all frequencies. Lower sampling frequencies require fewer data points to be collected and processed, decreasing energy consumption. The study found that the maximum accuracy achieved at a sampling frequency of 25 Hz was the same as that achieved at 100 Hz. This suggests that it is possible to maintain the same level of accuracy while operating at a lower sampling frequency, resulting in energy savings.

When we reduce the sampling frequency to 1 Hz, we observe a significant reduction in the maximum accuracy, which implies that extremely low sampling frequencies may compromise the accuracy of the HAR system. Another finding is that reducing the sampling frequency also reduced the variation in energy consumption. The maximum and minimum accuracy difference decreased as the sampling frequency decreased, suggesting that lower frequencies resulted in more consistent energy consumption across different hyperparameter configurations.

The study indicates that reducing the sampling frequency in a HAR system leads to significant energy savings. While maintaining the same maximum accuracy as higher frequencies, a frequency of 25 Hz can achieve improved energy efficiency. However, extremely low frequencies, such as 1 Hz, may reduce accuracy. Additionally, lowering the sampling frequency reduces the energy variation, resulting in more consistent energy consumption across different hyperparameter configurations. These findings provide insights into optimizing the trade-off between accuracy and energy consumption in HAR systems for specific users by adjusting the sampling frequency and hyperparameters.

RQ 5 The goal of the RQ5 is to investigate how the mismatch between the sampling frequencies of the train and test sets affects the accuracy of a HAR system. The study analyzes the effect of having different sampling frequencies in the train and test sets. This mismatch can occur when the data used for training the HAR system is collected at a different sampling frequency than the data used for testing and evaluation. By examining the accuracy of the HAR system under sampling frequency mismatch, we aim to uncover how this inconsistency affects the system’s ability to classify activities correctly. It seeks to determine if and how the discrepancy in sampling frequencies impacts the performance

of the HAR system in accurately recognizing activities from the test set. This information can be valuable for understanding the limitations and challenges of using data collected at different sampling frequencies in real-world scenarios.

The study examines multiple sampling frequencies for both the train and test sets, including 100 Hz, 50 Hz, 25 Hz, 12.5 Hz, 5 Hz, and 1 Hz. We used these frequencies to investigate the impact of sampling frequency mismatch on the accuracy of the HAR system. We observe that some users were more affected by the mismatch between the sampling frequencies of the train and test sets than others. Individual differences in movement patterns, activity styles, or other factors could contribute to varying sensitivity to sampling frequency mismatch.

For test set sampling frequencies lower than 12.5 Hz (specifically 5 Hz and 1 Hz), the influence of the mismatch between the train and test set frequencies is more pronounced, suggesting that when the test set has a lower sampling frequency than the train set, the accuracy of the HAR system is more significantly affected. On the other hand, for test set sampling frequencies equal to or greater than 12.5 Hz, the mismatch between the train and test set frequencies had a relatively smaller impact on the accuracy of the HAR system, which implies that when the test set has a higher sampling frequency or a frequency comparable to the train set, the mismatch has less influence on the accuracy.

In summary, the study reveals that the mismatch between the train and test sets' sampling frequencies can impact the HAR system's accuracy. The degree of impact varies among users, with some being more affected than others. The influence of the mismatch is more pronounced when the test set has a lower sampling frequency than the train set. However, for test set frequencies equal to or greater than 12.5 Hz, the impact of the mismatch on accuracy is limited. These findings provide insights into the importance of considering sampling frequency consistency between the train and test sets to optimize the accuracy of HAR systems for different users and sampling scenarios.

RQ 6 The goal of RQ6 is to quantify the amount of energy that can be saved by utilizing Pareto-optimal hyperparameter configurations for a HAR system while still meeting the minimum accuracy required for a specific Quality of Service (QoS) level. Our goal is to determine the potential energy savings we can achieve by optimizing the hyperparameters of the HAR system. The study focuses on identifying Pareto-optimal hyperparameter configurations. We can identify these configurations and evaluate the trade-off between energy consumption and accuracy. We also intend to establish a minimum accuracy requirement for a specific QoS level. This requirement serves as a threshold that the HAR system must meet to ensure an acceptable level of performance. The QoS level may be defined based on user expectations, industry standards, or application requirements. For this study, we define a minimum accuracy of 75

We find that all users had hyperparameter configurations that met the minimum accuracy requirement, implying that it is possible to achieve the desired accuracy level for all users while optimizing the energy consumption of the HAR system. Depending on the user, we can achieve significant energy savings ranging

from 68.70% to 85.77% by utilizing the Pareto-optimal hyperparameter configurations. These configurations represent the trade-off between energy consumption and accuracy, allowing for improved energy efficiency without sacrificing the minimum required accuracy.

The maximum accuracy achieved varied among users. Some users had higher accuracy levels compared to others. For example, User 7 had the highest accuracy, while User 1 had the lowest accuracy among the studied users. Depending on the user, we observe accuracy drops ranging from 5.99% to 20.32% when considering the maximum accuracy obtained for the user and the first configurations with an accuracy greater than 75%. Despite these drops, the resulting accuracies remained within an acceptable range and still met the minimum requirement.

In summary, the study demonstrates that achieving the minimum required accuracy for a specific QoS level is possible while realizing significant energy savings through Pareto-optimal hyperparameter configurations. Different users may have variations in both maximum accuracy levels and the extent of accuracy drops, but overall, the configurations were able to meet the minimum accuracy requirement while significantly reducing energy consumption. These findings provide insights into the potential energy efficiency improvements that can be achieved in a HAR system while maintaining satisfactory performance levels.

5.4 Treats to Validity

The experimental study presented in this report includes specificities that may condition some conclusions. We also note that the study was planned, considering a self-adaptivity future HAR system in terms of runtime exploration of system parameters and incremental/online learning.

We have yet to intend to explore the features extracted from the raw data in this study. The set of features used was fixed and chosen because they provided good accuracy in previous studies. Analyzing the impact of the features on metrics such as accuracy, energy consumption, and response time is exciting and valuable for self-adaptivity. Still, it needs to be included to maintain the study focus.

The prototyping HAR system used a target embedded platform with a specific device, computing and memory characteristics, operating system, and Java technology with a Java Runtime Environment (JRE). Although the accuracy is independent of the target device and JRE, assuming the same dataset, set of features, and algorithm, the energy consumption and response times presented depend on the overall characteristics of the target computing system and execution environment used. We also note that a multithread version of the HAR system may impact energy consumption and response time, and the use of somewhat old devices may affect more energy consumption and longer execution time than the use of more up-to-date devices. However, we believe that most conclusions, especially relative comparisons, would still hold.

Variations in the target device's performance, such as fluctuations in CPU utilization, memory availability, or thermal conditions, can introduce variability

in response time and energy consumption measurements. Factors such as the operating system, other running processes, background tasks, and system configurations can affect the performance measurements, more precisely, response time and energy consumption. They all were mitigated by running the HAR system several times and reporting average values.

More than the absolute values measured in response time and energy consumption, one important outcome of this kind of study is the relative impact between configurations. This can be very important for HAR systems and the research on self-adaptivity. Most conclusions regarding relative impact are generalizable, and their changes when considering different target systems reinforced one of the study’s goals: quantitatively and qualitatively, showing the importance of researching self-adaptivity HAR systems.

The study focuses on a PAMAP2 dataset and an HAR system based on a traditional k NN algorithm. This constrains the kind of conclusions regarding the user activities, which may be too dependent on the k NN behavior, memory, and computing complexity. The algorithm’s performance at the activity level depends on the dataset and its representativeness regarding user activities. Using a different ML algorithm or dataset can influence the measured accuracy and consequently the Pareto frontiers and some conclusions and is also an important aspect to motivate self-adaptivity HAR systems.

This study’s accuracy, response time, and energy consumption metrics might not comprehensively represent the model’s performance. The absence of specific task-level values for different components (file reading, feature extraction, inference) might introduce uncertainty and limit the precision of the measurements. In addition, the specific hardware configuration of the Odroid embedded system might introduce some concerns if there are performance variations, overheating issues, or other hardware-related factors that affect the response time or energy consumption measurements.

The HAR system prototyped used the PAMAP2 dataset as input data to the system. This was realized by substituting the reading from sensors with reading from files where the raw data are stored. This way, we emulate the functioning of a real HAR system, also controlling the data we use. Although the reading from sensors imposes different execution time and energy consumption than the readings from files, they affect equally and proportionally the overall system performance and mitigate risks regarding the main conclusions.

Although the validity risks are associated with this kind of study, and especially to maintain the feasibility of the study, most conclusions presented are of useful importance to guide research on self-adaptivity HAR systems.

5.5 Analysis with Respect to Related Work

During this work, we conducted several experiments to evaluate the impact of some parameters (namely window size, overlap, the value of k , distance function, and sampling frequency) on the performance of a HAR system in terms of model performance (accuracy, F1-Score), energy consumption, and response time. However, the experimental results and conclusions are specific to the PAMAP2

dataset and the k NN algorithm. To confirm our conclusions, we compare them to the findings of the works identified in Section 2. Table XIV resumes the related work. We focus our comparison on window size, overlap, value of k , and sampling frequency. We analyze each hyperparameter individually to evaluate the impact on the system. To analyze the effect of each hyperparameter individually, we fixed the values of the remaining hyperparameters and select the configurations where only the hyperparameter under study changes. Table XII shows the values for the fixed hyperparameters and those used for the hyperparameter under study.

Table XII. Number of hyperparameter’s values used to evaluate their individual influence on the HAR system.

	Window Size (WS)	Overlap	k (k NN)
Window Size	100, 150, 250, 300, 350, 500, 550, 600, 650, 750, 800, 850, 900	250	250
Overlap (%)	50	0, 10, 30, 40, 60, 70, 80, 90	80
k (k NN)	10	9	1, 2, 3, 5, 6, 9, 10
Distance	Manhattan	Manhattan	Manhattan

As we already concluded, each user has its behavior when using the same configurations. To compare our results with the Related Work, we first need to know the influence of each hyperparameter individually for each User. We calculate the Pearson Correlation between the hyperparameters (window size, overlap, and k) and the performance metrics used to evaluate the system (accuracy, energy consumption, and response time). Table XIII shows the values of the correlations between the hyperparameters and performance metrics for each User.

Table XIII. Pearson Correlation between each hyperparameter and each performance metric (ACC - Accuracy; EC - Energy Consumption; RT - Response Time).

User	Window Size			Overlap			k (kNN)		
	ACC	EC	RT	ACC	EC	RT	ACC	EC	RT
1	0.5456	0.9994	0.9992	-0.5055	-0.9991	-0.9996	0.9830	0.9407	0.8265
2	0.9454	0.9992	0.9993	-0.9397	-0.9983	-0.9953	0.9238	0.8856	0.9670
3	0.8939	0.9993	0.9987	-0.7819	-0.9997	-0.9998	0.8717	0.8587	0.7764
4	0.9100	0.9993	0.9990	-0.9696	-0.9993	-0.9997	0.9481	0.8184	0.8769
5	0.8618	0.9996	0.9992	-0.7672	-0.9985	-0.9975	0.9777	0.9455	0.9467
6	0.7969	0.9992	0.9992	-0.9457	-0.9993	-0.9987	0.8505	0.8784	0.8743
7	0.3993	0.9992	0.9993	-0.8288	-0.9997	-0.9994	0.6678	0.8965	0.6645
8	0.8437	0.9984	0.9993	-0.2874	-0.9997	-0.9996	0.9932	0.9404	0.8393

Window size positively correlates with accuracy, energy consumption, and response time. This indicates that these performance metrics increase when the window size also increases. This correlation is stronger for energy consumption and response time. Regarding accuracy, the correlation is stronger for some users. For example, for User 7, the correlation between window size and accuracy is weaker than for the remaining Users. For this specific case, the accuracy increases (from 71% to 89%) until a window size of 500, and after that, it starts decreasing (from 89% to 82%). Overall, larger window sizes lead to higher accuracies.

The overlap increase leads to decreased accuracy, energy consumption, and response time. The negative correlation between overlap and the performance metrics confirms this. Like window size, the correlation is stronger for energy consumption and response time. For all Users, higher overlapping decreases energy consumption and response time. As for accuracy, some users, such as Users 1 and 8, are less affected by the overlap. For these Users, the influence of overlap in the accuracy differs significantly from the remaining Users. There are increases and decreases for different values of overlap. For example, the highest accuracy is achieved for an overlap of 60%. In contrast, the maximum accuracy for the remaining users is achieved for an overlap inferior to 50%.

The value of k is the hyperparameter with a weaker influence on the performance metrics. Changes in the k lead to small accuracy, energy consumption, and response time changes. For most users, these changes are inferior to 5% for accuracy, 2 mJ for energy consumption, and 2 ms for response time. However, the increase in the value of k translates into increased accuracy, response time, and energy consumption. The positive correlation between k and the performance metrics confirms that. Overall, higher values of k lead to higher accuracies, energy consumption, and response time.

Table XIV. Detailed information regarding the Related Work.

Study	Hyperparameters	Dataset	Number of Activities	Metrics	Inference Algorithm
Banos et al. [34]	Window Size (s) (0.25 to 7)	REALDISP [35]	33	F1-Score	C4.5, k NN, Naïve Bayes, Nearest Centroid
Garcia et al. [36]	Window Size (samples) (100 to 1000) Overlap (0.0 to 0.9)	PAMAP2 [22, 23]	12	Accuracy, Energy, Execution Time	k NN, VFDT, Naive Bayes, Ensemble
Wang et al. [37]	Window Size (s) (0.5 to 7)	Private	12	F1-Score	SVM, k NN, Decision Tree, Naïve Bayes, Adaboost
Mohsen et al. [39]	k (1 to 20)	UCI-HAR [40]	6	Accuracy	k NN
Liu et al. [41]	k (3 to 9)	HAPT [42] Smartphone [43]	9 6	Accuracy	k NN
Ramón et al. [44]	Sampling Frequency (Hz) (18 to 238)	15 HAR Datasets	6 to 44	Mean geometric of sensitivity and specificity	CNN
Niazi et al. [45]	Sampling Frequency (Hz) (5, 10, 20, 25, 50, 100) Window Size (s) (1, 2, 3, 5, 10)	Private	23	Average expected value	Random Forest
Zheng et al. [46]	Sampling Frequency (Hz) (1, 5, 10, 50)	Private	6	Accuracy Energy	SVM
This Work	Sampling Frequency (Hz) (1, 5, 12.5, 25, 50, 100) Window Size (samples) (50 to 900) Overlap (0 to 0.9) k (1 to 10) Distance (E, M, C)	PAMAP2 [22, 23]	12	Accuracy, F1-Score, Energy, Inference Time	k NN

Mohsen et al. [39] and Liu et al. [41] study the influence of the value of k on a k NN-base HAR system. Mohsen et al. [39] evaluate their studies on the

UCI-HAR dataset and conclude that the accuracy increases with the increase of the value of k . The best accuracy is obtained using values of k between 8 and 20. Increasing the value of k above 8 does not yield any significant improvement. On the other side, Liu et al. [41] evaluate the effect of different values of k , between 3 and 9, on the accuracy using the HAPT [42] and Smartphone [43] dataset. These authors conclude that increasing the value of k increases the accuracy of the models. However, beyond a k value of 6, the accuracy decreased with the increase of k . Although our results on the effect of the value of k on the HAR system are aligned with the related work, we do not observe significant increases in accuracy. Although the accuracy increases with the increase of the value of k , the increase is inferior to 5%. Also, we do not observe a decrease in the accuracy for k values beyond 6, such as Liu et al. [41]. As expected, we also observe an increase in energy consumption and response time when increasing the value of k . However, we could not compare it with the related work since none of the authors explored the effect of the value of k in these performance metrics.

Another hyperparameter explored in the work presented in the Related Work is overlap. Garcia et al. [36] study the influence of the overlap in accuracy, energy consumption, and execution time for the PAMAP2 dataset. They conclude that as for accuracy, the overlap shows more fluctuations in terms of accuracy. However, the best factors are concentrated between 10% and 50%. Increasing the overlap factor also increases the energy spent and execution time. Regarding accuracy, the results achieved are very similar to ours. We also observe that the best overlap is between 10% and 50%. Although we focus on the energy consumption and response time per instance, we also have measured the global energy consumption and execution time. Our results are similar to the author's, and larger overlappings lead to higher energy consumption and execution time. However, when considering per instance instead globally, we concluded that higher overlapping leads to decreased energy consumption and response time.

Window size is one of the most explored hyperparameters in the literature. Banos et al. [34] studied the influence of the window size in the REALDISP [35] dataset using as a metric the F1-Score. They vary the window size between 0.25 s and 7 s and show that windows with 2 s achieve the best results. They also conclude that larger window sizes do not always translate into better performances for the models. Garcia et al. [36] explore the influence of window sizes between 100 and 1000 samples for the PAMAP2 dataset for accuracy, energy consumption, and execution time. They conclude that smaller window sizes result in less accuracy, while larger ones provide a more accurate model. In terms of energy and execution time, smaller windows consume less energy and take less time than bigger windows. Wang et al. [37] use a private dataset to explore the window size between 0.5 s and 7 s. The results show a significant improvement in classification performance using an increased window size. However, considerable window size leads to significant recognition latency, i.e., response time. Niazi et al. [45] use 1 s, 2 s, 3 s, 5 s, and 10 s for the window size while evaluating the average expected value for a private dataset. The better results are spread around larger window sizes. Comparing these results with our work, we

verify that our conclusion is the same for the works of Garcia et al. [36], Wang et al. [37], and Niazi et al. [45], bigger window sizes translate into better recognition performance. Like Wang et al. [37] and Garcia et al. [36], we show that bigger window sizes lead to a longer response time and require more energy. Unlike Banos et al. [34], and for the values we studied, we show that bigger windows increase the model’s accuracy.

Although the sampling frequency is not a hyperparameter, it has been studied by many authors and significantly influences the system’s performance. Niazi et al. [45] use 5 Hz, 10 Hz, 20 Hz, 25 Hz, 50 Hz, and 100 Hz for sampling frequency. The best results are spread around high sampling rates. Zheng et al. [46] use 1 Hz, 5 Hz, 10 Hz, and 50 Hz sampling frequencies and evaluate their impact on the accuracy and energy consumption. The results show that the accuracy has only improved slightly with the sampling rate increase from 1 Hz to 50 Hz. In terms of energy, there is an increase in energy consumption with increased sampling frequency. Santoyo-Ramón et al. [44] evaluate the impact of the sampling frequency in 15 different datasets. The datasets used have sampling frequencies between 18 Hz and 238 Hz. The results show that the system performance only degrades when the sampling rate is set to 10–15 Hz. The detection ratio improves when the initial rate is reduced to values between 20 and 40 Hz. The conclusions achieved by Santoyo-Ramón et al. [44] are the most similar to ours. Regarding the model’s performance, we show no significant difference in sampling frequencies between 12.5 Hz and 100 Hz. However, specifically, for a sampling frequency of 1 Hz, we observe a significant degradation in the model’s performance. For the computational cost, smaller sampling frequencies lead to lower energy consumption and response time. Zheng et al. [46] also confirm that higher sampling frequencies translate into higher energy consumption. They also achieve the lowest accuracy for a sampling frequency of 1 Hz. Our conclusions differ from Niazi et al. [45] as they observed better results for higher sampling frequencies (in the case of 50 Hz). However, we verify that for some cases, sampling frequencies of 12.5 Hz achieve better results than the other higher frequencies.

Overall, our results align with most of the work identified in the related work, i.e., the influence of the hyperparameters is the same for both cases, even though different datasets and inference algorithms are being used. However, there are cases where our conclusions differ from the related work. For example, Niazi et al. [45] show that the best model performance is achieved for a maximum sampling frequency of 50 Hz. Our results show that lower sampling frequencies perform better than bigger ones in some situations. Our conclusion is stronger in similarity to the conclusions of Garcia et al. [36], since both use the same dataset and experimental setup. The conclusion for the sampling frequency is more influenced by the datasets used since a large variety of devices were used to collect the data. Most of the studies presented in the Related Work evaluate the influence on the model’s performance. Only some exceptions (Garcia et al. [36] and Zheng et al. [46]) have studied the influence on energy consumption and execution time. When targeting the implementation of a HAR system on a device to use in real life, it is essential to consider, in addition to the model’s perfor-

mance, its impact on the device in terms of energy consumption and response time.

6 Conclusion

Human activity recognition (HAR) is a research area that has been increasingly addressed due to the widespread of mobile devices, such as smartphones, with sensing capabilities. These devices have enough processing power and memory to implement HAR systems. Although more sensors integrated into these devices allow more accurate HAR systems, it increases energy consumption and thus decreases the device’s battery life.

To be more efficient, HAR systems shall be able to adapt to the device constraints, the user, and the environment. For example, when the device is running out of battery, the system should be able to adjust its behavior to reduce energy consumption and, in this way, increase the battery life of the device. For example, different people have different walking and motion patterns, and these patterns for the same person may change during their lifetime, caused by aging, diseases, or accidents. Not addressing this problem can result in a loss of accuracy.

One way to change the system’s behavior is by changing its hyperparameters. Hyperparameters control the learning process and can affect the resulting model and its performance wildly regarding accuracy, response time, and energy consumption. The optimal performance of a HAR system depends on several hyperparameters. To understand how the hyperparameters can influence the system, in this report, we studied the impact of a selected set of hyperparameters, namely window size, overlap, the value of k , and distance function, and also other parameter sampling frequency, on a k NN-based HAR system in terms of accuracy, response time, and energy consumption, using the PAMAP2 dataset.

We conducted several experiments to study the influence of the hyperparameters in a HAR system. First, we explored the configuration space to select the hyperparameters (configurations) values that maximized the accuracy and minimized the response time. All the remaining experiments were conducted using the configurations provided by this exploration. We have used the PAMAP2 data organization by users to simulate different users for the system.

As expected, the achieved results show that hyperparameters significantly impact the system’s accuracy, response time, and energy consumption. The same configurations have different implications for different users. Each user had a different number and configurations belonging to the Pareto-front, and the range values of the performance metrics were also different. For example, User 1 requires more energy to achieve an accuracy of 82% than most users to achieve accuracies higher than 90%. In another example, users 1 and 8 did not achieve an accuracy higher than 82% and 87%, respectively, while all other users achieved accuracies higher than 90%. These results reinforced the importance of studying the hyperparameters and the necessity of a system adapting to the user.

Overall, window size and overlap were the hyperparameters with a more significant impact on the accuracy, response time, and energy consumption. This is because window size and overlap impose the number of samples read from sensors. Windows with more samples require more time and energy to extract the features necessary to infer activities. Higher overlaps imply more calls to the inference task and globally more energy consumption.

At the activity level, there is a need to consider self-adaptivity. A configuration with high global performance may not be adequate for some activities. For example, configuration 818 has a global F1-Score of 0.80, but only leads to 0.3 for the activity sitting. However, configuration 375 has a global F1-Score of 0.82 and 0.67 for the activity sitting. These results show the importance of considering the activities individually when developing a HAR system instead of considering only the global performance of the model.

The sampling frequency is not considered a hyperparameter, but it also significantly impacts HAR system behaviors with differences according to the user and activity. Although all users are affected by the reduction of the sampling frequency, User 8 is much more affected than the other users. The reduction of the sampling frequency negatively affects the activity of nordic walking and rope jumping for User 8. Once again, this highlights the importance of a self-adaptive system. As expected, lowering the sampling frequency leads to lower both energy consumption and response time.

When implementing a HAR system on a device for use in real-life scenarios, it is important to evaluate the performance of the inference algorithm but also the impact of the HAR system on the device regarding energy consumption and response time. In addition, studying the hyperparameters and their influence is essential when developing a self-adaptive HAR system.

Our ongoing work is focused on continuing the study of hyperparameters' impact on HAR systems. We expect to study datasets with a different number of activities and characteristics from the PAMAP2 dataset. We also plan to evaluate the impact of the hyperparameters on other Machine Learning (ML) algorithms. Although each ML algorithm has its own set of hyperparameters, the window size and overlap hyperparameters evaluated in this study are common to traditional HAR systems based on ML algorithms. For future work, we plan to leverage on this study to research self-adaptive HAR system techniques aware of the user, device, and target service.

References

1. P. J. S. Ferreira, J. M. P. Cardoso, and J. Mendes-Moreira, "knn prototyping schemes for embedded human activity recognition with online learning," *Computers*, vol. 9, no. 4, 2020.
2. A. Jain and V. Kanhangad, "Human activity classification in smartphones using accelerometer and gyroscope sensors," *IEEE Sensors Journal*, vol. 18, no. 3, pp. 1169–1177, 2018.

3. S. Mohamad, M. Sayed-Mouchaweh, and A. Bouchachia, "Online active learning for human activity recognition from sensory data streams," *Neurocomputing*, vol. 390, pp. 341–358, 2020.
4. V. Hernandez, T. Suzuki, and G. Venture, "Convolutional and recurrent neural network for human activity recognition: Application on american sign language," *PLOS ONE*, vol. 15, p. e0228869, 02 2020.
5. A. Gupta and H. P. Gupta, "YogaHelp: Leveraging Motion Sensors for Learning Correct Execution of Yoga With Feedback," *IEEE Transactions on Artificial Intelligence*, vol. 2, no. 4, pp. 362–371, 2021.
6. S. Zhang, Z. Wei, J. Nie, L. Huang, S. Wang, and Z. Li, "A review on human activity recognition using vision-based method," *Journal of Healthcare Engineering*, vol. 2017, pp. 1–31, 07 2017.
7. M. Shoaib, S. Bosch, O. Incel, H. Scholten, and P. Havinga, "A survey of online activity recognition using mobile phones," *Sensors*, vol. 15, pp. 2059–2085, 01 2015.
8. X. Su, H. Tong, and P. Ji, "Activity recognition with smartphone sensors," *Tsinghua Science and Technology*, vol. 19, pp. 235–249, 06 2014.
9. W. Sousa Lima, E. Souto, K. El-Khatib, R. Jalali, and J. Gama, "Human activity recognition using inertial sensors in a smartphone: An overview," *Sensors*, vol. 19, p. 3213, 07 2019.
10. T. Cover and P. Hart, "Nearest neighbor pattern classification," *IEEE Transactions on Information Theory*, vol. 13, no. 1, pp. 21–27, 1967.
11. S. Kaghyan and H. Sarukhanyan, "Activity recognition using k-nearest neighbor algorithm on smartphone with tri-axial accelerometer," *International Journal of Informatics Models and Analysis (IJIMA)*, *ITHEA International Scientific Society, Bulgaria*, vol. 1, pp. 146–156, 2012.
12. M. Kose, O. D. Incel, and C. Ersoy, "Online human activity recognition on smart phones," *Workshop on Mobile Sensing: From Smartphones and Wearables to Big Data*, vol. 16, no. 2012, pp. 11–15, 2012.
13. P. Paul and T. George, "An effective approach for human activity recognition on smartphone," in *2015 IEEE International Conference on Engineering and Technology (ICETECH)*, 2015, pp. 1–3.
14. S. Sani, N. Wiratunga, and S. Massie, "Learning deep features for knn-based human activity recognition." in *ICCBR*, A. A. Sanchez-Ruiz and A. Kofod-Petersen, Eds. CEUR Workshop Proceedings, 2017, pp. 95–103.
15. P. Siirtola and J. Rönning, "User-independent human activity recognition using a mobile phone: Offline recognition vs. real-time on device recognition," in *Distributed Computing and Artificial Intelligence*, S. Omatu, J. F. De Paz Santana, S. R. González, J. M. Molina, A. M. Bernardos, and J. M. C. Rodríguez, Eds. Berlin, Heidelberg: Springer Berlin Heidelberg, 2012, pp. 617–627.
16. Y. Celik, S. Stuart, W. L. Woo, L. T. Pearson, and A. Godfrey, "Exploring human activity recognition using feature level fusion of inertial and electromyography data," in *2022 44th Annual International Conference of the IEEE Engineering in Medicine & Biology Society (EMBC)*, 2022, pp. 1766–1769.
17. G. S. Mubibya and J. Almhana, "Improving human activity recognition using ml and wearable sensors," in *ICC 2022 - IEEE International Conference on Communications*, 2022, pp. 165–170.
18. Y. Xia, J. Ma, C. Yu, X. Ren, B. A. Antonovich, and V. Y. Tsviatkou, "Recognition system of human activities based on time-frequency features of accelerometer data," in *2022 International Conference on Intelligent Systems and Computer Vision (ISCV)*, 2022, pp. 1–5.

19. G. Luo, "A review of automatic selection methods for machine learning algorithms and hyper-parameter values," *Network Modeling Analysis in Health Informatics and Bioinformatics*, vol. 5, no. 1, pp. 1–16, 2016.
20. M. Claesen and B. D. Moor, "Hyperparameter search in machine learning," *CoRR*, vol. abs/1502.02127, 2015. [Online]. Available: <http://arxiv.org/abs/1502.02127>
21. B. Wang and N. Z. Gong, "Stealing hyperparameters in machine learning," in *2018 IEEE Symposium on Security and Privacy (SP)*, 2018, pp. 36–52.
22. A. Reiss and D. Stricker, "Introducing a new benchmarked dataset for activity monitoring," in *2012 16th International Symposium on Wearable Computers*, 2012, pp. 108–109.
23. A. Reiss and D. Stricker, "Creating and benchmarking a new dataset for physical activity monitoring," in *ACM International Conference Proceeding Series*, 06 2012.
24. Y. Qu, Y. Tang, X. Yang, Y. Wen, and W. Zhang, "Context-aware mutual learning for semi-supervised human activity recognition using wearable sensors," *Expert Systems with Applications*, vol. 219, p. 119679, 2023.
25. M. A. A. Al-qaness, A. Dahou, M. A. Elaziz, and A. M. Helmi, "Multi-resatt: Multilevel residual network with attention for human activity recognition using wearable sensors," *IEEE Transactions on Industrial Informatics*, vol. 19, no. 1, pp. 144–152, 2023.
26. L. Trinh and B. Ha, "An incorporation of deep temporal convolutional networks with hidden markov models post-processing for sensor-based human activity recognition," in *Proceedings of the 11th International Symposium on Information and Communication Technology*, ser. SoICT '22. New York, NY, USA: Association for Computing Machinery, 2022, p. 96–102.
27. W. Huang, L. Zhang, S. Wang, H. Wu, and A. Song, "Deep ensemble learning for human activity recognition using wearable sensors via filter activation," *ACM Trans. Embed. Comput. Syst.*, vol. 22, no. 1, oct 2022.
28. X. Cheng, L. Zhang, Y. Tang, Y. Liu, H. Wu, and J. He, "Real-time human activity recognition using conditionally parametrized convolutions on mobile and wearable devices," *IEEE Sensors Journal*, vol. 22, no. 6, pp. 5889–5901, 2022.
29. Z. Yang, M. Qu, Y. Pan, and R. Huan, "Comparing cross-subject performance on human activities recognition using learning models," *IEEE Access*, vol. 10, pp. 95 179–95 196, 2022.
30. D. Marinov and D. Karapetyan, "Hyperparameter optimisation with early termination of poor performers," *CoRR*, vol. abs/1907.08651, 2019. [Online]. Available: <http://arxiv.org/abs/1907.08651>
31. J. Bergstra and Y. Bengio, "Random search for hyper-parameter optimization," *Journal of Machine Learning Research*, vol. 13, no. 10, pp. 281–305, 2012.
32. M. Feurer and F. Hutter, *Hyperparameter Optimization*. Cham: Springer International Publishing, 2019, pp. 3–33.
33. J. Bergstra, R. Bardenet, Y. Bengio, and B. Kégl, "Algorithms for hyper-parameter optimization," in *Advances in Neural Information Processing Systems*, J. Shawe-Taylor, R. Zemel, P. Bartlett, F. Pereira, and K. Q. Weinberger, Eds., vol. 24. Curran Associates, Inc., 2011.
34. O. Banos, J.-M. Galvez, M. Damas, H. Pomares, and I. Rojas, "Window size impact in human activity recognition," *Sensors*, vol. 14, no. 4, pp. 6474–6499, 2014.
35. O. Baños, M. Damas, H. Pomares, I. Rojas, M. A. Tóth, and O. Amft, "A benchmark dataset to evaluate sensor displacement in activity recognition," in *Proceedings of the 2012 ACM Conference on Ubiquitous Computing*, ser. UbiComp '12. New York, NY, USA: Association for Computing Machinery, 2012, p. 1026–1035.

36. K. D. Garcia, T. Carvalho, J. Mendes-Moreira, J. M. P. Cardoso, and A. C. P. L. F. de Carvalho, "A study on hyperparameter configuration for human activity recognition," in *14th International Conference on Soft Computing Models in Industrial and Environmental Applications (SOCO 2019)*, F. Martínez Álvarez, A. Troncoso Lora, J. A. Sáez Muñoz, H. Quintián, and E. Corchado, Eds. Cham: Springer International Publishing, 2020, pp. 47–56.
37. G. Wang, Q. Li, L. Wang, W. Wang, M. Wu, and T. Liu, "Impact of sliding window length in indoor human motion modes and pose pattern recognition based on smartphone sensors," *Sensors*, vol. 18, no. 6, 2018.
38. L. Y. Hu, M. W. Huang, S. W. Ke, and C. F. Tsai, "The distance function effect on k-nearest neighbor classification for medical datasets," *SpringerPlus*, vol. 5, no. 1, 2016.
39. S. Mohsen, A. Elkaseer, and S. G. Scholz, "Human activity recognition using k-nearest neighbor machine learning algorithm," in *Sustainable Design and Manufacturing*, S. G. Scholz, R. J. Howlett, and R. Setchi, Eds. Singapore: Springer Singapore, 2022, pp. 304–313.
40. D. Garcia-Gonzalez, D. Rivero, E. Fernandez-Blanco, and M. R. Luaces, "A public domain dataset for real-life human activity recognition using smartphone sensors," *Sensors*, vol. 20, no. 8, 2020.
41. Z. Liu, S. Li, J. Hao, J. Hu, and M. Pan, "An efficient and fast model reduced kernel knn for human activity recognition," *Journal of Advanced Transportation*, vol. 2021, pp. 1–9, 06 2021.
42. J.-L. Reyes-Ortiz, L. Oneto, A. Samà, X. Parra, and D. Anguita, "Transition-aware human activity recognition using smartphones," *Neurocomputing*, vol. 171, pp. 754–767, 2016.
43. D. Dua and C. Graff, "UCI machine learning repository," 2017. [Online]. Available: <http://archive.ics.uci.edu/ml>
44. J. Antonio Santoyo-Ramón, E. Casilari, and J. Manuel Cano-García, "A study of the influence of the sensor sampling frequency on the performance of wearable fall detectors," *Measurement*, vol. 193, p. 110945, 2022.
45. A. Niazi, D. Yazdansepar, J. Gay, F. Maier, L. Ramaswamy, K. Rasheed, and M. Buman, "Statistical analysis of window sizes and sampling rates in human activity recognition," in *HEALTHINF 2017 - 10th International Conference on Health Informatics, Proceedings; Part of 10th International Joint Conference on Biomedical Engineering Systems and Technologies, BIOSTEC 2017*, E. van den Broek, A. Fred, H. Gamboa, and M. Vaz, Eds. SciTePress, 2017, pp. 319–325.
46. L. Zheng, D. Wu, X. Ruan, S. Weng, A. Peng, B. Tang, H. Lu, H. Shi, and H. Zheng, "A novel energy-efficient approach for human activity recognition," *Sensors*, vol. 17, no. 9, 2017.
47. F. Hutter, H. Hoos, and K. Leyton-Brown, "An efficient approach for assessing hyperparameter importance," in *Proceedings of the 31st International Conference on Machine Learning*, ser. Proceedings of Machine Learning Research, E. P. Xing and T. Jebara, Eds., vol. 32, no. 1. Beijing, China: PMLR, 22–24 Jun 2014, pp. 754–762.
48. S. Arlot and A. Celisse, "A survey of cross-validation procedures for model selection," *Statistics Surveys*, vol. 4, pp. 40 – 79, 2010.
49. A. Bifet, G. Holmes, R. Kirkby, and B. Pfahringer, "Moa: Massive online analysis," *J. Mach. Learn. Res.*, vol. 11, pp. 1601–1604, 2010.
50. T. Akiba, S. Sano, T. Yanase, T. Ohta, and M. Koyama, "Optuna: A next-generation hyperparameter optimization framework," in *Proceedings of the 25th*

A Individual Users - Hyperparameters

A.1 All Configurations

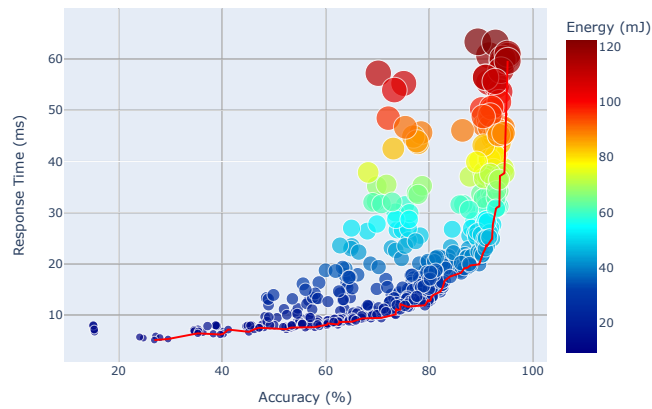


Fig. 19. Energy Consumption, Response Time, and Accuracy of the configurations for User 2.

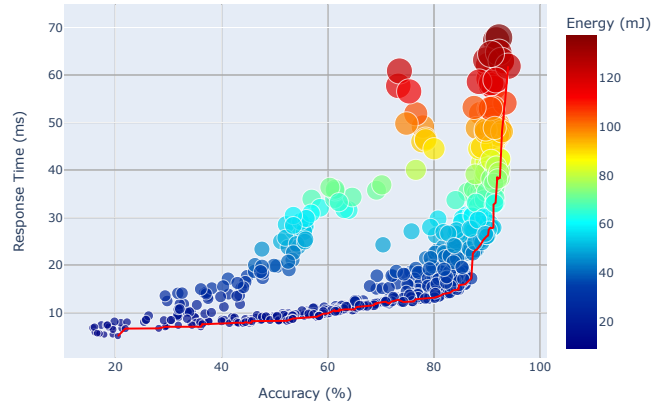


Fig. 20. Energy Consumption, Response Time, and Accuracy of the configurations for User 3.

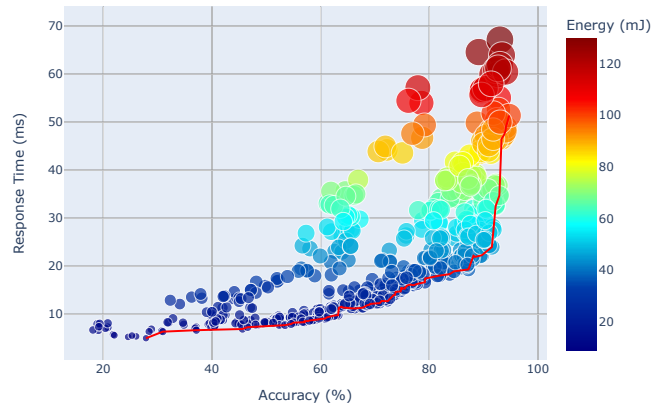


Fig. 21. Energy Consumption, Response Time, and Accuracy of the configurations for User 4.

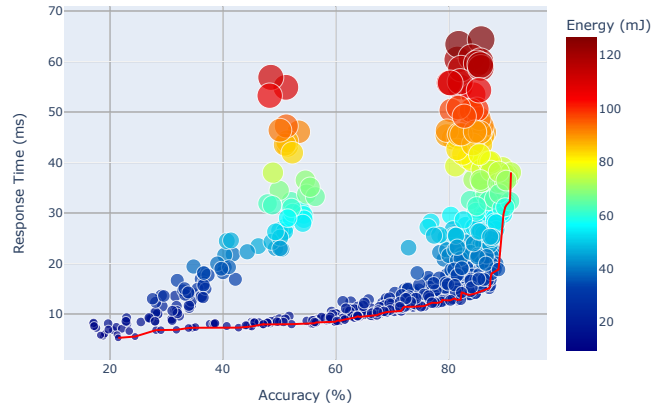


Fig. 22. Energy Consumption, Response Time, and Accuracy of the configurations for User 5.

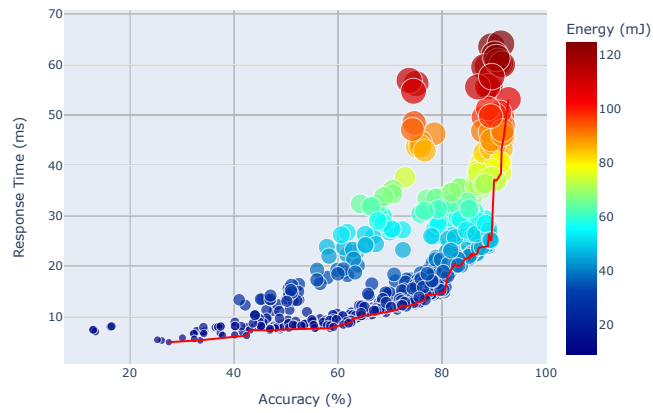


Fig. 23. Energy Consumption, Response Time, and Accuracy of the configurations for User 6.

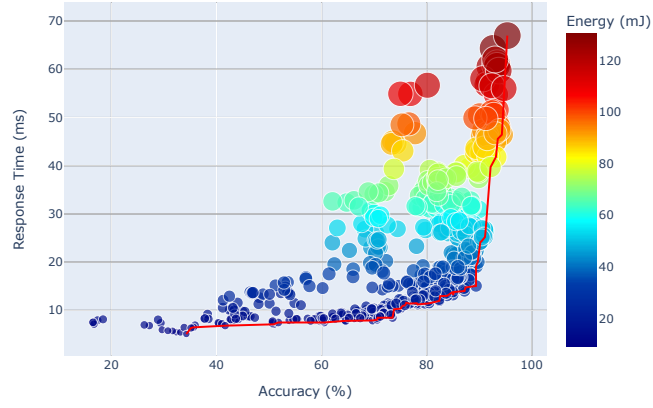


Fig. 24. Energy Consumption, Response Time, and Accuracy of the configurations for User 7.

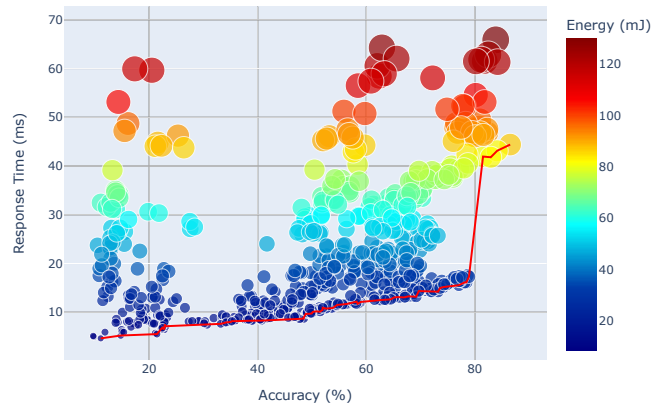


Fig. 25. Energy Consumption, Response Time, and Accuracy of the configurations for User 8.

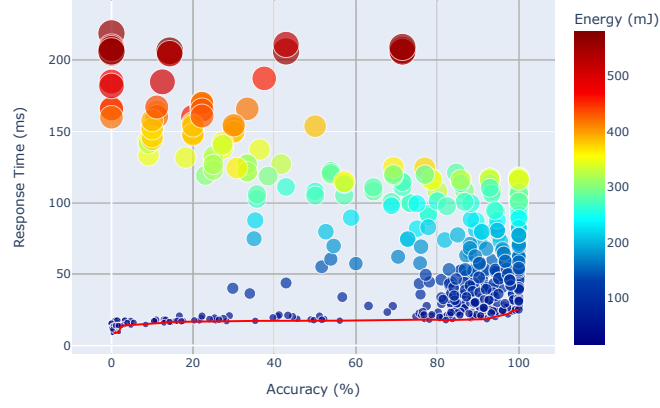


Fig. 26. Energy Consumption, Response Time, and Accuracy of the configurations for User 9.

A.2 Pareto-Front configurations with an accuracy greater or equal to 75%

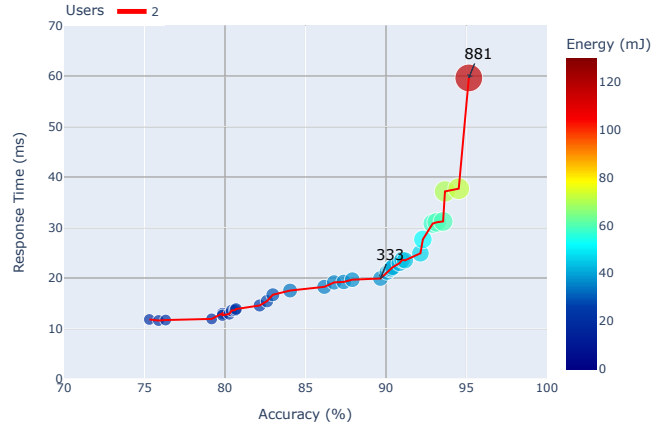


Fig. 27. Pareto-Front for User 2 with configurations with an accuracy greater than 75%. Some configurations highlighted (configuration ID is shown).

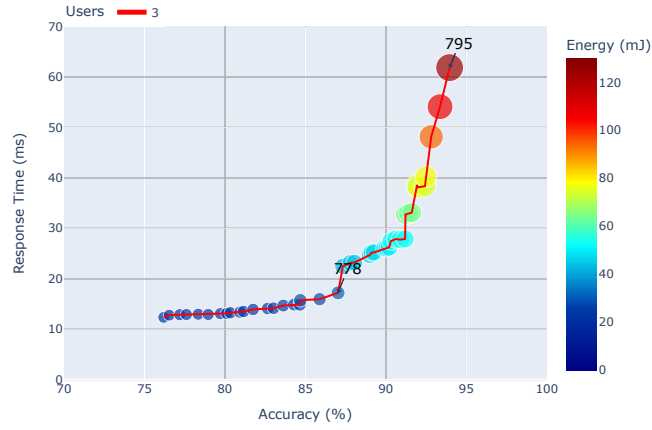


Fig. 28. Pareto-Front for User 3 with configurations with an accuracy greater than 75%. Some configurations highlighted (configuration ID is shown).

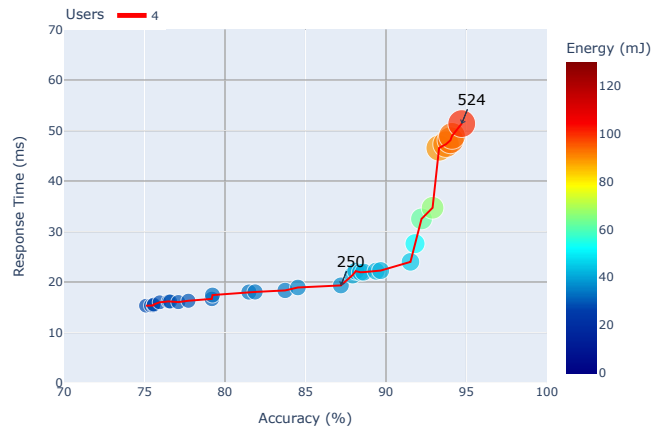


Fig. 29. Pareto-Front for User 4 with configurations with an accuracy greater than 75%. Some configurations highlighted (configuration ID is shown).

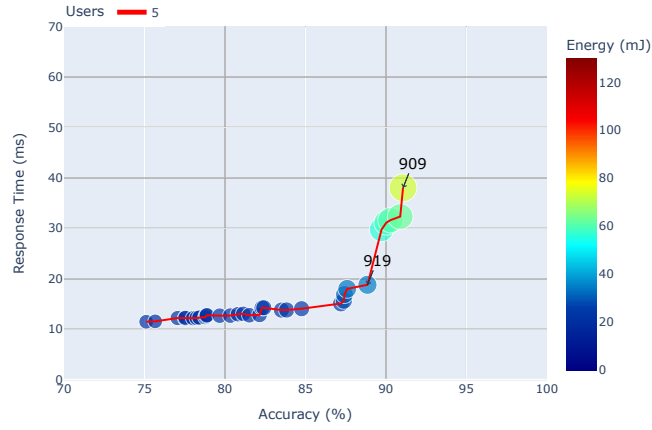


Fig. 30. Pareto-Front for User 5 with configurations with an accuracy greater than 75%. Some configurations highlighted (configuration ID is shown).

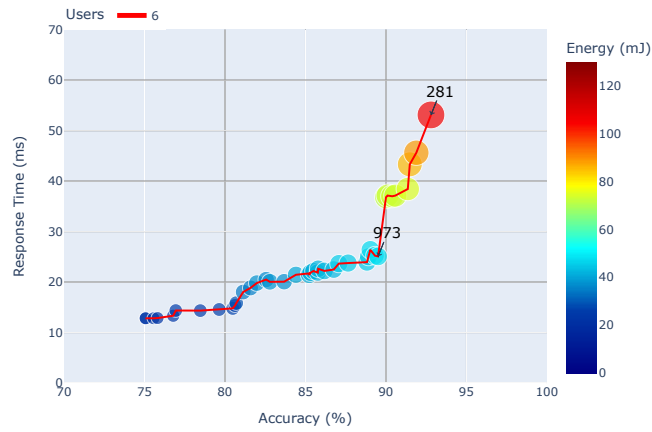


Fig. 31. Pareto-Front for User 6 with configurations with an accuracy greater than 75%. Some configurations highlighted (configuration ID is shown).

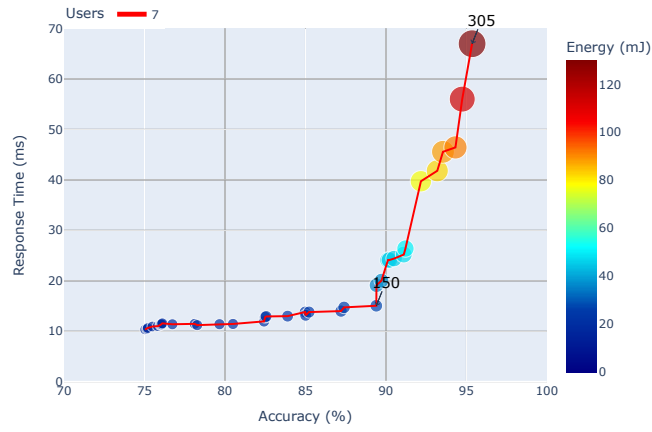


Fig. 32. Pareto-Front for User 7 with configurations with an accuracy greater than 75%. Some configurations highlighted (configuration ID is shown).

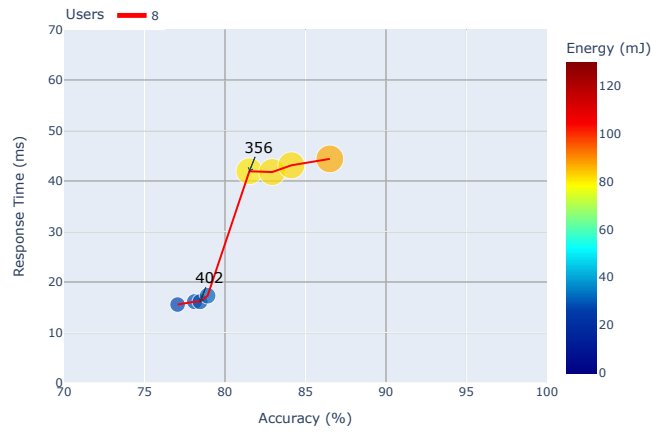


Fig. 33. Pareto-Front for User 8 with configurations with an accuracy greater than 75%. Some configurations highlighted (configuration ID is shown).

B Individual Users - Sampling Frequency

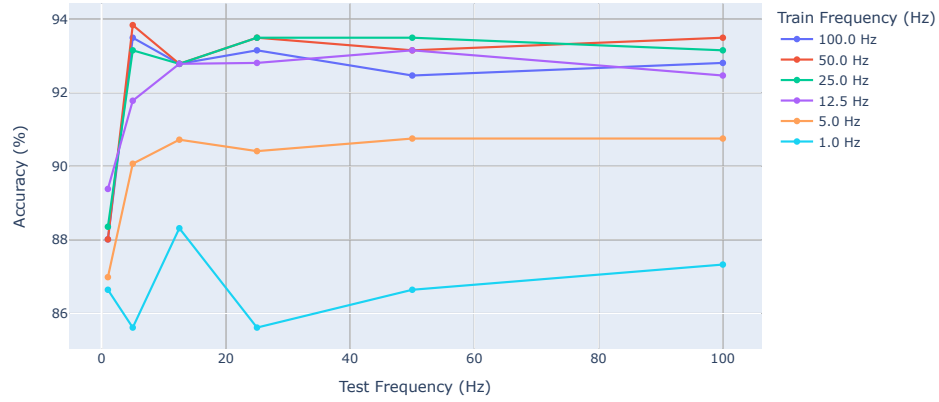


Fig. 34. Variation of the sampling frequency of the train and test sets for User 2, from 1 Hz to 100 Hz.

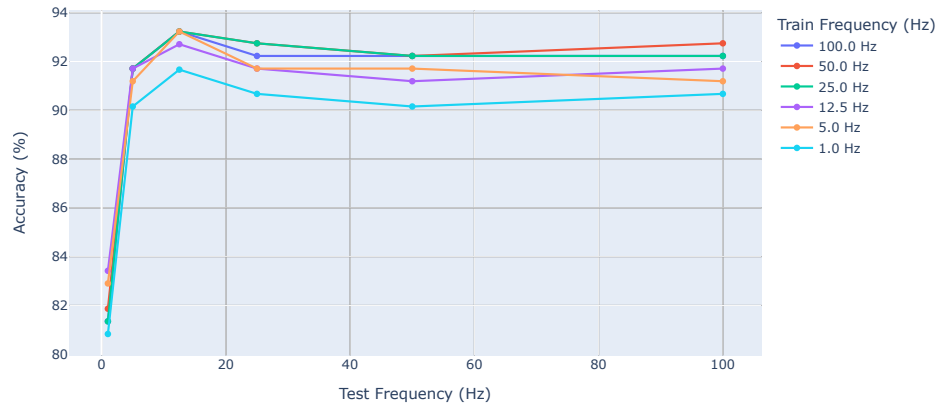


Fig. 35. Variation of the sampling frequency of the train and test sets for User 3, from 1 Hz to 100 Hz.

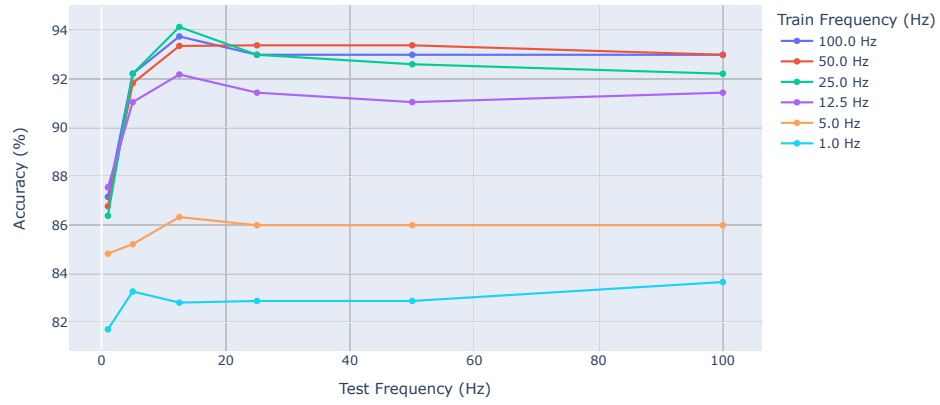


Fig. 36. Variation of the sampling frequency of the train and test sets for User 4, from 1 Hz to 100 Hz.

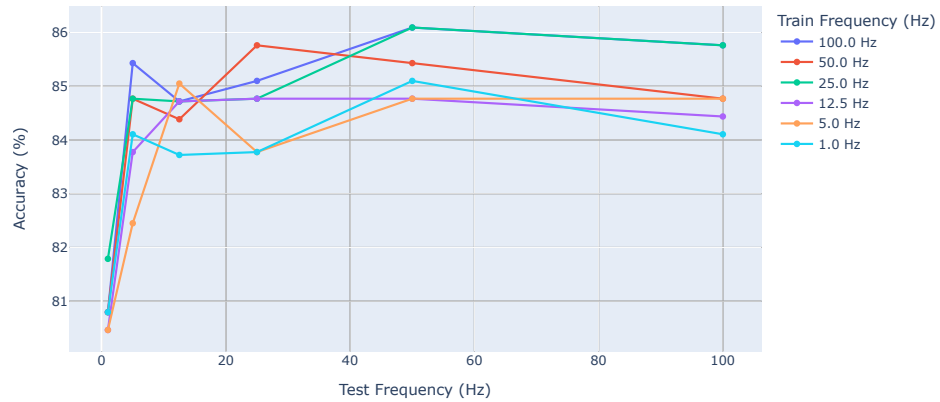


Fig. 37. Variation of the sampling frequency of the train and test sets for User 5, from 1 Hz to 100 Hz.

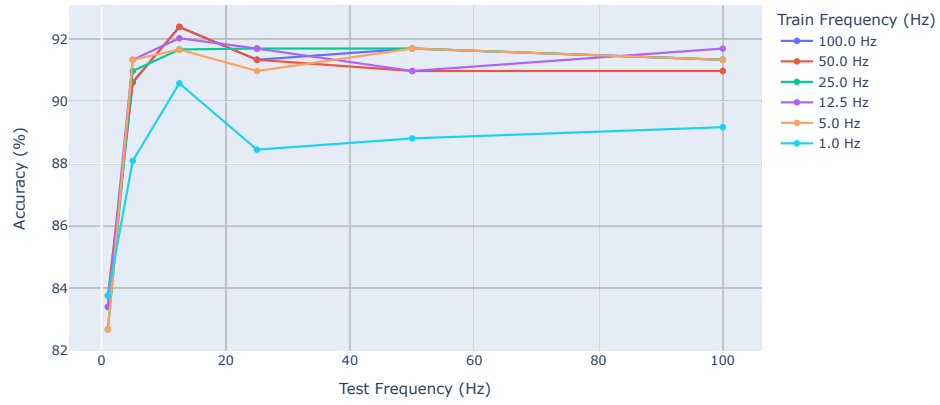


Fig. 38. Variation of the sampling frequency of the train and test sets for User 6, from 1 Hz to 100 Hz.

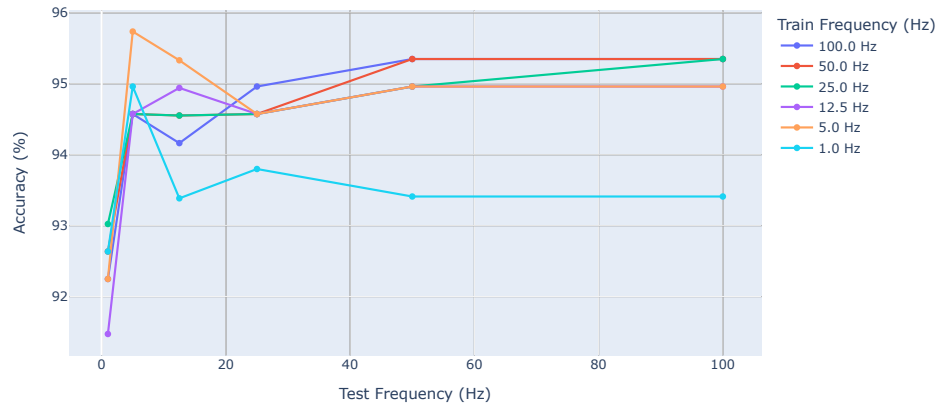


Fig. 39. Variation of the sampling frequency of the train and test sets for User 7, from 1 Hz to 100 Hz.

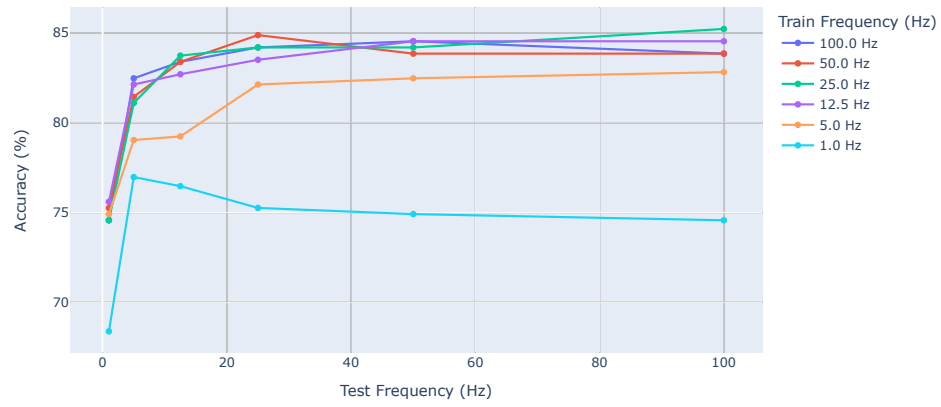


Fig. 40. Variation of the sampling frequency of the train and test sets for User 8, from 1 Hz to 100 Hz.